Journal of Electrical and Computer Engineering

Big Data for Digital Image Processing

Lead Guest Editor: Muhammad Rashad
Guest Editors: Xinhua Cai, Qun Zhao, and Xianyi Cheng

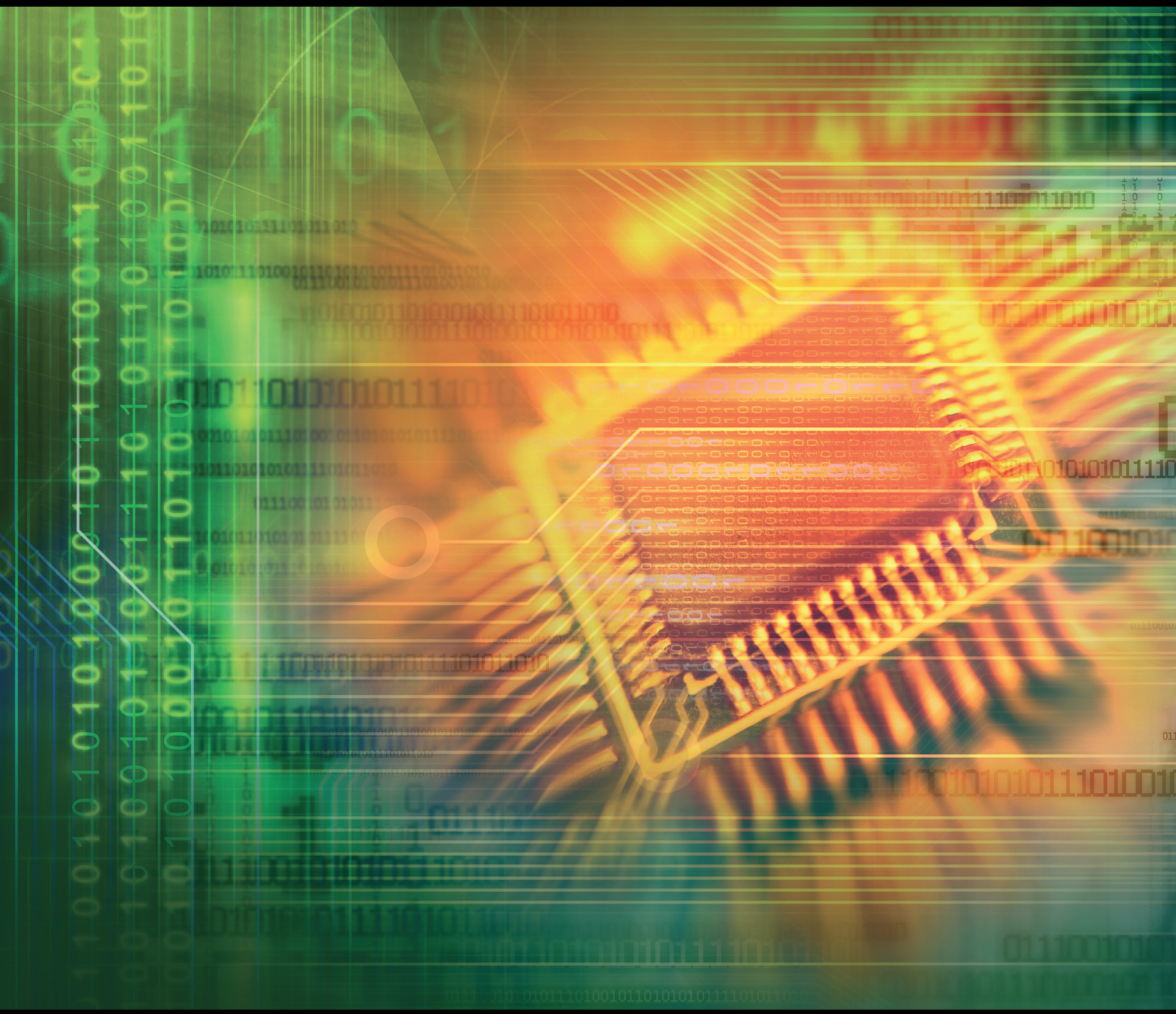

Big Data for Digital Image Processing

Journal of Electrical and Computer Engineering

Big Data for Digital Image Processing

Lead Guest Editor: Muhammad Rashad
Guest Editors: Xinhua Cai, Qun Zhao, and Xianyi Cheng

Contents

Hindawi
Journal of Electrical and Computer Engineering
Volume 2024, Article ID 9876494, 1 page
https://doi.org/10.1155/2024/9876494

Retraction

Retracted: Optimization of Business English Teaching Based on the Integration of Interactive Virtual Reality Genetic Algorithm

Journal of Electrical and Computer Engineering

Received 23 January 2024; Accepted 23 January 2024; Published 24 January 2024

This article has been retracted by Hindawi following an investigation undertaken by the publisher [1]. This investigation has uncovered evidence of one or more of the following indicators of systematic manipulation of the publication process:

(1) Discrepancies in scope

(2) Discrepancies in the description of the research reported

(3) Discrepancies between the availability of data and the research described

(4) Inappropriate citations

(5) Incoherent, meaningless and/or irrelevant content included in the article

(6) Manipulated or compromised peer review

The presence of these indicators undermines our confidence in the integrity of the article's content and we cannot, therefore, vouch for its reliability. Please note that this notice is intended solely to alert readers that the content of this article is unreliable. We have not investigated whether authors were aware of or involved in the systematic manipulation of the publication process.

In addition, our investigation has also shown that one or more of the following human-subject reporting requirements has not been met in this article: ethical approval by an Institutional Review Board (IRB) committee or equivalent, patient/participant consent to participate, and/or agreement to publish patient/participant details (where relevant).

Wiley and Hindawi regrets that the usual quality checks did not identify these issues before publication and have since put additional measures in place to safeguard research integrity.

We wish to credit our own Research Integrity and Research Publishing teams and anonymous and named external researchers and research integrity experts for contributing to this investigation.

The corresponding author, as the representative of all authors, has been given the opportunity to register their agreement or disagreement to this retraction. We have kept a record of any response received.

References

[1] X. Ma, "Optimization of Business English Teaching Based on the Integration of Interactive Virtual Reality Genetic Algorithm," *Journal of Electrical and Computer Engineering*, vol. 2022, Article ID 2455913, 9 pages, 2022.

Hindawi
Journal of Electrical and Computer Engineering
Volume 2024, Article ID 9840526, 1 page
https://doi.org/10.1155/2024/9840526

Retraction

Retracted: Analysis of Comprehensive Artificial Neural Network Computer Media Aided Construction of Economic Forecasting Model

Journal of Electrical and Computer Engineering

Received 23 January 2024; Accepted 23 January 2024; Published 24 January 2024

This article has been retracted by Hindawi following an investigation undertaken by the publisher [1]. This investigation has uncovered evidence of one or more of the following indicators of systematic manipulation of the publication process:

(1) Discrepancies in scope

(2) Discrepancies in the description of the research reported

(3) Discrepancies between the availability of data and the research described

(4) Inappropriate citations

(5) Incoherent, meaningless and/or irrelevant content included in the article

(6) Manipulated or compromised peer review

The presence of these indicators undermines our confidence in the integrity of the article's content and we cannot, therefore, vouch for its reliability. Please note that this notice is intended solely to alert readers that the content of this article is unreliable. We have not investigated whether authors were aware of or involved in the systematic manipulation of the publication process.

Wiley and Hindawi regrets that the usual quality checks did not identify these issues before publication and have since put additional measures in place to safeguard research integrity.

We wish to credit our own Research Integrity and Research Publishing teams and anonymous and named external researchers and research integrity experts for contributing to this investigation.

The corresponding author, as the representative of all authors, has been given the opportunity to register their agreement or disagreement to this retraction. We have kept a record of any response received.

References

[1] T. Li, "Analysis of Comprehensive Artificial Neural Network Computer Media Aided Construction of Economic Forecasting Model," *Journal of Electrical and Computer Engineering*, vol. 2022, Article ID 7981393, 8 pages, 2022.

Hindawi
Journal of Electrical and Computer Engineering
Volume 2024, Article ID 9765875, 1 page
https://doi.org/10.1155/2024/9765875

Retraction

Retracted: Multimedia Vision Improvement and Simulation in Consideration of Virtual Reality Reconstruction Algorithms

Journal of Electrical and Computer Engineering

Received 23 January 2024; Accepted 23 January 2024; Published 24 January 2024

This article has been retracted by Hindawi following an investigation undertaken by the publisher [1]. This investigation has uncovered evidence of one or more of the following indicators of systematic manipulation of the publication process:

(1) Discrepancies in scope

(2) Discrepancies in the description of the research reported

(3) Discrepancies between the availability of data and the research described

(4) Inappropriate citations

(5) Incoherent, meaningless and/or irrelevant content included in the article

(6) Manipulated or compromised peer review

The presence of these indicators undermines our confidence in the integrity of the article's content and we cannot, therefore, vouch for its reliability. Please note that this notice is intended solely to alert readers that the content of this article is unreliable. We have not investigated whether authors were aware of or involved in the systematic manipulation of the publication process.

In addition, our investigation has also shown that one or more of the following human-subject reporting requirements has not been met in this article: ethical approval by an Institutional Review Board (IRB) committee or equivalent, patient/participant consent to participate, and/or agreement to publish patient/participant details (where relevant).

Wiley and Hindawi regrets that the usual quality checks did not identify these issues before publication and have since put additional measures in place to safeguard research integrity.

We wish to credit our own Research Integrity and Research Publishing teams and anonymous and named external researchers and research integrity experts for contributing to this investigation.

The corresponding author, as the representative of all authors, has been given the opportunity to register their agreement or disagreement to this retraction. We have kept a record of any response received.

References

[1] J. He, "Multimedia Vision Improvement and Simulation in Consideration of Virtual Reality Reconstruction Algorithms," *Journal of Electrical and Computer Engineering*, vol. 2022, Article ID 4968588, 10 pages, 2022.

Hindawi
Journal of Electrical and Computer Engineering
Volume 2024, Article ID 9758163, 1 page
https://doi.org/10.1155/2024/9758163

Retraction

Retracted: Design of Image Processing Technology Support System in Human-Computer Collaborative Visual Design Assisted by Artificial Intelligence Technology

Journal of Electrical and Computer Engineering

Received 23 January 2024; Accepted 23 January 2024; Published 24 January 2024

This article has been retracted by Hindawi following an investigation undertaken by the publisher [1]. This investigation has uncovered evidence of one or more of the following indicators of systematic manipulation of the publication process:

(1) Discrepancies in scope

(2) Discrepancies in the description of the research reported

(3) Discrepancies between the availability of data and the research described

(4) Inappropriate citations

(5) Incoherent, meaningless and/or irrelevant content included in the article

(6) Manipulated or compromised peer review

The presence of these indicators undermines our confidence in the integrity of the article's content and we cannot, therefore, vouch for its reliability. Please note that this notice is intended solely to alert readers that the content of this article is unreliable. We have not investigated whether authors were aware of or involved in the systematic manipulation of the publication process.

Wiley and Hindawi regrets that the usual quality checks did not identify these issues before publication and have since put additional measures in place to safeguard research integrity.

We wish to credit our own Research Integrity and Research Publishing teams and anonymous and named external researchers and research integrity experts for contributing to this investigation.

The corresponding author, as the representative of all authors, has been given the opportunity to register their agreement or disagreement to this retraction. We have kept a record of any response received.

References

[1] Y. Song, "Design of Image Processing Technology Support System in Human-Computer Collaborative Visual Design Assisted by Artificial Intelligence Technology," *Journal of Electrical and Computer Engineering*, vol. 2023, Article ID 9363644, 15 pages, 2023.

Hindawi
Journal of Electrical and Computer Engineering
Volume 2023, Article ID 9843297, 1 page
https://doi.org/10.1155/2023/9843297

Retraction

Retracted: Filtering Algorithm for Positioning Accuracy of the Logistics Tracking System Based on the 3D Virtual Warehousing Logistics Demonstration System

Journal of Electrical and Computer Engineering

Received 15 August 2023; Accepted 15 August 2023; Published 16 August 2023

This article has been retracted by Hindawi following an investigation undertaken by the publisher [1]. This investigation has uncovered evidence of one or more of the following indicators of systematic manipulation of the publication process:

(1) Discrepancies in scope

(2) Discrepancies in the description of the research reported

(3) Discrepancies between the availability of data and the research described

(4) Inappropriate citations

(5) Incoherent, meaningless and/or irrelevant content included in the article

(6) Peer-review manipulation

The presence of these indicators undermines our confidence in the integrity of the article's content and we cannot, therefore, vouch for its reliability. Please note that this notice is intended solely to alert readers that the content of this article is unreliable. We have not investigated whether authors were aware of or involved in the systematic manipulation of the publication process.

Wiley and Hindawi regrets that the usual quality checks did not identify these issues before publication and have since put additional measures in place to safeguard research integrity.

We wish to credit our own Research Integrity and Research Publishing teams and anonymous and named external researchers and research integrity experts for contributing to this investigation.

The corresponding author, as the representative of all authors, has been given the opportunity to register their agreement or disagreement to this retraction. We have kept a record of any response received.

References

[1] G. Sun and F. Qiao, "Filtering Algorithm for Positioning Accuracy of the Logistics Tracking System Based on the 3D Virtual Warehousing Logistics Demonstration System," *Journal of Electrical and Computer Engineering*, vol. 2022, Article ID 5963140, 9 pages, 2022.

Hindawi
Journal of Electrical and Computer Engineering
Volume 2023, Article ID 9838757, 1 page
https://doi.org/10.1155/2023/9838757

Retraction

Retracted: Based on Knowledge Recognition and Using Binomial Distribution Function to Establish a Mathematical Model of Random Selection of Test Questions in the Test Bank

Journal of Electrical and Computer Engineering

Received 15 August 2023; Accepted 15 August 2023; Published 16 August 2023

This article has been retracted by Hindawi following an investigation undertaken by the publisher [1]. This investigation has uncovered evidence of one or more of the following indicators of systematic manipulation of the publication process:

(1) Discrepancies in scope

(2) Discrepancies in the description of the research reported

(3) Discrepancies between the availability of data and the research described

(4) Inappropriate citations

(5) Incoherent, meaningless and/or irrelevant content included in the article

(6) Peer-review manipulation

The presence of these indicators undermines our confidence in the integrity of the article's content and we cannot, therefore, vouch for its reliability. Please note that this notice is intended solely to alert readers that the content of this article is unreliable. We have not investigated whether authors were aware of or involved in the systematic manipulation of the publication process.

Wiley and Hindawi regrets that the usual quality checks did not identify these issues before publication and have since put additional measures in place to safeguard research integrity.

We wish to credit our own Research Integrity and Research Publishing teams and anonymous and named external researchers and research integrity experts for contributing to this investigation.

The corresponding author, as the representative of all authors, has been given the opportunity to register their agreement or disagreement to this retraction. We have kept a record of any response received.

References

[1] Y. Chang, "Based on Knowledge Recognition and Using Binomial Distribution Function to Establish a Mathematical Model of Random Selection of Test Questions in the Test Bank," *Journal of Electrical and Computer Engineering*, vol. 2021, Article ID 2250300, 8 pages, 2021.

Hindawi
Journal of Electrical and Computer Engineering
Volume 2024, Article ID 9758163, 1 page
https://doi.org/10.1155/2024/9758163

Retraction

Retracted: Design of Image Processing Technology Support System in Human-Computer Collaborative Visual Design Assisted by Artificial Intelligence Technology

Journal of Electrical and Computer Engineering

Received 23 January 2024; Accepted 23 January 2024; Published 24 January 2024

This article has been retracted by Hindawi following an investigation undertaken by the publisher [1]. This investigation has uncovered evidence of one or more of the following indicators of systematic manipulation of the publication process:

(1) Discrepancies in scope

(2) Discrepancies in the description of the research reported

(3) Discrepancies between the availability of data and the research described

(4) Inappropriate citations

(5) Incoherent, meaningless and/or irrelevant content included in the article

(6) Manipulated or compromised peer review

The presence of these indicators undermines our confidence in the integrity of the article's content and we cannot, therefore, vouch for its reliability. Please note that this notice is intended solely to alert readers that the content of this article is unreliable. We have not investigated whether authors were aware of or involved in the systematic manipulation of the publication process.

Wiley and Hindawi regrets that the usual quality checks did not identify these issues before publication and have since put additional measures in place to safeguard research integrity.

We wish to credit our own Research Integrity and Research Publishing teams and anonymous and named external researchers and research integrity experts for contributing to this investigation.

The corresponding author, as the representative of all authors, has been given the opportunity to register their agreement or disagreement to this retraction. We have kept a record of any response received.

References

[1] Y. Song, "Design of Image Processing Technology Support System in Human-Computer Collaborative Visual Design Assisted by Artificial Intelligence Technology," *Journal of Electrical and Computer Engineering*, vol. 2023, Article ID 9363644, 15 pages, 2023.

Hindawi
Journal of Electrical and Computer Engineering
Volume 2023, Article ID 9363644, 15 pages
https://doi.org/10.1155/2023/9363644

Research Article

Design of Image Processing Technology Support System in Human-Computer Collaborative Visual Design Assisted by Artificial Intelligence Technology

Yan Song

Zhengzhou Railway Vocational & Technical College, Zhengzhou, Henan 450000, China

Correspondence should be addressed to Yan Song; 10497@zzrvtc.edu.cn

Received 31 December 2021; Revised 28 March 2022; Accepted 23 March 2023; Published 8 May 2023

Academic Editor: Muhammad Rashad

Aiming at the problems of high cleaning intensity, low efficiency, and hidden safety hazards of high-altitude curtain walls, this study proposes that the image processing method is a kind of image processing technology in human-computer collaborative visual design. The algorithm uses generalized mapping to scramble the picture and then expands and replaces the scrambled pictures one by one through the image processing technical support system. Studies have shown that this calculation method has mixed pixel values, good diffusion performance, and strong resistance performance. The pixel distribution of the processed image is relatively random, and the features of similar loudness are not relevant. It is proved through experiments that the above calculation methods have strong safety performance.

1. Introduction

With the development of science and technology and Internet technology, multimedia digital products are widely used in all walks of life. Nowadays, many security issues are gradually exposed in the dissemination and use of multimedia data information. The characteristics of digital pictures are large data and high correlation between data. In the past, traditional processing methods used for multimedia processing have the disadvantage of low efficiency [1, 2]. The development of a new type of chaotic system, which makes multimedia image processing have the characteristics of high efficiency and high safety performance, is a research boom in recent years. There are many types of image data processing in human-computer collaborative visual design. Due to the high dimensions, image processing in human-computer collaborative visual design leads to undesirable results. The multigranularity algorithm of image data in human-computer collaborative visual design proposed in literature [3] should not be applied to the fusion of high-level data clusters because image data in human-computer collaborative visual design cannot be processed to the hypotenuse boundary. In literature [4], a weighted processing algorithm for image data processing in human-computer collaborative visual design is proposed. The error in the processing result is relatively large. In the literature [5], due to the dispersiveness of the algorithm in the use process, the image data processing analysis in the human-computer collaborative visual design based on a priori information is proposed.

This study designs a robot control system with STM 32 and LPC 4300 as the control core. The control system adopts a motion control method based on electric push rods, servo motors, and vacuum suction cups and adds an image recognition control system. This paper studies the image processing method in the human-machine collaborative visual design of the high-order chaotic calculation method. The experimental analysis shows that this method has strong resistance to exhaustive supply and system analysis attacks, high computational efficiency, and high security performance.

2. Control System Design Methods

As shown in Figure 1, the man-machine image processing technology support system here mainly includes man-

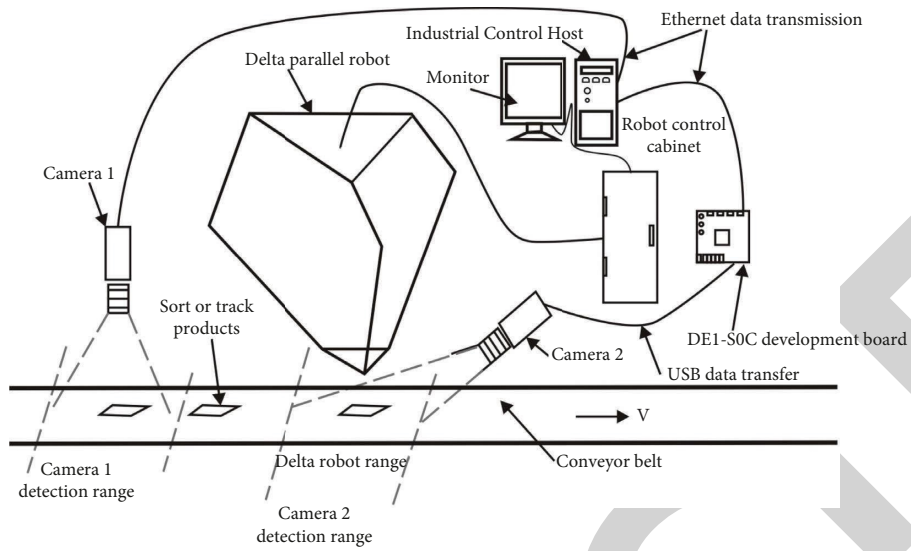

Figure 1: Human-machine image processing technology support system.

machine, transmission mechanism, and vision system. The dynamic capture experiment platform constitutes a semi-closed circulating conveying system to ensure that the capture target moves cyclically on the conveyor belt [6].

2.1. Control System Hardware Design. According to the design requirements, the hardware design of the system includes two parts: the hardware design of the main controller based on STM 32 and the hardware design of the machine vision control system based on LPC 4300 [7], and a simplified block diagram of the hardware design of the control system is shown in Figure 2.

The hardware of the man-machine image processing technology support system in this article mainly composed of light source, CCD industrial camera, camera lens, and artificial intelligence technology. The specific hardware selection is as follows.

2.1.1. Light Source. The light source has a huge impact on data collection and system performance. In the human-machine vision system, a good light source can highlight the characteristics of the captured target as much as possible. The part that needs to be detected and the part that needs to be captured can achieve a greater difference, thereby ensuring the feature difference of the target to be detected in other backgrounds. The characteristic comparison of different light sources is shown in Table 1.

Considering the actual working situation of the human-machine grasping system in the grasping process, because the brightness of the fluorescent lamp is relatively large, it is suitable for large-area uniform lighting and the price is cheap [8, 9]. Therefore, to ensure better lighting effects, this article uses fluorescent lamps as humans. The light source installation design of the vision system is shown in Figure 1.

2.1.2. CCD Industrial Camera. Choosing a suitable industrial camera is very important for the human-machine vision control system. In this study, the visual inspection area based on artificial intelligence technology is 300 mm × 200 mm, and the accuracy should be kept within 0.5 slowly. Therefore, the No. 1 industrial camera uses a 2 million pixel (1600 × 1200) camera. The No. 2 industrial camera uses a 2 million pixel (1280 × 960) camera. Because the frame rate has a great impact on the real-time feedback of the human-machine visual inspection system, the frame rate cannot be too low [4]. Based on the above analysis, the parameters of the No. 1 industrial camera and the No. 2 industrial camera are shown in Tables 2 and 3.

2.1.3. Lens Model Selection. Considering that the resolution of the lens needs to be matched with the resolution of the industrial camera, too low resolution will reduce the accuracy of visual inspection and too much pursuit of high resolution will increase additional production costs. The focal length between the No. 1 industrial camera and the No. 2 industrial camera can be solved by the lens focal length calculation formula [10].

$$f = w * \frac{D}{W}. \tag{1}$$

Among them, D represents the object distance; w represents the total length of the visual sensor; W represents the length of the actual project corresponding to the visual sensor. Then, it can be calculated from the above parameters that the focal length of the No. 1 industrial camera is $f = 8.5 * 300/200 = 12.75$ mm, and the focal length of the No. 2 industrial camera is $f = 4.8 * 300/200 = 7.2$ mm. After comprehensive consideration, the No. 1 industrial camera uses the Computar M3Z1228C-MP lens produced by Japan's CBC Company. The specific parameter configuration is shown in Table 4. The No. 2 industrial camera uses

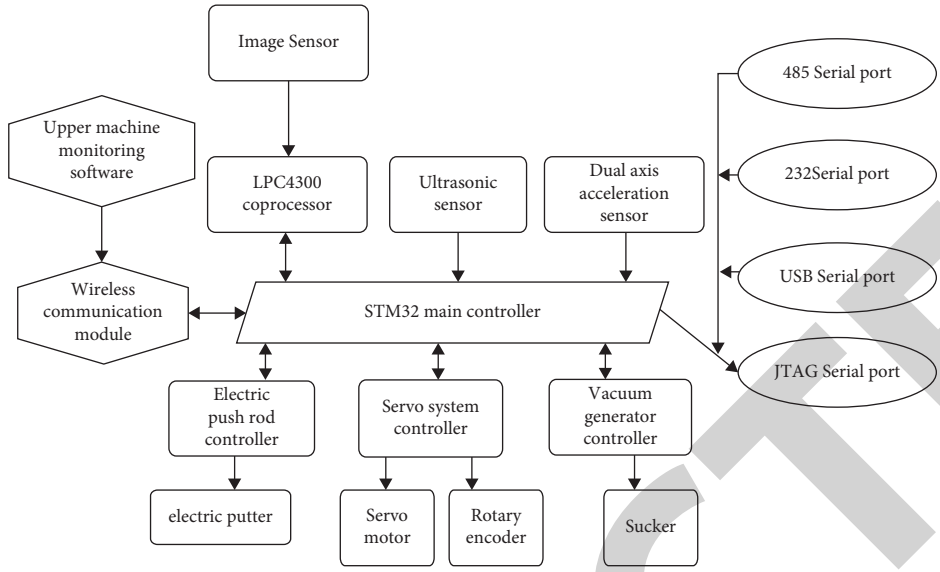

Figure 2: Simple block diagram of control system hardware design.

Table 1: Comparison of characteristics of different light sources.

Light source	Color	Life/h	Light intensity	Features
Halogen light	White, yellowish	5000–7000	Very bright	More fever, cheaper
Fluorescent lamp	White, greenish	5000–7000	Bright	Cheap, large area lighting
LED	Red, yellow, green, white, blue	60000–100000	Brighter	Cheap, small area lighting
Fiber light source	Optional	5000–7000	Bright	Less heat, uniform lighting
Electroluminescent tube	Determined by the luminous frequency	5000–7000	Brighter	Less fever, cheaper

Table 2: Parameters of industrial camera No. 1

Project	Parameter
Industrial camera model	DMK-23G74
Color	Black and white
Chip size	1/1.8 8.5 mm × 6.8 mm
Pixel	1600 × 1200
Pixel size	4.4 μm × 4.4 μm
Sensor	CCD
Frame rate	20
Interface method	C/CS interface

Table 3: Parameters of No. 2 industrial camera.

Project	Parameter
Industrial camera model	MV-UB 130GM
Color	Black and white
Chip size	1/1.3 4.8 mm × 3.6 mm
Pixel	1280 × 960
Pixel size	3.75 μm × 3.75 μm
Sensor	CMOS
Frame rate	36
Interface method	CS interface

Table 4: Lens parameters of No. 1 industrial camera.

Project	Parameter
Lens model	M3Z1228C-MP
Focal length	12.36 mm
Target surface size	2/3
Maximum imaging size	8.8 mm × 6.6 mm
Aperture range	F1.4-F16C
Working distance	0.1–∞
Interface method	C interface

Table 5: Lens parameters of No. 2 industrial camera.

Project	Parameter
Lens model	M0814-MP2
Focal length	12–36 mm
Target surface size	2/3
Maximum imaging size	8.8 mm × 6.6 mm
Aperture range	F1.4-F16C
Working distance	0.2–∞
Interface method	C interface

Computar M0814-MP2 lens. The specific parameter configuration is shown in Table 5.

The hardware design of the machine vision control system is to use the image sensor OV9715 as the image input and the LPC4300 processor as the image processing unit to realize the positioning of cleaning obstacles and the identification of cleaning objects during the cleaning process, so as to realize the intelligentization of the cleaning process. The LPC4300 is an asymmetric digital signal controller with dual core architectures of ARM3 CortexTM-M4 and Cortex-M0. It can handle a large number of data transmission and

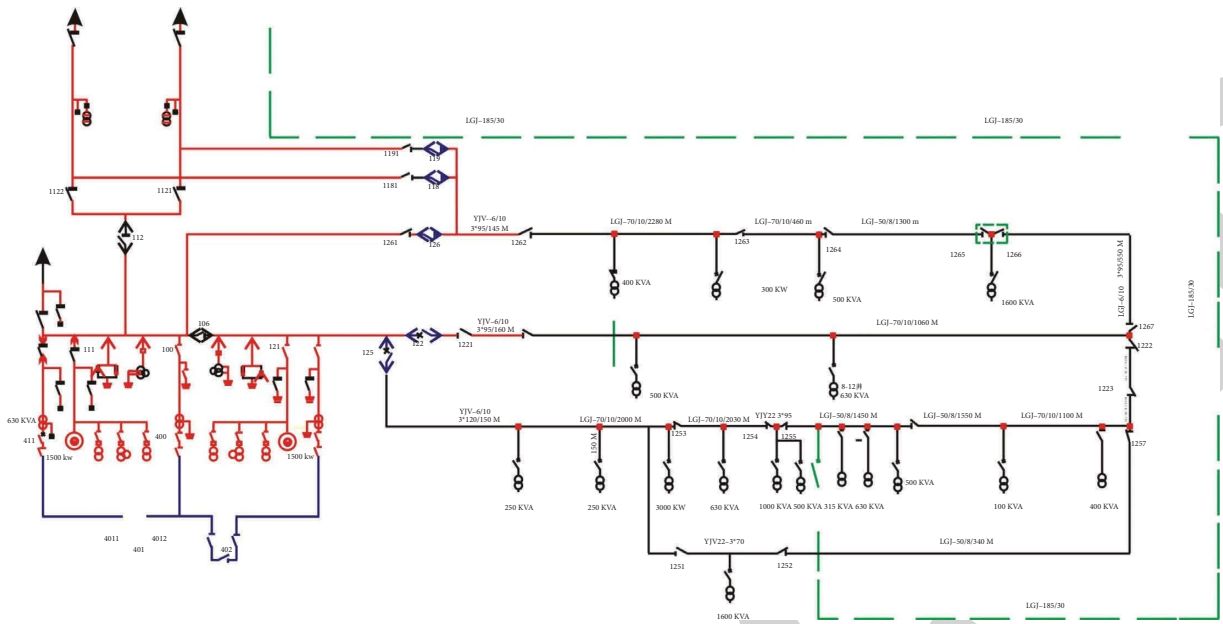

Figure 3: Hardware design of the machine vision module.

I/O processing tasks and can execute up to 204 MHz at high speed.

The OV9715 is a high-performance vision sensor with a resolution of 1 million. An ultrawide-angle lens can be used when distortion correction and image joining are required. With the first-class low-light performance of 3300 mV/(lux-sec), images can be captured under almost any lighting conditions. Figure 3 shows the hardware design of the machine vision module [11].

As shown in Figure 3, the hardware design of the image processing module includes the construction of the LPC4300 minimum system and the OV9715 drive circuit, the rudder interface and the JTAG debugging interface. The LPC4300 processor controls the steering gear to adjust the lens direction of the image processor and scans the cleaning area. The LPC4300 recognizes the image information from the image sensor and finally transmits the recognition result to STM 32. It supports communication between LPC4300 and STM 32.

2.2. Control System Software Design. Figure 4 shows the overall flow of the cleaning robot software design. The upper computer UI interface uses the wireless communication module to control the control system and set the action parameters. The control system plans the action path of the robot by collecting the data information of each sensor and the parameter information sent by the upper computer and sends the planned results to the electric push rod control system, vacuum generator control system, and servo control system. Control the washing of limbs and robotic arms.

Main controller software design: The design of the main controller application program adopts the C language program design and uses the function program library formally provided by ST Company. The functions that realize the software design of the main controller include collecting sensor data, making electric push rod, servo motor, and vacuum generator control program, and arm washing trajectory and walking trajectory plan. Figure 5 shows human-computer interaction and wireless serial. Through the demonstration, the creation of communication program and software design process of master controller are important in the design of master controller software [10].

The working system of the robot is divided into two working modes: manual working mode and intelligent working mode. In manual operation, the operator controls the robot by jog to complete the cleaning operation, which mainly realizes the monitoring and visualization of the cleaning process by the camera. Different from human work, intelligent work does not require human intervention in the robot cleaning process. The image processing module locates the cleaning obstacles and recognizes the cleaning object to automatically complete the cleaning task [11].

Image processing module software design: The software design of the image processing module is mainly the process of identifying and processing cleaning objects. During the image recognition process, the cleaning robot trains the current object in advance to obtain the feature quantity of the target object and creates an effective feature quantity mapping table. When the system is working, it extracts the characteristic value of the currently collected work object, matches it with the value of the characteristic quantity mapping table, and completes the identification of the target object. Figure 6 shows the software design flow of the image processing module.

As shown in Figure 6, the cleaning robot needs to perform preprocessing operations on the image during the image processing process. This is to simplify the image data to the greatest extent and also to improve the detectability of useful information. Image segmentation is the technique and process of segmenting an image into a number of specific

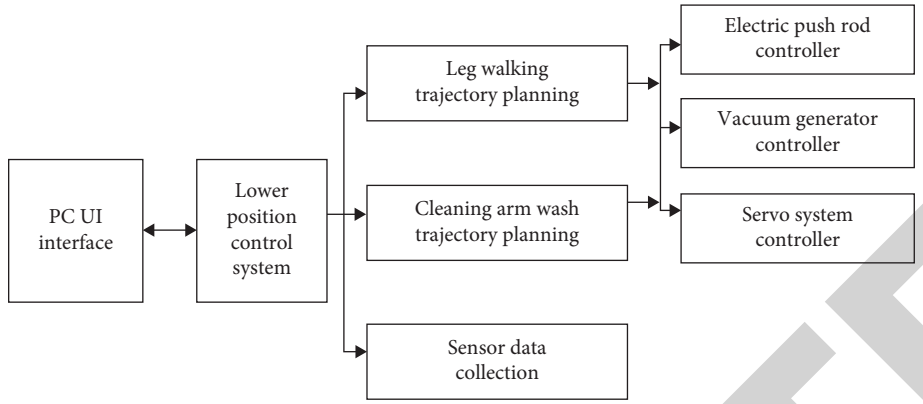

Figure 4: The overall process of system software design.

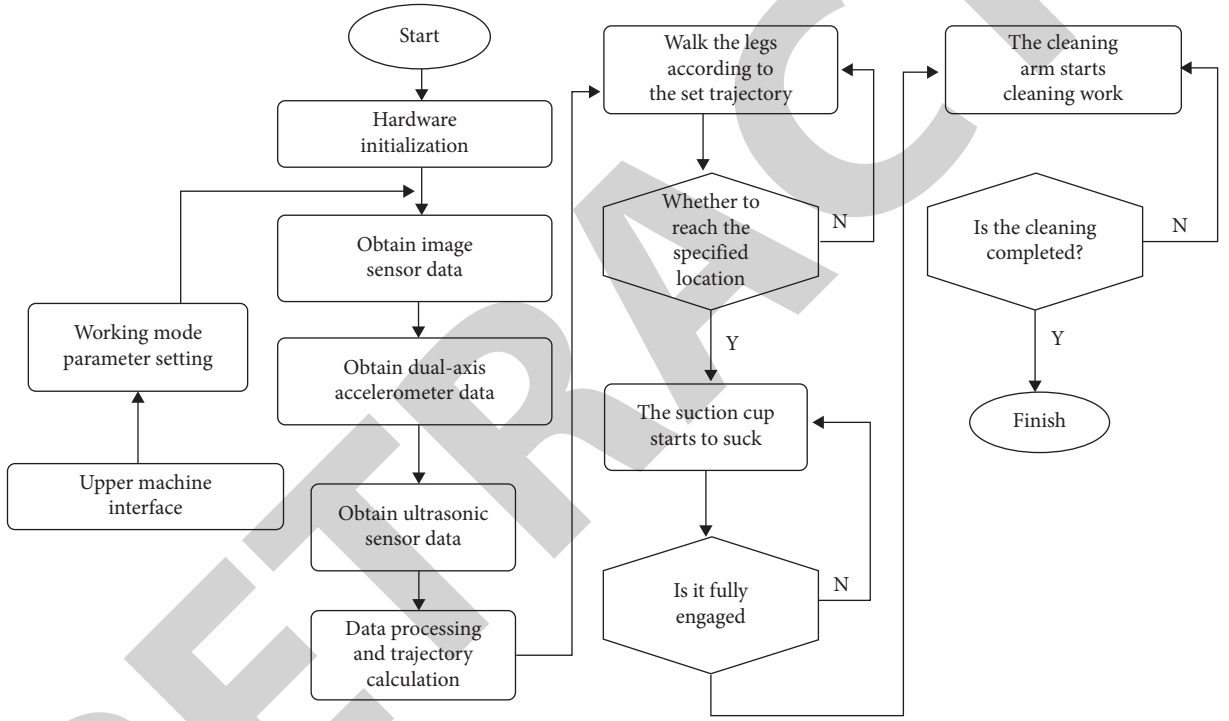

Figure 5: The main controller software design process.

areas with unique properties and proposing objects of interest. Image feature value extraction establishes a feature mapping table to match the target object to find the most effective feature from multiple features. Image matching refers to the comparison between the extracted features and the feature mapping table to achieve the purpose of target object recognition [12].

2.3. Determining the Calibration of the Positional Relationship. To enable the system to interact and track objects correctly, the positional relationship between the vision system and the conveyor belt, the robot and the conveyor belt must be calibrated. As shown in Figure 7, the coordinate system O_r-$X_rY_rZ_r$ established in the man-machine system. Suppose the business coordinate system established by the No. 1 industrial camera is O_{c1}-$X_{c1}Y_{c1}Z_{c1}$, and the field of the view coordinate system established by the conveyor plane XY in this industrial camera vision is O_{v1}-$X_{v1}Y_{v1}Z_{v1}$; the coordinate system established under the No. 2 camera is O_{c2}-$X_{c2}Y_{c2}Z_{c2}$, and the conveyor plane in this industrial camera vision. The field of the view coordinate system established by XY is O_{v2}-$X_{v2}Y_{v2}Z_{v2}$; on the conveyor belt, follow the conveyor XY plane, take the conveyor movement direction as the X axis, and use the right-hand rule to establish the world coordinate system O_w-$X_wY_wZ_w$, where O_w is the Z_{v2} axis of the O_{v2}-$X_{v2}Y_{v2}Z_{v2}$ of the coordinate system O_{v2}-$X_{v2}Y_{v2}Z_{v2}$ and the plane of the robot conveyor belt. The intersection meets the coincidence of O_w and O_{v2}. O_{v1} is the intersection point between the Z_{v1} axis of the coordinate system O_{v1}-$X_{v1}Y_{v1}Z_{v1}$ and the plane of the robot conveyor belt.

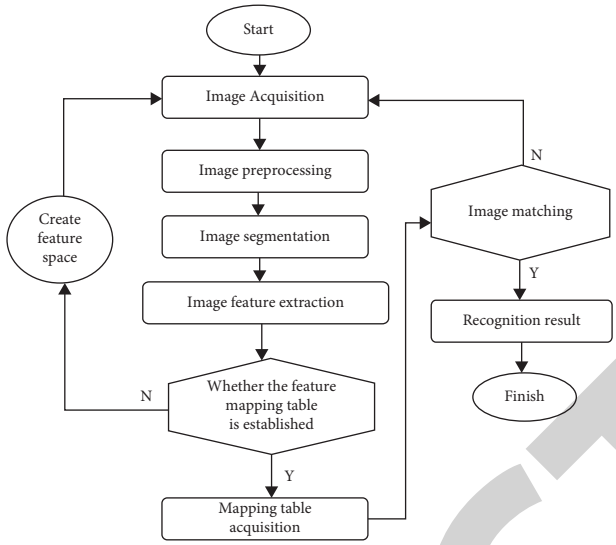

Figure 6: Image processing module software design flow.

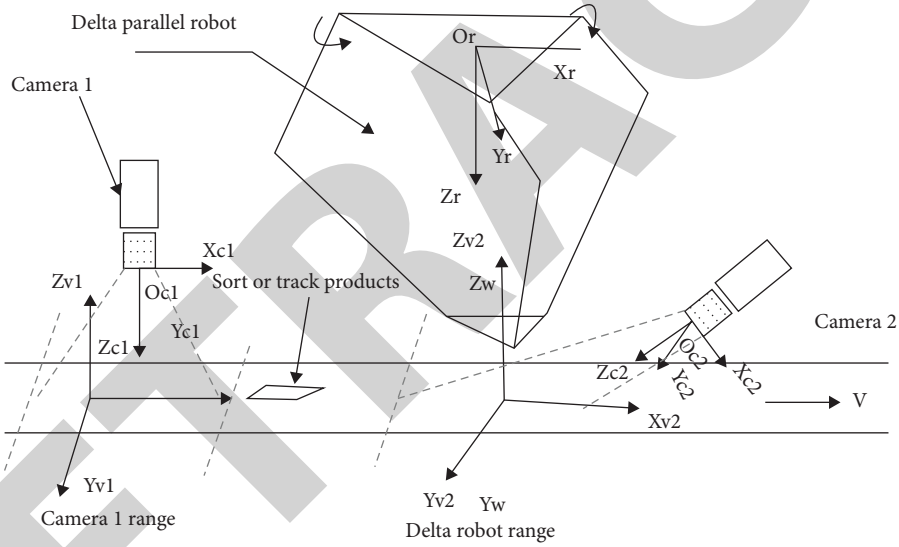

Figure 7: The relationship of the coordinate system of the man-machine control system.

It can be seen from Figure 7 that the position coordinates of a certain point $p(x_p, y_p, z_p)$ under the vision of camera No. 1 in the camera's vision area can be obtained by means of rotation and translation. If the transformation matrix from the coordinate system of camera 1 to the coordinate system of the field of view is R_{c1v1} and the translation vector is T_{c1v1}, then

$$V_{v1} = R_{c1v1}V_p + T_{c1v1}. \tag{2}$$

The industrial camera No. 1 uses point P in the coordinates, and the position coordinate formula of this point in the world coordinate system is shown in (2). Rotation coordinates are represented by R_{v1w}; translation vectors are represented by T_{v1w}.

$$V_w = R_{v1w}V_{v1} + T_{v1w}. \tag{3}$$

Similarly, for point P in the industrial camera No. 2, the position coordinates in its field of view and the rotation and translation conversion formula to the world coordinates are

$$\begin{aligned} V_{v2} &= R_{c2v2}V_p + T_{c2v2}, \\ V_w &= R_{v2w}V_{v1} + T_{v2w}. \end{aligned} \tag{4}$$

Similarly, for point P in the world coordinate system, its rotation plane formula in the machine coordinate system is as follows:

$$V_r = R_{wr}V_w + T_{wr}. \tag{5}$$

For the human-machine vision system and conveyor belt, the calibration between the robot itself and the conveyor belt is mainly based on the calculation of the abovementioned rotation matrices $R_{c1v1}, R_{c2v2}, R_{v1w}, R_{wr}$ and $T_{c1v1}, T_{c2v2}, T_{v2w}, T_{wr}$ based on the obtained data.

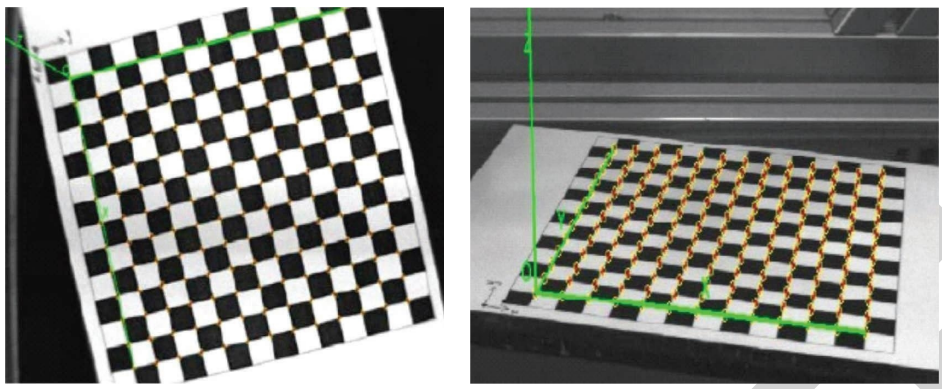

(a) (b)

Figure 8: Obtaining the calibration board coordinate system. (a) The coordinate system of the calibration plate obtained by the No. 1 camera; (b) the coordinate system of the calibration plate obtained by the No. 2 camera.

3. Calibration between the Target Images

3.1. Calibration of the Parameters between the Two Industrial Camera Coordinate Systems and the Field of View Coordinate System

3.1.1. Calculate the Plane Equation Corresponding to the Conveyor Belt in the Industrial Camera Coordinate System. As can be seen from Figure 8, place the calibration board at different positions in the field of view of the industrial camera to capture the image of the target, store the image at the same time, use the MATLAB calibration toolbox to read the saved internal parameter calibration, and then use the function of external parameter acquisition to calibrate the external parameters in each image. The acquisition of external parameter calibration is to use the coordinate system on the calibration board to obtain the coordinate system in the industrial camera through rotation and translation. Carry out plane fitting to the position coordinates of these origins and finally determine the plane equation where the calibration plate is currently located, as shown in Figure 8.

Based on the above working principles and experimental methods, the origin coordinates of the calibration coordinate system are shown in Table 6, when the grasping target collected by the industrial camera No. 1 is at 15 different positions, and the calibration board is obtained when the industrial coordinates of No. 2 are collected at 15 different positions. The coordinates of the origin under the coordinates are shown in Table 7.

By fitting the above data through MATLAB, the expressions of the field of view plane equations of the No. 1 industrial camera and the No. 2 industrial camera can be calculated:

$$\begin{aligned} 0.016802x - 0.007094y + z - 333.031718 = 0, \\ 0.009708x + 2.584124y + z - 511.581412 = 0. \end{aligned} \tag{6}$$

Table 6: The coordinates of the origin of the calibration board of the No. 1 industrial camera.

No.	X (mm)	Y (mm)	Z (mm)
1	−58.5264	−63.8011	333.5227
2	67.6947	41.3830	332.1067
3	37.7501	62.0916	332.6778
4	56.3415	48.2775	332.3378
5	−67.1456	−55.6965	333.7113
6	−44.3639	−73.2236	333.1287
7	−77.4116	−52.2072	333.8364
8	−47.7349	−74.0932	333.1775
9	41.0552	55.7552	332.6581
10	57.1042	45.3162	332.7124
11	37.0819	65.8596	332.9051
12	73.0015	59.5045	332.8345
13	−86.7054	−65.0509	333.8390
14	−86.7688	−58.1968	334.0540
15	−37.1688	−59.2738	333.4790

Table 7: The coordinates of the origin of the calibration board of the No. 2 industrial camera.

No.	X (mm)	Y (mm)	Z (mm)
1	−3.5967	16.4759	469.2558
2	−39.8526	16.4012	468.6889
3	−97.4704	16.5184	468.9079
4	92.1832	−25.9968	577.0119
5	3.7051	−25.7642	576.9291
6	−6.7059	30.0554	432.8186
7	−97.5993	30.4785	432.8319
8	−0.8004	13.3125	477.6422
9	−108.9302	13.9342	477.9089
10	−108.9306	14.8525	476.8875
11	107.6221	−14.8473	549.3964
12	18.2715	−14.4572	549.4243
13	122.1851	−28.2901	583.4863
14	13.0369	−28.2903	583.5664
15	−3.5967	−20.2878	563.0148

3.1.2. Coordinate System Establishment and Parameter Calibration. After obtaining the plane equation, assuming the intersection point $O - X_vY_vZ_v$ of the plane equation and the Z_v axis in the industrial camera coordinate system $Q(0, 0, q)^T$, $q_1 = 333.031718, q_2 = 511.581412$ can be calculated according to the expressions (3.31) and (3.32), and

then select one from the captured target image. The image of the calibration board is used as the reference image. Assuming that the external parameter corresponding to this image is (R_{vc}, T_{Vc}), R_{vc}, T_{Vc} in turn represents the rotation matrix and translation vector from the coordinate system of the calibration board to the coordinate system of the industrial camera. Select the Q point as the origin, the XY plane selects the transmission belt plane [13, 14], and construct the coordinate system $O_{v-}X_vY_vZ_v$ parallel to the X axis in the reference image, as shown in Figure 9. The $O-XYZ$ in the figure is the coordinate system of the calibration board corresponding to the reference image.

From the coordinate system of the industrial camera to the field of view coordinate system, the rotation matrix and parallel movement vector equation,

$$\begin{cases} R_{cv} = R_{vc}^{-1}, \\ T_{cv} = -R_{vc}^{-1}T_{vc}. \end{cases} \tag{7}$$

The coordinate reference image selected from the images collected by the industrial camera is Figures 10(a) and 10(b) in turn. Then, obtain the external parameters through MATLAB and obtain the formulas (8) and (9) of the conversion matrix of the industrial camera.

$$M_{v1c1} = \begin{bmatrix} R_{v1c1} & T_{v1c1} \\ 0 & 0 \end{bmatrix} = \begin{bmatrix} -0.0024 & 0.9998 & -0.0182 & 0 \\ 0.9999 & 0.0025 & 0.0082 & 0 \\ 0.0082 & -0.0182 & -0.9998 & 333.0317 \\ 0 & 0 & 0 & 1 \end{bmatrix}, \tag{8}$$

$$M_{v2c2} = \begin{bmatrix} R_{v2c2} & T_{v2c2} \\ 0 & 0 \end{bmatrix} = \begin{bmatrix} -0.9999 & -0.0126 & -0.0015 & 0 \\ -0.0061 & -0.3689 & -0.9294 & 0 \\ 0.0112 & 0.9294 & -0.3690 & 511.5814 \\ 0 & 0 & 0 & 1 \end{bmatrix}. \tag{9}$$

Then, the corresponding translation parameters from the industrial camera coordinate system to the field of view coordinate system can be derived from the expression (9), as shown in the formulas (10) and (11).

$$M_{c1v1} = \begin{bmatrix} R_{c1v1} & T_{v1c1} \\ 0 & 0 \end{bmatrix} = \begin{bmatrix} -0.0024 & 0.9999 & -0.0082 & -2.7444 \\ 0.9998 & 0.0025 & 0.0182 & 6.0739 \\ -0.0182 & -0.0082 & -0.9998 & 333.5135 \\ 0 & 0 & 0 & 1 \end{bmatrix}, \tag{10}$$

$$M_{c2v2} = \begin{bmatrix} R_{c2v2} & T_{v2c2} \\ 0 & 0 \end{bmatrix} = \begin{bmatrix} -0.9999 & 0.0061 & -0.0112 & -5.7148 \\ -0.0126 & -0.3689 & 0.9294 & -475.43949 \\ -0.0015 & -0.9294 & -0.3690 & 188.7874 \\ 0 & 0 & 0 & 1 \end{bmatrix}. \tag{11}$$

3.1.3. Parameter Calibration from the Industrial Field of View Coordinate System to the World Coordinate System. For the parameter calibration of the field of view coordinate system and the world coordinate system of the industrial camera, the conveyor belt is selected as the XY plane, and the space coordinate system is constructed according to the right-hand rule. Therefore, the coordinate system between the field of view coordinate system and the world coordinate system of the industrial camera can be regarded as the change between the two-dimensional plane coordinate system as shown in Figure 11. In the figure, $O_{v1-}X_{v1}Y_{v1}$ is the field of view coordinate system 1 corresponding to the No. 1 industrial camera; $O_{v2-}X_{v2}Y_{v2}$ is the field of view coordinate system 2 corresponding to the No. 2 industrial camera. $O_{w-}X_wY_w$ is the world coordinate system, in which O_{v2} and O_w overlap.

It can be seen from Figure 11 that assuming that O_{v1} moves vector $T_{v1w} = [a, b, 0]^T$ relative to the world coordinate system, the conversion matrix from the field of view coordinate system of the industrial camera to the

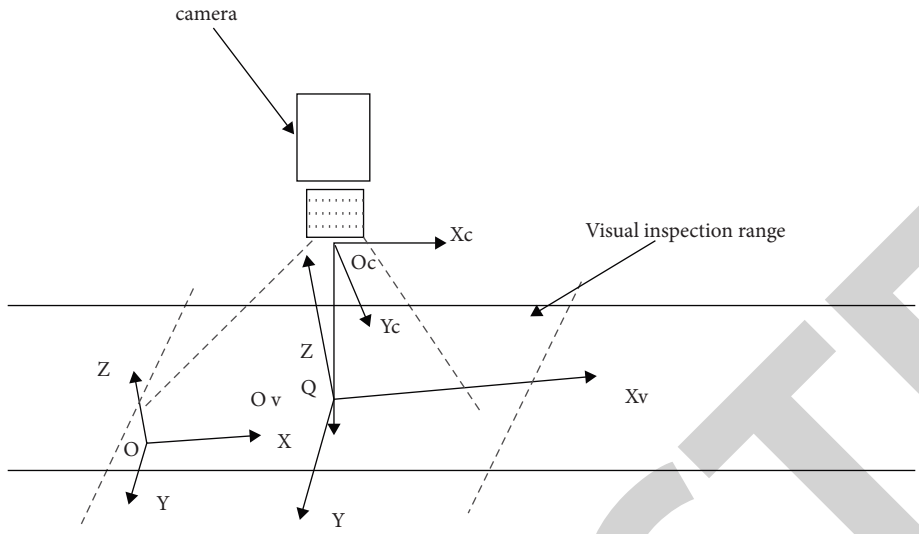

Figure 9: The relationship between the camera coordinate system and the field of view coordinate system.

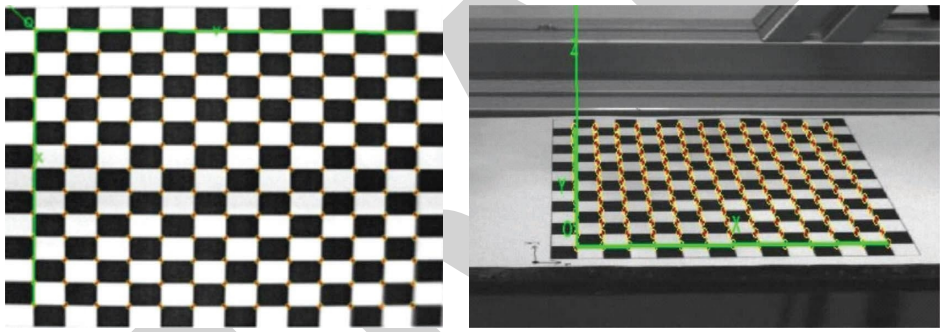

(a) (b)

Figure 10: Reference coordinate system image. (a) The reference coordinate system image of camera 1; (b) the reference coordinate system image of camera 2.

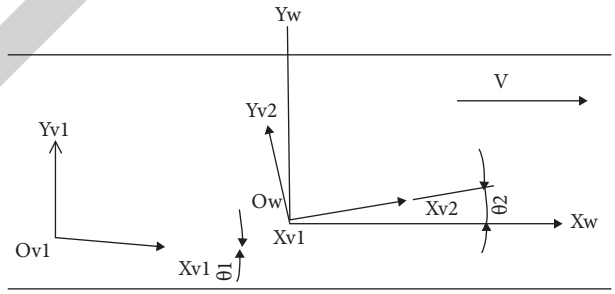

Figure 11: Conversion relationship between the field of view coordinate system of the industrial camera and the world coordinate system.

world coordinate system can be expressed by following formula:

$$M_{v1w} = \begin{bmatrix} R_{v1w} & T_{v1w} \\ 0 & 0 \end{bmatrix} = \begin{bmatrix} \cos\theta_1 & \sin\theta_1 & 0 & a \\ -\sin\theta_1 & \cos\theta_1 & 0 & b \\ 0 & 0 & 1 & 0 \\ 0 & 0 & 0 & 1 \end{bmatrix}. \quad (12)$$

Then, the matrix transformed from the field of view coordinate system 2 of the industrial camera to the world coordinate system is as follows:

$$M_{v2w} = \begin{bmatrix} R_{v2w} & T_{v2w} \\ 0 & 0 \end{bmatrix} = \begin{bmatrix} \cos\theta_2 & \sin\theta_2 & 0 & 0 \\ -\sin\theta_2 & \cos\theta_2 & 0 & 0 \\ 0 & 0 & 1 & 0 \\ 0 & 0 & 0 & 1 \end{bmatrix}. \quad (13)$$

The θ_1 and θ_2 in expressions (3.33) and (3.34) are the angles at which the field of view coordinate system of the corresponding industrial camera rotates with the Z axis as the center by the right-hand rule and then coincides with the world coordinate system. Therefore, as long as θ_1, θ_2, and T_{v1w} can be calibrated, the parameters of the corresponding transformation matrix can be obtained. The calibration process in this article is to place a positioning plate at the front of the conveyor belt and then place the target ball of the laser tracer on the positioning plate, locate as shown in Figure 12.

The image is collected by the industrial camera; use MATLAB to read the corresponding parameters in the industrial camera and then refer to the translation vector calibrated by the internal parameters; then, the industrial coordinate system corresponding to the origin of the coordinate system established by each calibration board can be obtained coordinate. Images of two calibration plates was taken by the same industrial camera at different positions; the angle formed by the line of the origin position coordinates of the corresponding calibration plates at different positions and the field of view coordinates of the industrial camera is the θ angle to be calibrated. As shown in Figure 13, the $O_{v-}X_vY_v$ and $O_{v-}X_v'Y_v'$ in the figure both transform the field of view coordinates of the industrial camera to the coordinate system of the origin of the calibration plate in the current image.

The corresponding coordinates of O_v and O_v' obtained by calibration under the coordinates of the industrial camera are V_c and V_c' in turn. Then, the formulas (12) and (13) can be transformed into the field of view coordinates. Assume that the transformed coordinates are V_v and V_c', satisfying both $V_v = (x_v, y_v, 0)^T$ and $V_v' = (x_v', y_v', 0)^T$. Then, the formula for the angle between the field of view coordinate system and the world coordinate system is as follows:

$$\theta_{vw} = \arctan\left(\frac{y_v' - y_v}{x_v' - x_v}\right). \quad (14)$$

From the results of the above calibration, combined with the transition coordinate system $O_{t-}X_tY_t$ in Figure 14, the

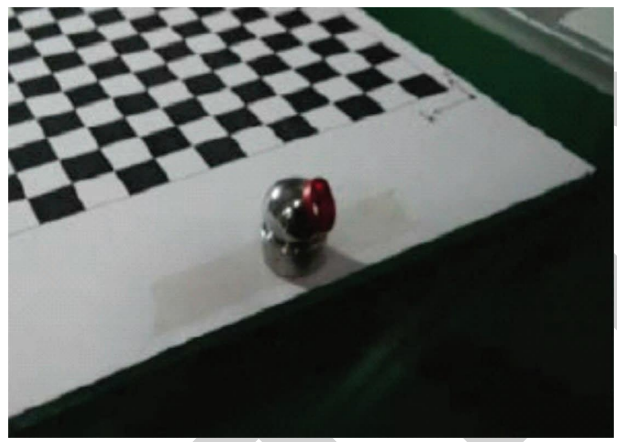

Figure 12: The placement of the target ball on the calibration plate.

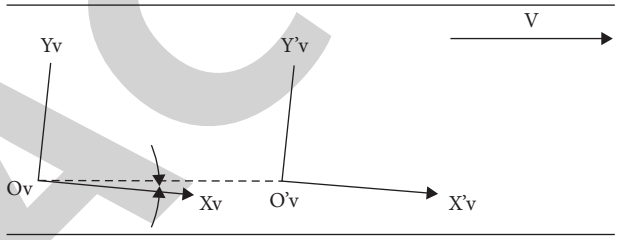

Figure 13: The rotation angle from the visual coordinate system to the world coordinate system.

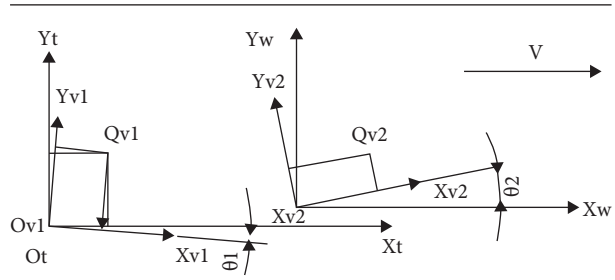

Figure 14: Schematic diagram of translation between the field of view coordinate system 1 and world coordinate system.

total length of the line segment $o_{v1}o_{v2}$ can be obtained by calculating the coordinates of the two points Q_{v1} and Q_{v2} obtained by laser tracking detection. The position coordinates of Q_{v1} and Q_{v2} corresponding to the industrial camera can be solved, and then, they can be transformed into corresponding field of view coordinates 1 and field of view coordinates 2 by formula (13) and formula (14).

According to Figure 14, Q_{v1} and Q_{v2} can be transformed into the corresponding coordinate system of $O_{t-}X_tY_t$ and $O_{w-}X_wY_w$. In addition, the position coordinate in the coordinate system is the position coordinate $Q_{v1}O_{t-}X_tY_t(x_1, y_1, 0)Q_{v2}O_{w-}X_wY_w(x_2, y_2, 0)$ in the coordinate system; then, the formula (15) of the translation

vector $T_{v1w} = (a, b, 0)^T$ can be obtained. Among them, S represents the distance measured by laser tracking.

$$T_{v1w} = \begin{bmatrix} a \\ b \\ 0 \end{bmatrix} = \begin{bmatrix} s + x_1 - x_2 \\ y_1 - y_2 \\ 0 \end{bmatrix}. \tag{15}$$

According to the above method and working mechanism, the two points corresponding to the field of view of the No. 1 and No. 2 industrial cameras on the calibration board were measured in order of 10 sets of experimental values in the industrial coordinate system, as shown in Table 8. The s value of the corresponding line segment $Q_{v1}Q_{v2}$ is shown in Tables 9 and 10.

According to formulas (13–15), the angle $\theta_1 = 3.136522$rad that the industrial camera No. 1 rotates around the Z axis and transforms to world coordinates is solved, and the angle $\theta_{12} = -0.012518$rad that the industrial camera No. 2 rotates around the Z axis and transforms to the world coordinates is solved. From formula (14) and Table 10, the translation vector $T_{v1w} = (629.942\text{mm}, -5.816852\text{mm}, 0)^T$ of the field of view coordinate system of the industrial camera No. 1 relative to the world coordinate system can be solved, and the corresponding conversion formula is as follows:

$$M_{v1w} = \begin{bmatrix} R_{v1w} & T_{v1w} \\ 0 & 1 \end{bmatrix} = \begin{bmatrix} -0.9999 & 0.0051 & 0 & 629.9424 \\ -0.0051 & -0.9999 & 0 & -5.8169 \\ 0 & 0 & 1 & 0 \\ 0 & 0 & 0 & 1 \end{bmatrix},$$

$$M_{v2w} = \begin{bmatrix} R_{v2w} & T_{v2w} \\ 0 & 1 \end{bmatrix} = \begin{bmatrix} -0.9999 & 0.0125 & 0 & 0 \\ 0.0125 & 0.9999 & 0 & 0 \\ 0 & 0 & 0 & 1 \\ 0 & 0 & 0 & 1 \end{bmatrix}. \tag{16}$$

4. Experiment and Result Analysis

4.1. Mean Filtering and Binarization to Obtain the Target Image. Binarization of the obtained target image is the basis for the completion of target recognition and location positioning. However, the acquisition of the target image is mainly affected by many factors such as brightness, sensor accuracy, conveyor belt movement deviation, and so on. It is necessary to perform necessary filtering processing on the target image to be acquired and then perform image binarization.

$$g(x, y) = \frac{1}{9} \sum_{i=-1}^{1} \sum_{j=-1}^{1} f(x + i, y + j). \tag{17}$$

At the same time, in this article, to avoid the problem of unclear image caused by the noise interference of the average filter processing of the target image, the pixel value of the filtered image is compared with the slot value of the original image, and the slot value of the two is compared. The gray value of the image is determined by the size of the image. Assuming that it represents a filtered target image, T represents a nonnegative gap value determined during the actual processing, as shown in equation (18). $g'(x, y)$

$$g'(x, y) = \begin{cases} g(x, y), & |f(x, y) - g(x, y)| < T, \\ f(x, y), & \text{others.} \end{cases} \tag{18}$$

When the filtered image is binarized, Figure 15 is obtained. It can be seen from the analysis of Figure 15 that the target area processed by the above method is clearly visible.

4.2. Obtain the Connected Area of the Target Image. The acquisition of the connected area of the image mainly marks the pixels of the same area uniformly so that this area can be distinguished from different areas, which helps to accurately identify the target in the area and accurately locate it. At present, there are many methods to extract the connected domain of a region. In this article, we use the extraction algorithm of the target connected domain based on route coding. This method only needs a Run Lengthrun-length list and an array, and sorts all courses according to the rules of 8 area connectivity to realize the rapid extraction of the connected areas of the target image.

To implement this Algorithm 1, you need to build a linked list pointer pRunLenth and an integer array. If there is an array of N length, in terms of run length, the data structure that can be used to describe is as follows:

Define the size of the target image $M \times N$, and M represents the width value of the target image and N represents the height value of the object image, which can be the coordinates of each scanned image. The integer variable uses pTemp to indicate the tentative route pointer, pCur to indicate the current route pointer, and pPer to indicate the previous route pointer. $(i, j)1 \le i \le N, 1 \le j \le Mk = 0$ is initialized to NULL in turn.

Complete the forward loop of the path connection table through the temporary path pointer and find the path up to the sequence number of the previous row. Next, referring to equation (19), the connection status is obtained. The equation R represents the number of the previous row, and m represents the m-th row from the right to the left of the previous row. At the time of $p\text{Temp}(i-1)$, the m-th route representing the previous row was connected to the route at that time. At that time, it indicated that the m-th route forward was inconsistent with the route at that time. con = 1con = 0.

$$\text{con}_R^m = \begin{cases} 1 \quad \text{if} \begin{cases} p\text{Cur} -> i\text{Start} < p\text{Temp} -> i\text{Start} - 1 \\ p\text{Cur} -> i\text{End} \ge p\text{Temp} -> i\text{End} - 1 \end{cases}, \\ 1 \quad \text{if} \begin{cases} p\text{Cur} -> i\text{Start} \ge p\text{Temp} -> i\text{Start} - 1 \\ p\text{Cur} -> i\text{End} \le p\text{Temp} -> i\text{End} - 1 \end{cases}, \\ 0 \quad \text{others}. \end{cases} \tag{19}$$

Table 8: The value of the origin of the calibration plate in the coordinates of the No. 1 camera.

No.	x_c (mm)	y_c (mm)	z_c (mm)	x_c' (mm)	Y_c' (mm)	z_c' (mm)
1	−86.6224	−72.6984	333.3297	−86.7652	−58.1956	333.4254
2	−36.9902	−73.2582	333.4086	−37.1864	−59.2267	333.4564
3	−64.5139	−72.3965	333.7712	−64.7162	−57.3053	333.7012
4	−64.5512	−69.4667	333.7544	−64.6978	−58.6447	333.6302
5	−56.6054	−65.0509	334.0392	−56.7688	−58.1967	334.1542
6	−62.6211	−69.7435	333.2318	−62.7652	−59.2307	333.6246
7	−40.9992	−73.3284	333.9277	−40.1864	−57.4520	334.0492
8	−47.3179	−72.4622	332.9116	−47.4912	−57.3053	332.8636
9	−64.5211	−68.4372	333.7354	−64.6978	−58.2457	333.5367
10	−57.9371	−65.1032	334.4129	−58.1033	−58.1258	334.3489

Table 9: The origin of the calibration plate is in the 2 coordinates of the camera coordinate system.

No.	x_c (mm)	y_c (mm)	z_c (mm)	x_c' (mm)	y_c' (mm)	z_c' (mm)
1	124.0278	−20.1911	562.8838	23.7506	−19.5010	562.7106
2	76.6957	−19.8503	562.5072	12.6459	−19.4482	562.7851
3	110.6445	−22.7152	569.2870	49.5486	−22.5250	568.9284
4	94.5216	−22.7004	569.2402	21.0217	−22.3834	569.2005
5	119.8074	−21.2764	565.6998	40.6902	−20.9663	565.2179
6	87.7754	−21.0871	565.2967	17.7723	−20.8018	565.5518
7	114.7105	−29.6973	568.3270	48.0342	−29.3628	585.6951
8	85.5459	−29.4951	585.7893	14.1057	−29.2997	586.911
9	105.5589	−11.8971	541.4459	58.0852	−11.5703	541.2335
10	81.7106	−11.6781	541.1936	32.2806	−11.4452	541.4320

Table 10: Origin coordinate and its relative length.

No.	x_c (mm)	y_c (mm)	z_c (mm)	x_c' (mm)	y_c' (mm)	z_c' (mm)	S (mm)
1	−64.702	−62.968	333.487	67.101	−21.201	566.557	624.335
2	−58.063	−61.921	333.323	97.346	−18.863	599.971	593.062
3	−64.572	−57.837	333.538	88.254	−21.287	566.146	598.066
4	−51.712	−62.173	333.094	73.749	−19.013	599.997	617.473
5	−54.201	60.151	333.367	100.782	−19.981	562.242	596.688
6	49.874	60.151	332.571	−102.48	19.102	463.207	669.958
7	54.670	63.243	332.627	−15.624	20.667	458.327	580.132
8	50.103	60.801	332.587	−27.323	19.001	462.746	595.687
9	62.186	51.134	332.424	−43.846	23.582	451.062	620.383
10	63.824	49.764	332.060	−35.155	23.930	450.078	613.355

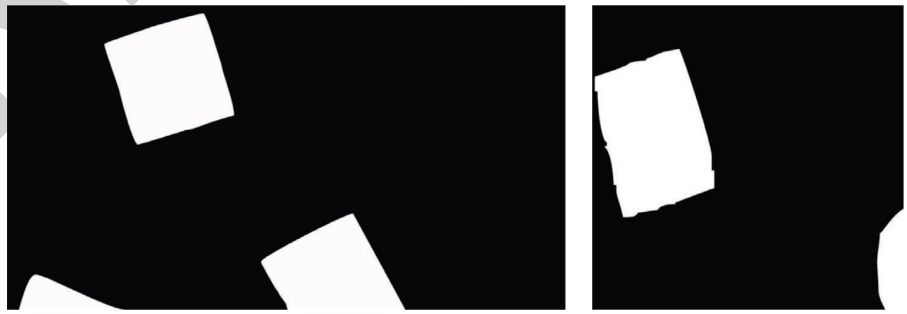

(a) (b)

Figure 15: The effect of target image binarization. (a) The image processed by the No. 1 camera; (b) the image processed by the No. 2 camera.

```
typedef struct tagRunLength
{
   int* pLable; //Pointer to the storage address of the label
   int iRow; //Current scan line number
   int iStart; //Run start column number
   int iEnd; //End of the run number
   tagRunLength* pForward; //Pointer to the previous run
   tagRunLength* pNext; //Pointer to the next run
}RunLength;
```

Algorithm 1: Data structure.

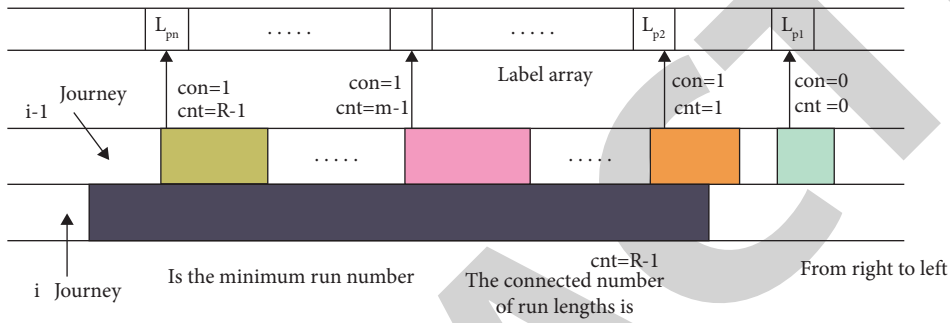

Figure 16: Connected domain processing of the target image.

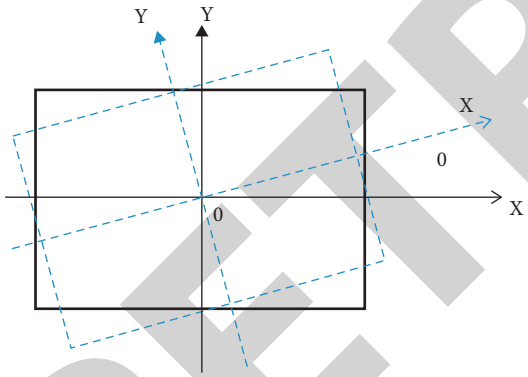

Figure 17: The angle between the smallest bounding rectangle and the regular posture.

The pCur of the current line number (i), the connected number of the pointing line can be expressed as $(i-1)$

$$\mathrm{cnt}_i = \sum_{m=0}^{R} \mathrm{con}_R^m. \tag{20}$$

For the previous line of $(i-1)$ according to the right-to-work traversal mode, refer to the expression 4.3 to judge the connectivity and calculate the run-length connectivity Cnt_i and its corresponding best sequence number $L\mathrm{min}$ according to the expression 23, as shown in Figure 16. When the number of connections of the route is satisfied, proceed to step 6. If the number of consecutive routes is satisfied, proceed to step 1.

Through the processing of the target image through the above steps, different connected domains in the image are, respectively, labeled differently.

4.3. Operation of the Smallest External Rectangle in the Connected Domain of the Image. The smallest bounding rectangle in the connected domain can not only be used to derive the rectangular degree of the target but also can be used to solve the target's position and posture θ (position and posture refers to the angle between the smallest bounding rectangle and the smallest outer rectangle of a specific posture value) as shown in Figure 17. Among them, the black solid line in the figure represents a regular posture, and the blue dashed line represents the minimum bounding rectangle of the target. This study adopts the method of constructing the rotation under the coordinates based on the center of the connected area of the image in the extraction of the smallest rectangle (Figure 17).

Assume that Si represents the minimum circumscribed rectangle of a specific posture in the established coordinate system $O - X_i Y_j$ and θi represents the rotation angle of the current coordinate relative to the coordinate system $O - X_i Y_j$. Then, the extraction process of the smallest bounding rectangle is as follows:

(1) In the initial stage, construct the coordinate system shown in Figure 18 based on the center of the target and calculate the minimum circumscribed rectangle and the corresponding area of the rectangle shown in Figure 18 that are parallel to the X axis and Y axis

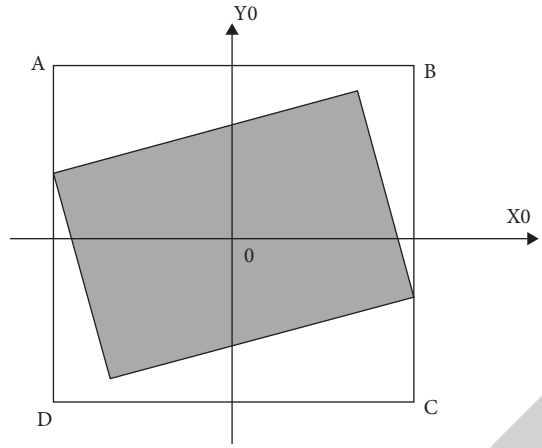

Figure 18: The circumscribed rectangle of the connected domain.

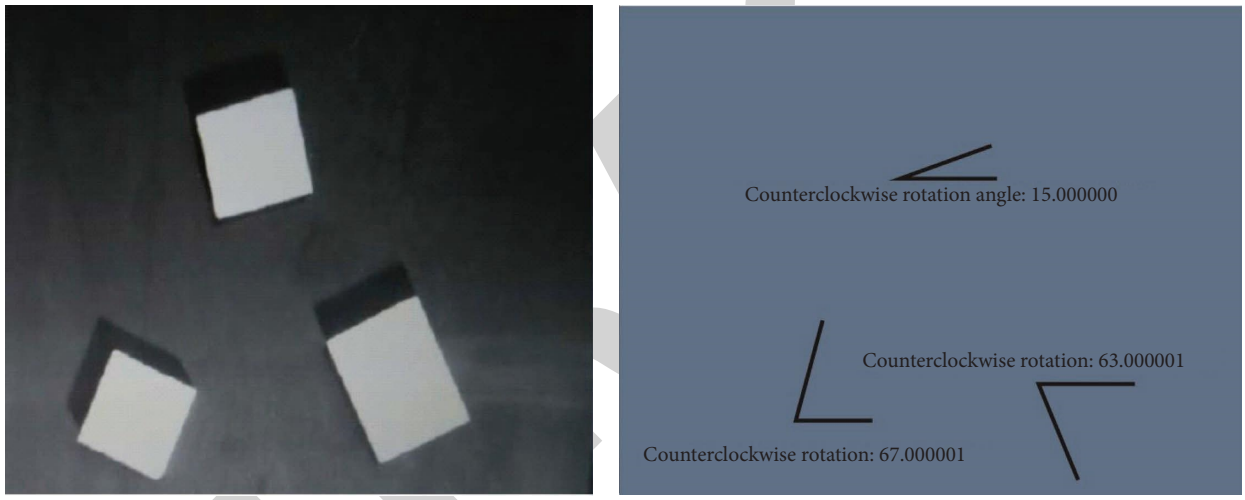

(a) (b)

Figure 19: Rotation angle detection of the target. (a) Target object on the conveyor belt; (b) detected rotation angle.

(2) Compared with the previous rotating coordinate system, the current rotating coordinate system has increased by an angle $\Delta\theta$. At the same time, calculate the corresponding minimum bounding rectangle and its area $S1$ after the rotation, and then, compare with the previous minimum area and mark the smallest of the two as $S_{\min}$. Also, the current rotation angle of $S_{\min}$ in the $O - X_i Y_j$ coordinate system is recorded as θi.

(3) Repeat step (2), always when the accumulated angle rotation exceeds the $180^\circ - \Delta = \Delta\theta$ result minus 900 to obtain the rotation angle of the corresponding regular posture, as shown in Figure 19.

5. Conclusions

As a new image processing and analysis algorithm that has gradually emerged in recent years, artificial intelligence technology can be used for the processing and analysis of image data processing in human-computer collaborative visual design. The data use different algorithms or perform multiple processing operations on the image under different conditions, and the operation results obtained by the processing operations are selected by appropriate methods to optimize the data processing and obtain the best results. This study introduces the image processing technology support system in the human-machine collaborative vision design and completes the hardware design and software design of the system's various functional modules. The experimental results show that the robot has image collection and recognition functions, which improves the robot's intelligence level.

Data Availability

The data used to support the findings of this study are available from the corresponding author upon request.

Hindawi
Journal of Electrical and Computer Engineering
Volume 2024, Article ID 9765875, 1 page
https://doi.org/10.1155/2024/9765875

Retraction

Retracted: Multimedia Vision Improvement and Simulation in Consideration of Virtual Reality Reconstruction Algorithms

Journal of Electrical and Computer Engineering

Received 23 January 2024; Accepted 23 January 2024; Published 24 January 2024

This article has been retracted by Hindawi following an investigation undertaken by the publisher [1]. This investigation has uncovered evidence of one or more of the following indicators of systematic manipulation of the publication process:

(1) Discrepancies in scope

(2) Discrepancies in the description of the research reported

(3) Discrepancies between the availability of data and the research described

(4) Inappropriate citations

(5) Incoherent, meaningless and/or irrelevant content included in the article

(6) Manipulated or compromised peer review

The presence of these indicators undermines our confidence in the integrity of the article's content and we cannot, therefore, vouch for its reliability. Please note that this notice is intended solely to alert readers that the content of this article is unreliable. We have not investigated whether authors were aware of or involved in the systematic manipulation of the publication process.

In addition, our investigation has also shown that one or more of the following human-subject reporting requirements has not been met in this article: ethical approval by an Institutional Review Board (IRB) committee or equivalent, patient/participant consent to participate, and/or agreement to publish patient/participant details (where relevant).

Wiley and Hindawi regrets that the usual quality checks did not identify these issues before publication and have since put additional measures in place to safeguard research integrity.

We wish to credit our own Research Integrity and Research Publishing teams and anonymous and named external researchers and research integrity experts for contributing to this investigation.

The corresponding author, as the representative of all authors, has been given the opportunity to register their agreement or disagreement to this retraction. We have kept a record of any response received.

References

[1] J. He, "Multimedia Vision Improvement and Simulation in Consideration of Virtual Reality Reconstruction Algorithms," *Journal of Electrical and Computer Engineering*, vol. 2022, Article ID 4968588, 10 pages, 2022.

Hindawi
Journal of Electrical and Computer Engineering
Volume 2022, Article ID 4968588, 10 pages
https://doi.org/10.1155/2022/4968588

Research Article

Multimedia Vision Improvement and Simulation in Consideration of Virtual Reality Reconstruction Algorithms

Jing He

College of Artificial Intelligence and Big Data, Chongqing Industry Polytechnic College, Chongqing, China

Correspondence should be addressed to Jing He; hejing@cqipc.edu.cn

Received 4 January 2022; Accepted 6 April 2022; Published 12 May 2022

Academic Editor: Muhammad Rashad

Due to the large noise and many discrete points of the image in the traditional image reconstruction process, the reconstruction quality of the image deviates greatly from the actual target. In this study, the virtual reality reconstruction algorithm is applied to multimedia vision, the virtual reality image is corrected by using the binocular offset positioning method, the denoising process is performed in the image reconstruction process, and the high-pass filter matrix is used to improve the image reproduction. At the same time, the three-dimensional reconstruction algorithm is used to perform correlation retrieval, the ensemble point set and the discrete point set are obtained, the maximum and minimum reconstruction degree areas are clarified, and the deviation reconstruction and peak relocation can be performed. Finally, the experimental test results show that the algorithm in this study can enhance the authenticity of image reconstruction, improve the accuracy of image corner detection, and effectively reduce the noise interference in the process of reconstructing the image.

1. Introduction

Multimedia virtual reality technology, as the most concerned image processing method, at present, can visually simulate images and use sensor equipment to complete the reconstruction of images of the target object, etc., to ensure that it can obtain visual data information in a specific environment, giving the experiencer this kind of personal experience, and while interacting with the virtual reality environment, it gives people more room for imagination [1, 2]. The so-called virtual reality is a virtual environment created by using digital technology. It creates a virtual environment and an imaginary world that cannot be felt in real life to resemble the real world and can also bring multiple perceptions such as vision, hearing, touch, and smell to the audience. What is created is a new three-dimensional perception experience, and the audience needs to use a display or data glove tool to experience the virtual world. The virtual reality reconstruction computing method has brought a new visual world to the audience. The current application of this method to many fields is a new development trend. The traditional multimedia visual form is that the audience follows the lens to experience, and the leading position of the work is the director [3]. The multimedia visual image is completely different from the traditional multimedia visual form. From the passive reception of information in the past to the current active reception, turning around is the dominant position of the work. The audience does not need to follow the lens to experience it but follow their own favorites. The visual perception and VR experience of people are different [4]. It can be seen that multimedia visual images are the future development trend of the film and television industry, and its technical characteristics and multimedia visual modes have brought new modes to the audience, allowing the images and the audience to interact.

The virtual reality reconstruction algorithm can effectively improve the accuracy of multimedia vision and the speed of image processing. Borrowing this algorithm can reduce the execution time of the algorithm. The average method can remove the interference of noise in the image reconstruction process to improve the accuracy of image reconstruction. On the basis of fully ensuring the quality of the reconstructed image, the robustness and feasibility of the enhanced algorithm will be widely used in all walks of life.

2. Basic Principles of Virtual Reality Reconstruction

The motion trajectory of the multimedia visual image is predicted in the reconstruction process, the motion trajectory is predicted and analyzed according to the image matching rule, similarity matching is performed on the feature points in the multimedia visual image, and the motion trajectory of the obtained search results is updated, in order to complete the purpose of multimedia visual image reconstruction.

T_i represents the i-th motion trajectory in the motion of multimedia visual images [5]. T_iDuring the movement of the multimedia visual image, T_i represents the coordinates corresponding to the target point in the current frame T_i (x, y). Age represents the total points of the audio track in the target action. Therefore, the following formula can be used to predict the motion trajectory of the multimedia visual image target:

(1) When age ≤2 is satisfied, then

$$\begin{cases} \Pr edX = x + (\text{Age} - 1)dx1, \\ \Pr edY = y + (\text{Age} - 1)dy1. \end{cases} \tag{1}$$

(2) When age >2 is satisfied, then

$$\begin{cases} \Pr edX = x + dx1 + (dx\ 1 - dx2), \\ \Pr edY = y + dy1 + (dy\ 1 - dy2). \end{cases} \tag{2}$$

In the formula, dx1 = x−LastX, dy1 = y−LastY; dx2 and dy2 respectively represent the coordinate position error values of the first two frames of the target track.

For the prediction points (PredX, PredY) of T_i corresponding to the motion trajectory of the kth frame of the moving target of the multimedia visual image, the target trajectory matching can be completed according to k+1 feature points in the search window corresponding to the region to obtain multimedia. The matching standard (X_p, Y_p) of the target motion trajectory of the visual image can represent the matching feature points of the target motion of the multimedia visual image as shown below.

Assuming that the target motion trajectory feature of the multimedia visual image actually exists, then it can be set as follows:

$$\begin{aligned} D_x^p &= X_p - \Pr edX\ , \\ D_y^p &= Y_p - \Pr edY\ . \end{aligned} \tag{3}$$

Then, the matching point of the motion trajectory corresponding to the multimedia visual image needs to meet

$$\left|D_x^p\right| \le \omega_x/2. \tag{4}$$

$$\left|D_y^p\right| \le \omega_y/2. \tag{5}$$

The ω_x and ω_y in the formula respectively indicate that the motion trajectory of the multimedia visual image can be searched in a short time. The prediction result suitable for the feature point of the motion track of the multimedia image is necessary for the corresponding coordinate value in the k+1 frame of the multimedia visual image. When there is a corresponding feature matching point, the target point of the multimedia visual image can be predicted by adding 1 to the matching value of T_i, and the motion track record is updated in time to complete the reconstruction of the multimedia visual image. The T_i operation expression is as follows:

$$\begin{aligned} &\left(D_x^p\right)^2 + \left(D_y^p\right)^2 = \min\left\{\left(D_x^m\right)^2 + \left(D_y^n\right)^2\right\}, \\ &m \in \left[0, \ldots, \pm \omega_x/2\right], n \in \left[0, \ldots, \pm \omega_y/2\right]. \end{aligned} \tag{6}$$

Assuming that the feature matching points corresponding to the above image reconstruction principles cannot be met, then (Pr edX, Pr edY) should be used as the corresponding coordinate value in the $k+1$ frame in the multimedia visual image.

According to the above analysis, we can deeply understand the basic principle of multimedia visual image motion trajectory reconstruction, according to this principle, the reconstruction of multimedia visual image can be quickly realized [6].

2.1. Characteristics of Multimedia Visual Images

Let the Audience Get a Real Sensory Experience in the Virtual World. If language is the main method of communication and the visual state of multimedia cannot control the sense of hearing and touch. The so-called multimedia vision is a state of reality and illusion that combines real feelings with concrete objects. It is not a code name to understand the expression of images. In other words, the illusory state is not an expression expounded by words. Users use the reorganization of illusory reality to understand the illusory world and feel the sensations brought by hearing, vision and touch. In multimedia visual works, users first experience sight and hearing, because multimedia visual works can mobilize human senses. At the same time, we should pay attention to the specific stories brought by the work itself. If the content of the work cannot touch the emotions of users, the experience of virtual reality will not be ideal. The content of a work cannot touch users, and even if the best media is used to express it, it cannot be confirmed by users. The images of multimedia visual works are different from previous images. In the past, the image is the sensory experience conveyed to the user. Multimedia visual images pay more attention to the

sublimation of user experience and emotion. Meredith Bricken is a reorganization method using illusory reality. If users can be substituted into the work, then this work is a success. This is the main feature of multimedia visual images, which express the connection between people and images, and a way of learning. For example, if the user chooses fish and birds in the illusory world, they can learn and acquire knowledge at the level of animals and experience the joyous world of animals.

Adjust the Photography Technology According to the Audience Experience. In multimedia visual works, users can freely adjust the angle according to personal preferences. From the user's point of view, in the early stage of shooting multimedia works, the most advanced technology is used to orderly shoot the works. Multimedia works not only express the viewing state of users but also a way of communicating with each other. Multimedia can be adjusted and updated at any time according to the user's hobbies, presenting the user's required works. However, this behavior of communicating with each other also takes away the user's ability to concentrate. For example, VR works will distract the audience's attention, and the result is that the audience does not want to face the director's camera. In other words, it is a story that can only be immersed in the illusory world but cannot touch the situation. When shooting multimedia visual works to avoid this shortcoming, the shooting team used a long lens to stagger the center of the stage, used stereo as the background, enhanced lighting and special effects to capture the user's eyes, and used vision and emotion to shoot the works. In the past filmmaking, it was the director's idea to use the camera's angle to carry out the filming from different angles, because the changes of multiple angles would make it impossible for users to teach and substitute into the plot of the story. Therefore, the director now uses special shooting methods and angles to replace the shots. The difference between multimedia visual images and traditional images is the audience's visual experience. VR uses characters that are immediately integrated into the work. According to the above analysis, the shooting methods of the two are also different. The multimedia visual images using the most advanced technology to shoot works can bring out the emotions of the works and can be adjusted according to the user's feelings at any time.

2.2. Traditional Visual Virtual Reality Reconstruction Algorithm

2.2.1. Phase-Correlated Three-Dimensional Stereo Matching. The multimedia visual phase correlation method can suppress the noise in the process of reconstructing the image, and the performance of the method is relatively moderate, which can optimize the virtual reality reconstruction method for the real simulation of the image [7]. The detailed operation steps of the algorithm are as follows:

If there are two sequences of multimedia visual images of the same type as f(n) and g(n), and the sizes are both represented by N, then the two corresponding discrete Fourier functions are expressed as follows:

$$F(k) = \sum_{n=-M}^{M} f(n) W_N^{kn} = A_F(k) e^{j\theta F(k)},$$
$$G(k) = \sum_{n=-M}^{M} g(n) W_N^{kn} = A_G(k) e^{j\theta G(k)}. \tag{7}$$

In the expression, $n = -M, \ldots, M$, $N = 2M + 1$, $W_N = e^{-j2n/N}$, the width of the multimedia image corresponding to $A_F(k)$ and $A_G(k)$, and the phase difference of the converted image between $e^{j\theta F(k)}$ and $e^{j\theta G(k)}$ can be expressed in a normalized manner.

$$\widehat{R}(k) = \frac{F(k)\overline{G(k)}}{|F(k)G(k)|} = e^{j\theta(k)}. \tag{8}$$

In the expression, $\overline{G(k)}$ is the expression of G(k) conjugate complex number, which satisfies $\theta(k) = \theta_F(k) - \theta_G(k)$, then the discrete Fourier inverse transformation function corresponding to $\widehat{R}$ is expressed as follows:

$$\widehat{r}(n) = \frac{1}{N} \sum_{n=-M}^{M} \widehat{R}(k) W_N^{-kn}. \tag{9}$$

If the sequence f(n) and g(n) of the multimedia visual image have a certain similarity, then the corresponding peak α can be obtained corresponding to the above expression, and the corresponding coordinate orientation is represented by δ, which means f(n) The relative offset corresponding to g(n) can quickly remove the visual deviation value between the two according to the peak feature, which can quickly and accurately realize the three-dimensional matching operation of the virtual reality image reconstruction.

2.2.2. Phase Correlation Visual Virtual Reality Reconstruction under the Mean Method. The use of the binocular offset positioning method is mainly to realize the correction of the reconstruction process of the multimedia visual image and at the same time can effectively maintain the corresponding baseline balance, as shown in Figure 1. Figure 1shows a schematic diagram of the visual virtual reality three-dimensional matching. So, the offset corresponding to the multimedia visual image can only appear on the epipolar line, and the calculation is performed in detail using the binocular offset positioning phase function to obtain the result of visual reconstruction. However, if the image illumination quality is poor, the accuracy of the matching method needs to be combined with the binocular offset positioning to improve the accuracy. At this time, the average method is used to ensure the authenticity of the image matching. The detailed operation process is shown in Figure 1.

It can be seen from Figure 1 that in a visual system for three-dimensional matching of multimedia visual images, L units of movement on the vertical axis corresponding to the sequence f(n) of the visual image can be performed to obtain $f_L(n)$ and the corresponding sequence. For $g_L(n)$, the corresponding phase correlation calculation can be performed for $f_L(n)$ and $g_L(n)$ to obtain $\widehat{r}_L(n)$, then its mean value can be expressed as follows:

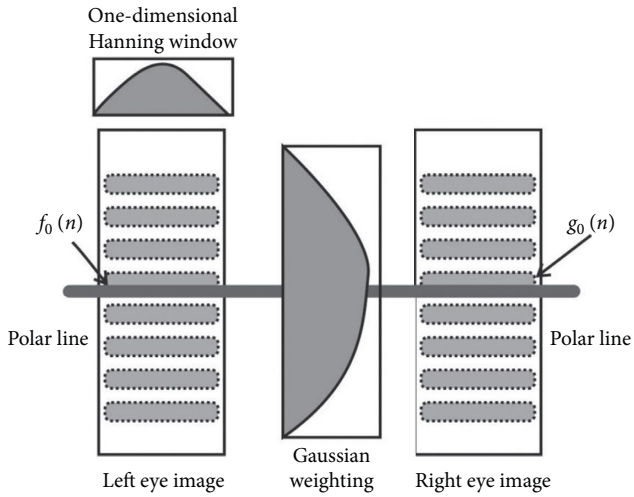

FIGURE 1: Visual virtual reality three-dimensional matching based on phase correlation.

$$\hat{r}_{ave}(n) = \frac{1}{2D+1} \sum_{L=-D}^{L=D} \hat{r}_L(n). \tag{10}$$

In the formula, $L = -D, \ldots, D$ and D are the reason for the relatively large change in the mean sequence. Then, 2D+1 is used as the total set corresponding to the mean sequence to obtain the coordinates of the peak α for effective stereo matching of visual deviation [8].

2.2.3. Three-Dimensional Matching Structure of Multimedia Visual Images. The process of multimedia visual image reconstruction is a kind of matching from coarse to fine, which can effectively improve the robustness of virtual reality algorithms, improve the resolution of the binocular structure corresponding to the multimedia visual image collection, and quickly find the corresponding matching points until the initial image resolution is improved, and the process is mainly as follows:

Multimedia visual simulation acquisition equipment uses images on both sides of the binocular and needs to be divided into resolutions according to multiple levels. At the same time, l max is used to complete the level-by-level matching. Among them, the image obtained in the first level of the multimedia visual image is represented by f_l, then the following expression can complete the expression of the upper level f_{l-1}:

$$f_{t-1}(x, y) = \frac{1}{4} \sum_{i=0}^{1} \sum_{j=0}^{1} f_{t-1}(2x + i, 2y + j). \tag{11}$$

In the above formula, when the correction is implemented, the multimedia visual image must maintain the parallel state of the epipolar lines, so the up and down shifts are considered. For example, in a device system based on landscape orientation, the starting point is $l = l$ max with the highest resolution.

The reference point in the left multimedia image can be expressed as $m = (m_1, m_2)$, then the corresponding azimuth coordinates in this area can be expressed by $(\lfloor 2^{-l\max} m_1 \rfloor, \lfloor 2^{-l\max} m_2 \rfloor)$, then for the image matching point corresponding to the right image of the multimedia vision, the azimuth coordinates in this area need to be fused, namely, $q_{l\max} = (\lfloor 2^{-l\max} m_1 \rfloor, \lfloor 2^{-l\max} m_2 \rfloor)$. Similarly at the $l = l$ max − 1 level, the point m calculates the set centered on the first level and the set centered on the corresponding point of the right image of the first level according to the coordinates of the first level direction, and if the lateral phase deviation is obtained, the corresponding azimuth coordinate point of the right image on the first level is $l = l$ max $- 1 m_l = (\lfloor 2^{-l} m_1 \rfloor, \lfloor 2^{-l} m_2 \rfloor)$ $(\lfloor 2^{-l} m_1 \rfloor, \lfloor 2^{-l} m_2 \rfloor) 2 q_{l+1} \delta_l q_l = (\lfloor 2^{-l} m_1 \rfloor, \lfloor 2^{-(l+1)} m_2 \rfloor + \delta_l)$. The above steps are repeatedly exercised to obtain accurate correction results. When I = 0, q=(m) can be obtained to achieve three-dimensional matching. Through the use of this algorithm, a sense of stereo matching can be achieved, and the positioning and analysis of special effects on the left side of the multimedia vision image will be applied to effectively improve the relative image matching pixels between the two [9].

Combined with the above-detailed analysis, it can be seen that the use of virtual reality algorithms can effectively improve multimedia vision in the image processing process. Due to the complex calculations, the current three-dimensional matching algorithms do not consider the impact of the surrounding environment. Then, the average value method is used to complete the calculation of sequence weights, and the resolution of multimedia visual images has been improved.

3. Improved Algorithm for Multimedia Visual Virtual Reality Reconstruction

3.1. Feature Extraction of Multimedia Visual Images. The feature extraction process of multimedia visual images is mainly based on the extraction of feature information of three-dimensional multimedia visual images, and at the same time, visual analysis is performed based on the changes in the characteristics of multimedia visual images. The value of the visual target is used to search for the three-dimensional coordinate value of the multimedia visual image. It is assumed that the projection of the multimedia geometry truly reflects the perspective transformation model, and the optimized conversion of the virtual reality algorithm is used to extract the characteristics of the multimedia visual dynamic image.

3.1.1. Feature Extraction of Visual Two-Dimensional Multimedia Target Image. After extracting the three-dimensional contour of the visual target, the target feature is obtained, which can segment the image and recognize the three-dimensional visual traveling image. The one-dimensional signal interval is extracted from the collected images along the contour of the visual walking image, and the maximum and minimum values of the obtained signal interval are used as the position points of the visual walking legs. The distance between these two points can be used as

the dynamics of the test object to reconstruct the feature vector. The two-dimensional coordinates obtained are as follows: $(c_1 z_1)$ represents the coordinates of the footing point, $(c_2 z_2)$ represents the coordinates of the knee joint, and $(c_3 z_3)$ represents the coordinates of the crotch, leaving the original visual two-dimensional multimedia target feature image described above.

3.1.2. Multimedia Visual Image Change Feature Generation. It is assumed that the equation of the multimedia geometric projection model formed by the keys in the visual dynamic image is as follows:

$$c_s = S(c). \tag{12}$$

In the formula, S(c) represents the key point $c = (c, z, v)$ in the multimedia environment to the two-dimensional image coordinate point in the two-dimensional target image. $c_s = (c_s z_s)$ represents the camera exchange, and the projection conversion model of the small hole camera can show the perspective conversion in the real environment model. There are object points, image points, and the origin of the coordinate system in the same two-dimensional multimedia plane, which are unified. The conversion model of the visual target can also be described by the three-dimensional target situation including c_s, c_o, and c. Different visual targets can produce a certain degree of collinearity, and the conversion formula is as follows:

$$p(c_s - c_o) = (c_o - c). \tag{13}$$

The formula converted from formula (5) is as follows:

$$p\left(\begin{pmatrix} c_s \\ z_s \\ 0 \end{pmatrix} - \begin{pmatrix} 0 \\ 0 \\ s \end{pmatrix}\right) = \begin{pmatrix} 0 \\ 0 \\ s \end{pmatrix} - \begin{pmatrix} c \\ z \\ s \end{pmatrix}. \tag{14}$$

According to formula (6), the expanded formula is as follows:

$$\begin{cases} p = \dfrac{v - s}{s} = \dfrac{s}{s} - 1, \\ c_s = -\dfrac{c}{s} = s\dfrac{c}{s - z}, \\ z_s = -\dfrac{z}{s} = s\dfrac{z}{s - z}. \end{cases} \tag{15}$$

In practical applications, $e_u(c_u, z_u, v_u)$ represents a point in the actual three-dimensional vision target image coordinate system after parallel movement and rotation and $e_g(c_g, z_g, v_g)$ represents a point corresponding to the camera coordinates in the multimedia camera. R represents the multimedia image coordinate point rotation conversion matrix, and E represents the multimedia image coordinate point parallel conversion matrix. Q indicates that the rotation matrix of the multimedia camera projects the camera coordinate points on the plane and obtains the point e(b, r) in the projection. The conversion formula is as follows:

$$\begin{bmatrix} U \\ Y \end{bmatrix} = Q\begin{bmatrix} C_u \\ Z_u \\ V_u \end{bmatrix} = Q\left[R\begin{bmatrix} C_u \\ Z_u \\ V_u \end{bmatrix} - E\right]. \tag{16}$$

Based on the key point data in the 3D visual target image, three conversion matrices of R, E, and Q can be obtained according to equation (18), where l represents the number of frames in the 2D multimedia visual image; $R_{l\times 3}$ ("I×3" is on the lower right side of "B") represents the matrix formed by rotation of the image per frame, and each element area in the matrix is broken down by the angle of the matrix rotation around c, z, and v axis; $E_{l\times 3}$ ("I×3" is on the lower right side of "E")represents the matrix formed by translation of the image per frame; the first row of $Q_{l3\times 2}$ ("3×2" is on the lower right side of "Q") represents the rotation of multimedia camera. The 3 element areas in the matrix are respectively rotated around each angle of c, z, v, axis; $P_{3\times 4}$ indicates that the 4 multimedia coordinate points are the original values of the shape points. Then, the calculation formula of the multimedia visual image feature after the optimization conversion of the nonlinear algorithm is as follows:

$$X_{sl} = \begin{pmatrix} R_{l\times 3} & E_{l\times 3} \\ P_{3\times 4} & Q_{3\times 2} \end{pmatrix}. \tag{17}$$

Multimedia Visual Image Motion Trajectory Feature Preprocessing. The acquired multimedia visual image is binarized, the image in the moving target is automatically updated, the adaptive threshold filtering method is used to realize the image processing, the multimedia visual image target motion trajectory to record is removed, and the three-dimensional visual image is extracted.

The moving targets in the acquired multimedia visual surveillance images are binarized [10]:

$$A_{k+1}(x, y) = \begin{cases} 1, \left[I_k(x, y) - G_k(x, y) > T_f\right], \\ 0, \text{else}. \end{cases} \tag{18}$$

Among them, $I_k(x, y)$ and $G_k(x, y)$ respectively represent the current image and background of the acquired multimedia visual moving target; T_f represents the binarization threshold.

By introducing an adaptive background update algorithm to adapt the background of the moving object image, it can effectively suppress the influence of the illumination and background changes of the multimedia visual image [11]. The calculation is shown as follows:

$$\alpha, \beta \in [0, 1]. \tag{19}$$

Based on the above reasoning, when the pixel location of the multimedia visual action image is the target, there is no need to replace the background by an autonomous update again. If the current pixel is not the target, then the relative pixel data of the multimedia visual action image need to be adjusted. Because the target action picture and natural environment noise in the multimedia visual monitoring picture come from the characteristics of the target itself, the

background needs to be updated by the autonomous threshold filtering operation:

$$T_S = S_{fst} \times \mu + S_{\text{end}} \times \sigma. \tag{20}$$

Among them, S_{fst} represents the maximum perimeter of the moving target in the multimedia visual image, S_{snd} represents the perimeter of the moving target second only to S_{fst}, and μ and s represent the weighting coefficients related to S_{fst} and S_{snd}, respectively.

$T_{\min}$ is set to indicate the minimum noise threshold in multimedia visual images:

$$S_{fst} > T_{\min}. \tag{21}$$

Then, formula (21)is executed, if

$$S_{fst} \le T_{\min}. \tag{22}$$

All multimedia visual images are not extracted as targets.

If the circumference of the i-th moving target of the multimedia visual image is greater than the threshold T_S, that is,

$$S_i > T_S. \tag{23}$$

The simulator prototype is extracted. Instead, it is thrown away.

3.2. Detail Texture Enhancement of Visual Images. In the case of using the phase correlation function for calculation, the target individual feature vector in the visual virtual reality reconstructed image has a great influence on the reconstructed data. If the target individual texture feature is assumed to be less, it is easy to produce errors, thereby increasing the reconstruction. The difficulty requires fine texture on the reconstructed image. Therefore, the superposition of high-frequency data in the selected image in the initial image can improve the texture characteristics of the original image and can improve the accuracy of the result.

In noise removal, for the image gray-scale sequence N in the reconstruction of visual virtual reality with x = P, the feature distribution in the edge region of the target individual is obtained, with the gray-scale conversion equation as follows:

$$\begin{aligned} S_c &= \left[S_0, S_1, \ldots, S_{Q-1}\right]_{\text{binary}} = \left[\sum_i^{Q-1} S_i \times 2^i\right]_{Dce}, \\ S_i &= \sum_j^{W\times W} I_x^j. \end{aligned} \tag{24}$$

Among them, Q is the number of gray scales in the vicinity of the target area, W is the conversion step size, and the denoising function is as follows:

$$\begin{aligned} x(k+1) &= Q_i(k)_x + w_i(k), \quad i = 1, 2, \ldots, m, \\ z(k) &= H_i(k)_x(k) + v_i(k), \quad i = 1, 2, \ldots, m. \end{aligned} \tag{25}$$

In the formula, $w_i(k)$ and $v_i(k)$ are the pixel noise in the edge area of the target individual. $Q_i(k)$ and $H_i(k)$ belong to a balanced distribution with a mean value of 0 and a variance of $S_i(k)$, and a fuzzy set $u = \{u_{ik}\}$ is constructed. Then, the feature decomposition of the texture is done to obtain the denoising output as follows:

$$\begin{aligned} I_{GSM} = I\left(C^N; D^N | s^N\right) &= \sum_{i=1}^{N} I\left(C_i; D_i | s_i\right) \\ &= \sum_{i=1}^{N} \left(h\left(D_i | s_i\right) - h\left(D_i | C_i s_i\right)\right) \\ &= \sum_{i=1}^{N} \left(h\left(g_i C_i + V_i | s_i\right) - h\left(V_i\right)\right). \end{aligned} \tag{26}$$

Taking into account the difference between the reconstructed image regions, $u^{(n)}(x, y, d)$ is used to describe the spatial texture feature information, the pixel gray interval is constructed in the gradient direction, and the iterative formula of the image denoising function is obtained:

$$\begin{aligned} u^{(n+1)}(x, y) &= u^{(n)}(x, y) + \delta u_1^{(n)}(x, y), \\ u_1^{(n)}(x, y) &= M\Delta_x u^{(n)}(x, y) + N\Delta_t u^{(n)}(x, y, d). \end{aligned} \tag{27}$$

The number of repeated steps is described as follows: Through the texture feature noise removal method, the impact on the image is reduced, and the improvement of the visual virtual reality reconstruction algorithm is realized $n = 1, 2, \ldots, T$.

Then, the image texture is enhanced, and (28) is used to perform high-pass filtering on the initial image, that is,

$$c(x, y) = \sum_{i=-n}^{n} \sum_{j=-m}^{m} f(i, j) g(x - i, y - j). \tag{28}$$

Here, f is the reconstructed initial image, c is the high-frequency region of feature selection, and g is a 3×3 hyperspherical matrix [12] as follows:

$$g = \begin{bmatrix} -1 & -1 & -1 \\ -1 & 8 & -1 \\ -1 & -1 & -1 \end{bmatrix}. \tag{29}$$

Then, the texture enhancement image f1 is obtained as follows:

$$f_1(x, y) = f(x, y) + c(x, y). \tag{30}$$

Among them, f1 is the texture image after detailed enhancement, f is the initial image, and c is the azimuth coordinates of the selected high-frequency region (x, y) image.

3.3. Improvement of Multimedia Visual Virtual Reality Reconstruction Algorithm. From the characteristics of the collected multimedia visual pictures, we study a reconstruction method of the illusory reality of the multimedia visual image based on the illusion reality reconstruction calculation, and at the same time, a model of the illusion reality reconstruction method is constructed. Using the

minimum value of the gradient projection target value, the gradient direction can be optimized to obtain the reconstructed visual image effect.

Assuming that the training 3D vision images form a sample set, the types of training 3D vision image sample sets are sufficient. In the j-th training 3D vision image sample set matrix, $J \in I^{\alpha-\beta}$ means the training 3D vision image sample dictionary and $\|g\|_1$ means in the j-th image The norm class of $J \in I^{\alpha}$; the norm of the j-th training three-dimensional visual image; m represents the visual image dictionary matrix; q, u represents the coefficient greater than zero, and the model formula based on the virtual reality reconstruction algorithm is as follows:

$$\min \|g\|_1 q.u.m = Jg + X_{sl}. \tag{31}$$

According to formula (9), it is necessary to determine the minimum value of $\|g\|_1$. The Newton's interior point blocking method is used to constrain the objective function with inequality, and the formula is as follows:

$$\begin{aligned} &\min \frac{1}{3}\|Jg - m\|_3^3 + \delta \sum_{k=1}^{n} o_k \\ &q.u. \longrightarrow -o_k \le g_k \le o_k, k = 1, \ldots, n. \end{aligned} \tag{32}$$

In the (g, o) region, according to the constraints of $-o_k \le g_k \le o_k$, the minimum value $(\dot{g}(\varepsilon), o(\varepsilon)), t \varepsilon n \in q[0, \infty)$ can be obtained, and the calculation formula of using the minimum interior point method to optimize the gradient direction is as follows:

$$\nabla^2 J_K(g, o) \cdot \begin{bmatrix} \Delta g \\ \Delta o \end{bmatrix} = -\nabla J_K(g, o) \in I^{2\alpha}. \tag{33}$$

Based on equation (11) to find the gradient direction, the gradient projection method is used to obtain the sparsely represented reconstructed visual image more quickly. The virtual reality reconstruction of 3D visual images is realized.

When the azimuth coordinates are known to search for the peak value, if a deviation occurs in the global search method, the relevance and restriction standards in the reconstruction level should be used to reduce the scope of the search and minimize the reconstruction deviation. It can be seen from the horizontal two-way restriction criterion that if the vertical error of the verification is close to 0, the vertical search interval needs to be reduced; when the multimedia visual image is processed for 3D reconstruction, the correlation of any reconstruction level can be used to shorten the horizontal search range [13, 14].

A low-pass filtering step is added to $\hat{r}(n_1, n_2)$ and then its peak value is calculated:

$$h(k_1, k_2) = \begin{cases} 1, |k_1| \le U_1, |k_2| \le U_2, \\ 0, \text{otherwise.} \end{cases} \tag{34}$$

Assuming that the horizontal and vertical quality inspection offset errors of multimedia visual images are relatively small, then the virtual reality reconstruction algorithm is used to ensure the accuracy of the offset calculation, especially when the data obtained have large deviations. The reconstruction structure of the image also cannot correct its normal function, but the limited area is relatively small, but it has not been reconstructed. Therefore, the values of U1 and U2 used can be used as the most ideal search values.

In the traditional reconstruction algorithm, the reconstruction process requires an evaluation and correction of the failure rate. However, there is an intermediate reconstruction process in the actual use situation, and the resulting incorrect reconstruction will cause the next resolution of the scene. At the same time, the selected method is mainly because the fixed threshold α_{th} is clearly compared with the peak α. However, the overall peak of each resolution has a large change, so more precise dynamic methods are used for determining the threshold α_{th}.

The peak α in any reconstruction level is statistically sorted and arranged into a set. Assuming that the edge of the restricted area of level 1 is the threshold α_{th}, then $q_l(m_l)$ can be calculated. If the phase correlation peak α is greater than or equal to the threshold α_{th}, it can be proved that the point is a gregarious point, that is,

$$\begin{aligned} q_{lc}(m_l) &= q_l(m_l), \\ d_{lc}(m_l) &= m_l - q_l(m_l). \end{aligned} \tag{35}$$

Suppose $\alpha < \alpha_{th}$, then it is proved that the point is a point away from the group, and the adjacent area 5× that does not contain the point is selected. For all points in the 5 intervals, a sequence is constructed by size, the middle value is taken, and it is defined as the d value of the point, which is as follows:

$$\begin{aligned} d_l'(m_l) &= \left(d_1^{med}, d_2^{med}\right), \\ q_l'(m_l) &= m_l - d_l'(m_l). \end{aligned} \tag{36}$$

Then, the phase correlation calculation is used to derive the new peak value. If $\alpha > \alpha_{th}$, then

$$\begin{aligned} q_{lc}(m_l) &= q_l'(m_l), \\ d_{lc}(m_l) &= m_l - d_l'(m_l). \end{aligned} \tag{37}$$

Otherwise, let $d_{lc}(m_l) = d_l'(m_l)$.

In the data obtained in the reconstruction of multimedia visual virtual reality, there are a small amount of allocation errors, which need to be conditionally restricted so that the subsequent three-dimensional model will not be affected, resulting in distortion of the visual virtual reality reconstruction image and reducing the real effect [9]. Some of its errors are limited through error reconstruction and peak relocation, but there are still a small number of errors that have not been filtered. Therefore, it is necessary to calculate the maximum and minimum depth values of the stereo model and determine its depth interval and threshold α_{th}, assuming that the corresponding reconstruction point is that the depth value is not within the determined interval, then it will not be output, and the reconstruction point $\alpha < \alpha_{th}$ will not be output at the same time.

The azimuth coordinate of the sample is set to be (x_l, y_l), the corresponding reconstruction point is (x_r, y_r), the peak

value is calculated to be α, and the bilateral disparity is $d = x_l - x_r$.

If $\alpha \geq \alpha_{th}$ and $d_{\min} < d < d_{\max}$ the relevant value is input into the 3D model, where $d_{\max}$ and $d_{\min}$ represent the maximum and minimum parallax values, respectively.

4. Simulation Data Analysis

4.1. Experimental Guidelines and Objects

4.1.1. Experimental Guidelines. In the background of the illusory reality reconstruction, the effect of the multimedia vision illusion reality reconstruction method is highlighted. The target trajectory of the multimedia vision picture can be used as a case, and the method in the literature is used to compare with the multimedia vision image reconstruction method in the illusion reality reconstruction method. The quasi-lateral conversion method of the virtual reality reconstruction rate RR obtained by comparing the above two calculation methods as follows:

$$M(\iota) = \frac{K_\iota}{K}. \tag{38}$$

In the formula. where K represents the total number of visual image samples in the test; M represents the number of visual image samples that are accurately reconstructed in the candidate samples.

4.1.2. Subject. The samples tested in the experiment are mainly ORL human motion visual images, a multimedia visual image database is constructed, and 500 visual images of ORL human motions are analyzed by comparing various algorithms. There are 50 people in total, and each person has 10 different actions and actions under different lights. The morphological visual image has a resolution of 112×92 and a gray scale of 256 levels. The test analysis was carried out using the RR evaluation form.

4.2. Experimental Results. In order to verify the comprehensive practicability of the proposed multimedia visual virtual reality reconstruction algorithm, a simulation is needed. The simulation environment is MATLA-BR2010a. The sample image used uses the C multimedia visual image M and the parameter of the simulated bilateral lateral balance system to correct the matching error to obtain more accurate system parameter information, as shown in Figure 2. Simultaneously, the simulation parameter values are as follows: the matching level $l_{\max}$ is 5, the window is 33×33, and the interval for setting the threshold α_{th} is 10%.

In order to compare the improved effect of the algorithm in this research, the image reconstruction algorithm of traditional literature [3] and the improved algorithm proposed in this research were used to reconstruct the sample image. The corner detection calculation results are shown in Figures 3 and 4:

The test results show that the virtual reality reconstruction method used in this study can detect the corner points of the sample image more effectively, and at the same time can more realistically describe the local maximum value of the multimedia visual image. Through comparative analysis, it can be seen that the use of image reconstruction methods in literature [3] has a small number of corner detections, which seriously affects the accuracy of multimedia visual image reconstruction.

Figure 2: Experimental sample.

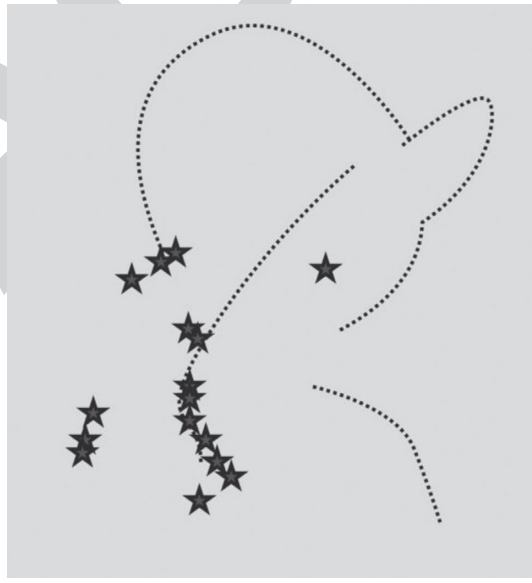

Figure 3: Document [3] algorithm.

The following further verifies the image reconstruction noise filtering effect of the research algorithm. The instrument used in the experiment is an oscilloscope. The greater the fluctuation of the waveform of the instrument interface, the greater the noise of the image and the lower its clarity, which reflects the reconstruction effects of different methods (Figures 5–8).

According to the analysis of the simulation results, it can be seen that the image reconstruction noise obtained by the traditional algorithm is too large, and the part of the image is fuzzy and unclear. The visual experience is poor, but

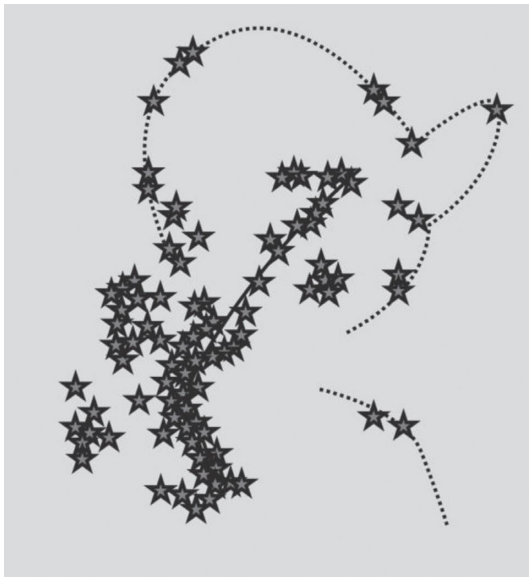

Figure 4: Research algorithm.

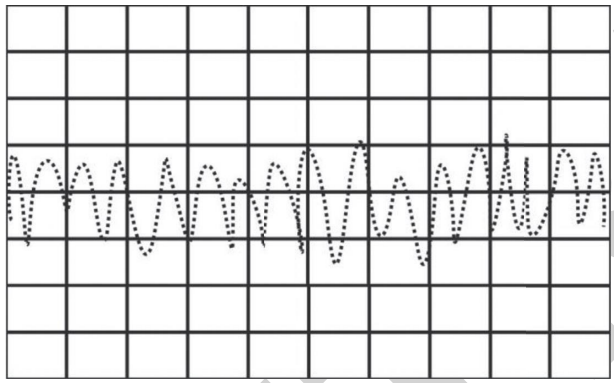

Figure 5: Original image noise.

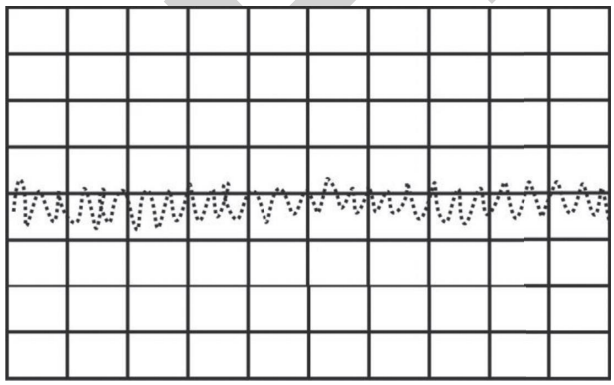

Figure 6: The noise effect after image reconstruction under the algorithm of literature [3].

applying the virtual reality reconstruction method to the process of multimedia visual reconstruction can effectively suppress noise interference, effectively improve the quality of multimedia visual image reconstruction, enhance the

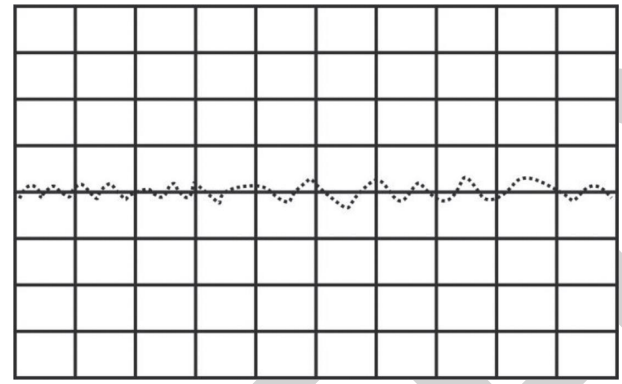

Figure 7: The noise effect after image reconstruction under the algorithm of literature [4].

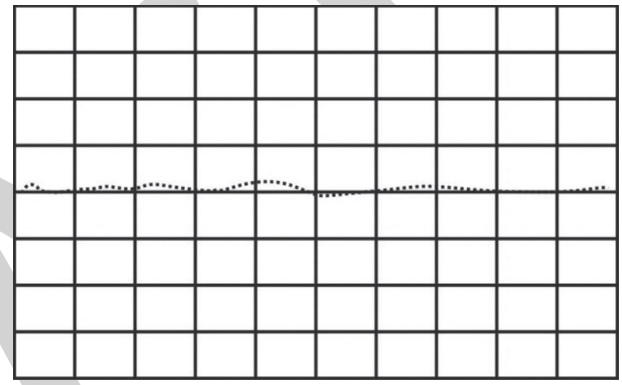

Figure 8: Research algorithm image reconstruction noise.

authenticity of the image, and promote the real visual experience of the user in virtual reality.

5. Conclusion

Based on the analysis of traditional algorithms, it is proposed to apply the virtual reality reconstruction algorithm to the simulation test of multimedia vision. Under the condition of ensuring the authenticity of the original image, the structure of the image can be optimized, and the peak value of the image can be efficiently performed according to the matching level. The threshold model of reconstructed image is retrieved and constructed, the accuracy of image evaluation and correction is improved, and this algorithm is used to reconstruct the image more realistically. In virtual reality, viewers can adjust their viewing angles and query information about the surrounding environment. This is a feeling that traditional images cannot give. The wrong data are evaluated and corrected, and then the maximum, minimum, and depth data are calculated. The improved transition noise is lower, the calculation speed is faster, and the visual experience is better, while maintaining its original robustness and feasibility.

Data Availability

The data used to support the findings of this study are available from the corresponding author upon request.

Hindawi
Journal of Electrical and Computer Engineering
Volume 2024, Article ID 9876494, 1 page
https://doi.org/10.1155/2024/9876494

Retraction

Retracted: Optimization of Business English Teaching Based on the Integration of Interactive Virtual Reality Genetic Algorithm

Journal of Electrical and Computer Engineering

Received 23 January 2024; Accepted 23 January 2024; Published 24 January 2024

This article has been retracted by Hindawi following an investigation undertaken by the publisher [1]. This investigation has uncovered evidence of one or more of the following indicators of systematic manipulation of the publication process:

(1) Discrepancies in scope

(2) Discrepancies in the description of the research reported

(3) Discrepancies between the availability of data and the research described

(4) Inappropriate citations

(5) Incoherent, meaningless and/or irrelevant content included in the article

(6) Manipulated or compromised peer review

The presence of these indicators undermines our confidence in the integrity of the article's content and we cannot, therefore, vouch for its reliability. Please note that this notice is intended solely to alert readers that the content of this article is unreliable. We have not investigated whether authors were aware of or involved in the systematic manipulation of the publication process.

In addition, our investigation has also shown that one or more of the following human-subject reporting requirements has not been met in this article: ethical approval by an Institutional Review Board (IRB) committee or equivalent, patient/participant consent to participate, and/or agreement to publish patient/participant details (where relevant).

Wiley and Hindawi regrets that the usual quality checks did not identify these issues before publication and have since put additional measures in place to safeguard research integrity.

We wish to credit our own Research Integrity and Research Publishing teams and anonymous and named external researchers and research integrity experts for contributing to this investigation.

The corresponding author, as the representative of all authors, has been given the opportunity to register their agreement or disagreement to this retraction. We have kept a record of any response received.

References

[1] X. Ma, "Optimization of Business English Teaching Based on the Integration of Interactive Virtual Reality Genetic Algorithm," *Journal of Electrical and Computer Engineering*, vol. 2022, Article ID 2455913, 9 pages, 2022.

Hindawi
Journal of Electrical and Computer Engineering
Volume 2022, Article ID 2455913, 9 pages
https://doi.org/10.1155/2022/2455913

Research Article

Optimization of Business English Teaching Based on the Integration of Interactive Virtual Reality Genetic Algorithm

Xiao Ma

School of Tourism English, Zhengzhou Tourism College, Zhengzhou 451464, China

Correspondence should be addressed to Xiao Ma; maxiao@zztrc.edu.cn

Received 28 December 2021; Accepted 8 March 2022; Published 22 April 2022

Academic Editor: Xianyi Cheng

With the continuous advancement of the global economy and the deepening of internationalization and openness, it is also necessary to keep pace with the times in the optimization of business English teaching. At this point, a genetic algorithm based on the interactive virtual reality (VR) should be established for the optimization of business English teaching to adapt to the future trend in business English teaching optimization more appropriately. In the business English teaching process at present, it is required to change the traditional teaching concept, adjust the previous teaching ideas, widen the horizon continuously, establish an international and diversified English teaching and training program, incorporate the outstanding foreign teaching models, and proactively absorb the excellent educational concepts to drive the development of the domestic business English teaching model more effectively. The results of the simulation experiment indicate that the improved algorithm designed in this article can reduce the computational overhead of the meta-algorithm to a great extent, and the improvement strategy is designed based on the evaluation results of practical examples.

1. Introduction

With the continuous progress of the economy, many domestic companies have started to develop overseas markets as China joined the World Trade Organization (WTO); and many foreign companies have also started to flood into the Chinese market and gradually implemented cross-border mergers, acquisitions, and joint ventures, which have tremendously improved the comprehensive strength of the enterprises [1, 2]. However, as foreign enterprises access the domestic market, there are cultural conflicts between company operators with different cultural backgrounds in various countries, which can lead to increasingly prominent conflicts and contradictions in the business cooperation and management of both parties and severely affect the healthy growth of the enterprises. Students majoring in English at colleges and universities are the future workforce of foreign company employees, and it is crucial to develop the intercultural communication skills of this workforce. In fact, many foreign language teachers have started to enhance the cultural competence of students, especially their cultural competence, in their practical teaching process. Classroom teaching of English is mainly focused on communication activities between teachers and students, and it is a system with significant social features. The corresponding evaluation indicator system and teaching model form the level of education weighed by business English evaluation indicators, which need to be combined based on the principle of stipulations before teaching and satisfaction after teaching. At present, with cloud computing, computer technology, big data analysis, and hypermedia technology as a basis for driving the continuous development of modern information technologies, it is possible to offer virtualized teaching services and fast teaching services to English learners and implement data information technology services such as universal interconnectivity, intelligibility, and data information mining on a huge data scale. The image-friendly learning interfaces can not only effectively improve the environmental atmosphere of business English teaching but also change the previous view of English teaching and the learning-based relationship between teachers and students.

In this article, an optimization model for the effectiveness of higher vocational business English teaching is designed based on interactive virtual reality genetic algorithm according to the features of higher vocational business English teaching. The optimization of business English teaching is implemented based on traditional education. It is evidently more advantageous and can drive students' motivation and enthusiasm for learning. The optimization of business English teaching is not merely a tool to assist education, but a game changer of modern education for improving and rebuilding learning methods, which is a qualitative leap of traditional education.

The ultimate goal of English learners is to be able to communicate fluently and effectively in business English, while a solid basic knowledge of English is a prerequisite to achieve this goal. It is evident that beginners need to pass a stage test before they can proceed to the next stage of their studies successfully. In general, business English learners have better performance in English studies, whereas non-business English learners have better performance in basic knowledge. In fact, students who achieve excellent results in the entrance exams may not have good skills in language expression in the current education system [3, 4]. Business English is not only about high test scores, but also about the learners' overall perception of language expression, the knowledge of language use, and the ability to express themselves. It is also crucial to pay attention to the "words" and "reasoning." However, in the practical teaching process, relying solely on "words" is not feasible because learners have different learning levels and abilities, and some students have relatively strong listening and speaking skills. There is still a gap in the oral and written language output levels among the students from the practical requirements, and not all students can achieve fully unimpeded English expression and communication.

As a branch of English for special purposes, business English is the English subject that people use when they are engaged in business activities in the workplace, which has professional, practical, and cross-cultural communicative features. At present, most of the courses in business English in China focus on cultivating students' basic language skills such as listening, speaking, reading, writing, and translating in English, as well as improving their business communication skills. However, the number and proportion of business English courses are often limited, and most of them are still at the theoretical level. As a result, the business practice and cross-cultural business communication skills of students cannot be effectively improved in teaching activities, which is a common issue business English teaching facing in China at present. In addition, due to the rapid progress of the economy and society, the areas involved in business activities are gradually expanding. The timeliness of the business English curriculum, that is, the ability to follow the development of the times and constantly update changes, is also an aspect that the construction of the business English curriculum system focuses on. In the society nowadays, whether the new economic situation can be effectively used to make up for the lack of professional curriculum construction and whether new ideas and thinking can be delivered in teaching activities are the issues that need to be considered in the overall development of the specialty.

2. Based on the Interactive Virtual Reality Genetic Algorithm

2.1. Interactive Virtual Reality Genetic Algorithm. The process of optimizing the effectiveness of higher vocational education business English teaching model based on interactive virtual reality genetic algorithm is described as follows:

$$I(S_1, S_2, \ldots, S_n) = \sum_{i=1}^{n} - p \log_2(p_i). \tag{1}$$

In the previous equation, $p_i = |C_i|/|S|$ stands for the probability of each sample in the category i.

Firstly, it is necessary to establish a sample model of information that constrains the optimization model of business English teaching and evaluation capacity [5, 6]. In combination with the nonlinear information fusion methods and time-series analysis methods, statistical analysis is carried out on the teaching competencies of internationalized English education. The business English teaching optimization model and the evaluation capability constraint indicator parameters are taken a set of nonlinear time series to establish a high-dimensional feature distribution space, which stands for the distribution model of business English analysis and evaluation parameters. The primary indicator parameters are constraints to the teaching capability of English international education, teacher level, investment in educational facilities, and policy relevance. Subsequently, a differential equation is established to build an information flow model representing the parameters that constrain the capacity to rank English international education.

$$x_n = x(t_0 + n\Delta t) = h[z(t_0 + n\Delta t)] + \omega_n. \tag{2}$$

In the previous equation, $h(\cdot)$ stands for the multivariate value function for the analysis and evaluation of the English international education pendulum class. In the feature distribution space, the following conditions need to be met to obtain the feature training subset:

(1) $\Sigma = \mathrm{diag}(\delta_1, \delta_2, \ldots, \delta_r), \delta_i = \sqrt{\lambda_i}, \forall i \neq j;$

(2) $\cup_{i=1}^{L} S_i = V - v_s.$

In the previous equations, $x_{n+1} = \mu x_n(1 - x_n)$ indicates the optimization evaluation indicator. With regard to multiple variable groups, the sequence of characteristic distributions $x(n)$ corresponding to the business English teaching optimization evaluation statistics can be used to construct the business English teaching optimization model based on the initial teaching-level measurement values as follows:

$$\begin{aligned} c_{1x}(\tau) &= E\{x(n)\} = 0, \\ c_{2x}(\tau) &= E\{x(n)x(n+\tau)\} = r(\tau), \\ c_{kx}(\tau_1, \tau_2, \ldots, \tau_{k-1}) &\equiv 0, \quad k \geq 3. \end{aligned} \tag{3}$$

When $Q = 2$, the level of teacher power and the level of distribution of educational resources for business English classroom evaluation comply with the $(2 + 1)$ subordinate continuous letter writing condition. That is, the class of English international education is analyzed and evaluated accordingly.

$$\psi_x(\omega) = \ln \Phi_x(\omega) = -\frac{1}{2}\omega^2\sigma^2. \tag{4}$$

Based on the constructed data information flow model, a set of scalar sampling sequence components is established for the exclusive parsing evaluation of English internationalization education and provides an accurate data input base for the lecture analysis evaluation of English internationalization education [7, 8].

The interactive virtual reality (VR) genetic algorithm is used to carry out the big data information model analysis of the business English teaching optimization, and the control objective function for the predictive estimation of business English teaching optimization model competencies is established as follows:

$$\begin{aligned} &\max_{x_{a,b,d,p}} \sum_{a\in A}\sum_{b\in B}\sum_{d\in D}\sum_{p\in P} x_{a,b,d,p}V_p, \\ &\text{s.t.} \sum_{a\in A}\sum_{d\in D}\sum_{p\in P} x_{a,b,d,p}R_p^{bw}(S)\, b \in B. \end{aligned} \tag{5}$$

Hence, a specific analysis of the health indicator system is established accordingly.

The level of teaching competencies of personalized learning support is evaluated quantitatively and recursively based on the gray model. It is assumed that the historical data on the distribution of teaching competencies of personalized learning support and the initial values of the features are fixed from the prediction of teaching competencies of personalized learning support to obtain the estimated probabilistic density generalized function as the following:

$$u_c(t) = Kx_c(t). \tag{6}$$

The statistical model for the predictive estimation of business English teaching optimization analysis capacity is u: $I \times IR^d \longrightarrow IR$. After $k-1$ iterations, $k \geq 1$, and the gray order sequence of business English teaching optimization analysis evaluation complies with $N(k) < L$. The interactive virtual reality genetic algorithm is used to obtain the output indicator of the personalized learning-supported lecture analysis evaluation, which is taken as the K-adjacent sample values of the distributed large data information stream, as shown in the following expression:

$$P_{1J} = \sum_{d_i\in KNN} \mathrm{Sim}(x, d_i)\, y\left(d_i, C_j\right). \tag{7}$$

The fusion method for big data information is used to establish a personalized learning support lecture, and the objective function is used to construct the interdomain classification for analyzing and evaluating the information flow of large, distributed data. That is, the objective function of the big data cluster is described as follows:

$$J_m(U, V) = \sum_{k=1}^{n}\sum_{i=1}^{c} \mu_{ik}^m (d_{ik})^2. \tag{8}$$

The studied English courses supported by personalized learning is explored, and the sequence of exponential correlation distribution of the evaluation is quantitatively analyzed to identify the method of K-value excellence [9]. The results of quantitative recursive feature extraction for educational analysis and evaluation can be obtained as follows:

$$x_n = a_0 + \sum_{i=1}^{M_{AR}} a_i x_{n-i} + \sum_{j=0}^{M_{MA}} b_j \eta_{n-j}. \tag{9}$$

x_{n-i} stands for the scalar time series; b_j stands for the oscillatory decay value of the personalized learning support alignment and analysis evaluation.

2.2. Establishment of the Business English Educator Model. As English language learners are as the main participants and experiences of business English teaching as well as the main subjects of the learners' resource acquisition, English personalized design needs to meet the individual needs of English language learners. For the purpose of better clarifying the attribution of the educators in the business English teaching system, it is necessary to establish models for the practical examples and educators. The business English teaching model is mainly used to establish user modules through the teaching of business English or through third-party agent software for real-time data acquisition and develop business English teaching programs based on the acquired data information. Due to the growing demand for English language learners to be in full, independent as well as developing personalized learning, teachers can help them meet their personalized learning requirements and develop reasonable and scientific learning plan tasks the students.

During the process of business English learning, business English learners can make multiple kinds of errors. Business English learners are not proficient in the learning rules of English knowledge points. As a result, errors can occur in the application process. In addition, many unfavorable factors such as the tension and inattention of the evaluation process can also lead to many errors of business English learners. In contrast to the business English teaching content based on the basic English knowledge level, the learning model proposed in this article is designed based on the error/misunderstanding model of business English learners, which can identify the errors/misunderstandings made by business English learners effectively. Through the analysis of the root causes for their occurrence, it can respond to the error correction methods in time. The internalization of English knowledge is completed by consolidation, and the learning efficiency of business English learners can be improved quickly. Business English teaching mines the action data of business English learners based on learning records so as to quickly identify errors/misunderstandings that occur in the business English teaching process. The business English

teaching model is established to address the errors or misunderstandings of business English learners. The system will identify the corresponding correction methods in the error database based on the errors that occur so that business English instructors can quickly identify the error content and identify the error types after the errors occur and provide timely feedback to the business English instructors on the correction measures. The error database is divided into the enumerated type and the generated type. Through analyzing the experience of designers and experts, the system can effectively determine the possible errors of business English teachers and locate the causes of errors by enumeration. The class of errors is mainly generated based on the inventory system, which provides a reference basis for business English instructors to collect and analyze the errors that may occur in the learning process of business English instructors on their own. In addition, we have found that it is very rare for all three states of a phoneme to occupy only one frame in each frame of the system. This results in a system with only one corresponding frame of state in both sound scientific computational knowledge evaluation system-s(Figure 1). If that state is skipped on the token transfer path, the HMM structure can still describe the phoneme in a business English teaching optimization system accurately. The HMM structure is illustrated in Figure 2.

If the transition path of the HMM structure is altered, the operation of token transfer will become more complicated. In any state HMM with n, the state transfer matrix transfer probability distribution needs to be met as the following:

$$\left.\begin{aligned} a_{ij} &\neq 0, \quad i = j \text{ and } i = j - 1, \\ a_{ij} &= 0, \quad \text{others.} \end{aligned}\right\} \tag{10}$$

Hence, there are $2n + 1$ transmission paths for each factor. However, there are seven transmission paths for HMM in three states. After cross-state conversion, there will be $3n + 1$ transmission paths for each speech factor, and there are 10 transmission paths for three states. Although the increase in the number of transition paths will increase the time complexity of the operation, the ratio of increase is limited. Thus, the scientific computational knowledge evaluation of English speech still has the advantage of the frame-based asynchronous system operation, which has ensured the presence of an observation value in each English phoneme to obtain more valuable phoneme information. Figure 3 shows the HMM structure across $n - 1$ states.

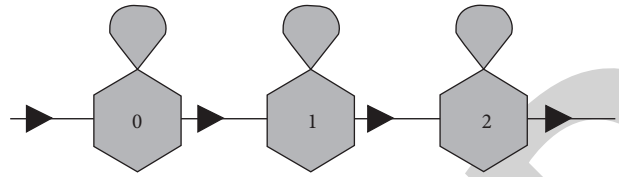

Figure 1: HMM state by state.

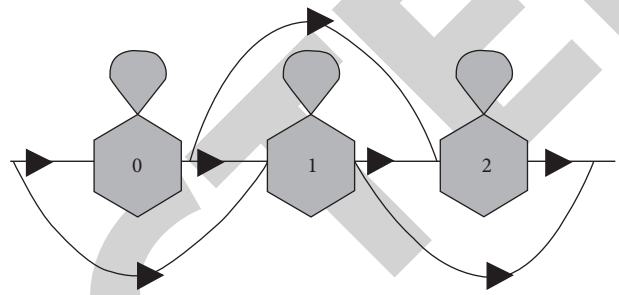

Figure 2: HMM across the single state.

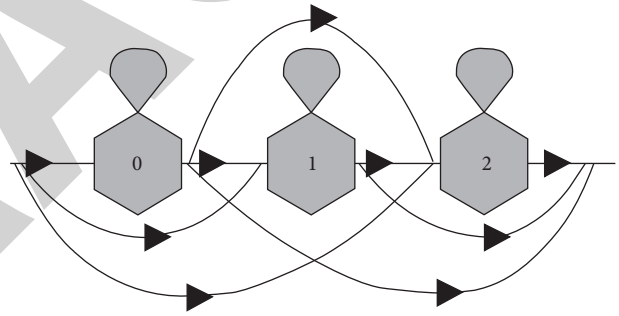

Figure 3: HMM across $n - 1$ states.

3. Health Evaluation Indicator for the Classroom Teaching of Business English and Its Measurement Analysis

3.1. Evaluation Indicators for the Business English Classroom Teaching System. In accordance with the health review theory of knowledge, the dynamics of the teaching delivery system is derived from the English teachers and students within the system through. English teaching and activities input system dynamics, which mainly promotes changes in the optimization model of business English teaching, which should be measured indirectly based on the external visible teaching model [10, 11]. The types of teaching activities and features of the business English teacher evaluation health indicator system are based on the analysis of the teaching process between business English teaching and students. The optimization model for business English teaching is mainly about English teacher preparation, English classroom education, providing special tutoring, types of student educational activities including students learning at the teacher, peer help within the teacher, and so on. The features of business English international teaching activities can be measured by using teacher motivation and the time used in the teaching process. The features of the learning patterns of students can be illustrated based on the enthusiasm of students for learning and the amount of time they have spent in learning. In the past, business English education required a common teaching mode of teachers and students and modern information as a teaching mode

of the education system, in which the information teaching resources and international teaching of business English are mainly used.

3.2. Organizational Structure Measurement Indicator for the Evaluation of Business English Classroom Teaching. In the evaluation indicators for business English teaching, individual English teachers and students use teaching models from teaching input energy as a rational distribution in the process of internationalized teaching system. Thus, certain teaching model can be constructed to ensure a smooth and efficient flow of energy. The organizational structure applicable to the international evaluation of business English is measured to establish the teaching evaluation indicators. The teachers and students need to meet each other's demand and adapt to each other. Teachers and students should supervise each other based on their own teaching activities. Thus, the ways of mutual energy transfer become more fluent, and the number of energy transformation increases. In general, the adaptability complies with four aspects, which include purpose adaptability, content adaptability, modality adaptability, and attitude adaptability in turn as the evaluation system of business English teachers between the roles of different activities. In this way, the teaching content and learning attitude are in line with the degree of teaching of both sides.

3.3. Resilience Indicator for the Evaluation of Business English Classroom Teaching. The resilience of the English course evaluation system refers to the capability of the teaching evaluation system to maintain the system caused and functioned normally when it is threatened from outside. The main influencing factors in the evaluation system are the teaching fatigue of English teachers in the teaching process, the lack of motivation of students to learn, and the existence of maladjustment in the information environment. The teaching organizational structure is threatened from outside, which will be the different perspectives of teachers' professional fatigue, interaction between students' learning and teachers' teaching activities, purpose, teaching content, teaching attitude, and teaching methods that cannot meet the actual demands of each one involved. It is necessary to overcome the problems that exist, such as the incompatibility with the modern information teaching environment, and the need to detect the risk factors, and to take appropriate measures to overcome the difficulties that may be encountered [12]. This will enable teachers and students to effectively use their educational skills, to detect the risk factors, and to organize their learning motivation and teaching structure in a way.

4. Examples and Result Analysis

4.1. Optimization of Attribute Selection for Data Sets. In the interactive virtual reality genetic algorithm-based model for optimizing the effectiveness of teaching business English in higher vocational education, n operations are required to determine the performance data on each one of the students. When there are more data, the operations become very slow, leading to a decrease in the efficiency of generating the interactive virtual reality genetic algorithm, so we reduce the computational overhead of the interactive virtual reality genetic algorithm and reduce the time consumption by redefining the selection criteria of the attributes in the data set.

In this article, the information quantity formula is optimized:

(1) It is assumed that $f(x)$ is continuous on $[a,b]$ and contains first-order as well as second-order derivatives in (a,b). Thus, the following can be obtained:If $f''(x) > 0$ in (a,b), then the shape on $[a,b]$ is concave.If $f''(x) < 0$ in (a,b), then the shape of $f(x)$ on $[a,b]$ is upper convex.

(2) If $f(x)$ is an upper convex function on the interval I, $\forall x_1, x_2 \in I, \lambda \in (0,1)$, then equation (11) below can be obtained:

$$\lambda f(x_1) + (1-\lambda) f(x_2) \leq f[\lambda x_1 + (1-\lambda) x_2]. \tag{11}$$

The function $\log_2 P$ in equation (1), which are consistent with $P_1 - P_2 = \Delta P \longrightarrow 0$. The function $\log_2 P$ is continuous on (0,1]. In accordance with equation (1), the concavity of the function $\log_2 P$ is checked, as described in the following equations:

$$(\log_2 P)' = \frac{1}{P \times \ln 2}, \tag{12}$$

$$(\log_2 P)'' = -\frac{1}{P^2 \times \ln 2} < 0. \tag{13}$$

In accordance with equation (1), the shape of the function obtained is upper convex on the definition domain (0,1].

(3) If $f(x)$ is an upper convex function on the interval I, then $\forall x_1, x_2, \ldots, x_n \in I$, $\lambda_1, \lambda_2, \ldots, \lambda_n > 0$, and $\lambda_1 + \lambda_2 + \cdots + \lambda_n = 1$, and the following equation can be obtained:

$$\lambda_1 f(x_1) + \cdots + \lambda_n f(x_n) \leq f(\lambda_1 x_1 + \cdots + \lambda_n x_n). \tag{14}$$

The formula for the volume of information is improved accordingly, as shown in the following equation:

$$I(S_1, S_2, \ldots, S_m)' = -\log_2 \sum_{i=1}^{m} P_i^2. \tag{15}$$

The improved information quantity formula is applied, and the classification accuracy of the interactive virtual reality genetic algorithm classifier changes as a result. Hence, on the basis of previous equation the information entropy formula can be modified, as shown in the following equation:

$$E(A)' = \sum_{j=1}^{m} \frac{\left|S_{1j} + S_{2j} + \cdots + S_{nj}\right|}{|S|} \times \left(-\log_2 \sum_{j=1}^{m} P_{1j}^2 + P_{2j}^2 + \cdots + P_{nj}^2 \right). \tag{16}$$

In the previous equation, P_j stands for the set of samples in the subset S_j that are included in the category C_i, and $(|S_{1j} + S_{2j} + \cdots + S_{nj}|/|S|)$ stands for the weight of the jth subset.

4.2. Optimization of Information Gain. In the process of increasing the training set, the interactive virtual reality genetic algorithm also changes significantly, and the number of examples increases during the process of tree establishment, the mutual information of individual features and the interactive virtual reality genetic algorithm will be transformed, which will influence the learning process of the subsequent data sets [13].

In the process of interactive virtual reality genetic algorithm, the amount of information is used as is the criterion for detecting attributes. In the interactive virtual reality genetic algorithm, the information gain is replaced by the Gini metric, and the performance after the replacement is more desirable than the former. The data set S Gini(S) for a data set containing classes is shown in the following equation:

$$\text{gini}(s) = 1 - \sum p_j \cdot p_j. \tag{17}$$

In the previous equation, p_j stands for the frequency of the jth type of data in S, and Gini increases proportionally to the information gain.

The most prominent defect of the interactive virtual reality genetic algorithm is that the interactive virtual reality genetic algorithm is unstable. In this article, the relevant improvements are made based on the operation. Compared with the operation of Gini, the detection indicator of Gini selects the minimum value of Gini. The modified method for dealing with the above problem is based on the Gini split indicator, in which the smallest residual value is selected as the new indicator for attribute selection, and the original information gain is supplemented accordingly.

The improved formula for the information gain is shown as follows:

$$\text{gain}_{\text{left}} = 1 - \text{gain}(A)' = 1 - \frac{I(S_1, S_2, \ldots, S_m) - aE(A)}{m}. \tag{18}$$

In the previous equation, a stands for the attribute priority value, which takes values in the range of (0,1].

The minimum value $\text{gain}_{\text{left}}$ is selected as the new test attribute benchmark, which can not only solve the problem that the interactive virtual reality genetic algorithm easily accepts attributes with multiple fetched values, but also improve the classification efficiency of the interactive virtual reality genetic algorithm and reduce its instability.

4.3. Simulation Results. In this article, simulation experiments are carried out specifically to verify the effectiveness. The computational cost is calculated, and the results are shown in Figure 4.

Subsequently, the optimized interactive virtual reality genetic algorithm is used to construct an optimization model for the effectiveness, and the results are tested in a higher vocational institution for practical effectiveness optimization, as shown in Figure 5.

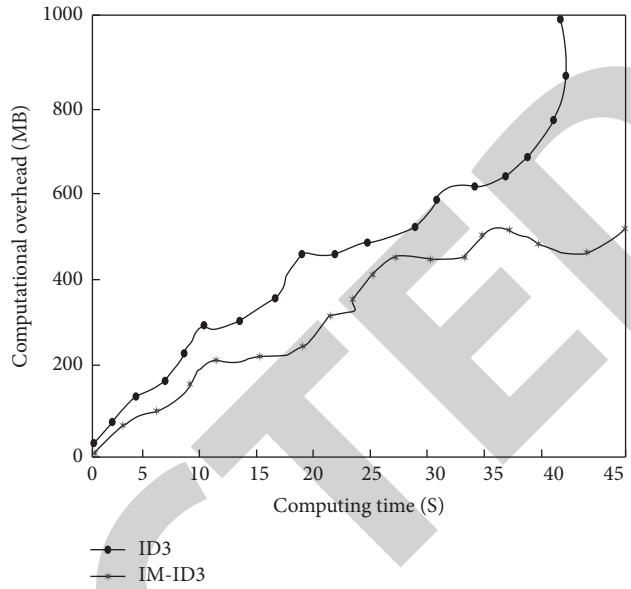

Figure 4: Results of interactive virtual reality (VR) genetic algorithm in optimizing the construction effectiveness of higher vocational business English teaching.

From the simulation experiments, it can be concluded that the above optimization algorithm not only saves computing overhead, but also improves the optimization results of the effectiveness of teaching business English in higher vocational education.

For the purpose of verifying the system performance, the popular business English teaching evaluation systems (HMM system, endpoint detection system, and Audry system) at present are used and compared with the system proposed in this article. The overall control and result output of the system are processed by MATLAB software. The speech models were constructed by business English teaching evaluation and feature extraction of the four systems. The average evaluation rates and evaluation times of the four evaluation systems after 10 training sessions are shown in Table 1.

So far, it can be known that the online English speech teaching evaluation system designed in this thesis has a significantly higher evaluation rate than the HMM system and the endpoint detection system has a slightly higher evaluation rate than the Audry system. In the aspect of evaluation time, the system proposed in this article is almost the same as the HMM system and the evaluation time is significantly less than the Audry system and the endpoint detection system. For the purpose of enhancing the convincingness of a higher evaluation rate of the system proposed in this article than the Audry system 9, the curves are depicted for the evaluation rate of single training business English teaching in the above training group of 10 training sessions, as shown in Figure 6. This has revealed that the evaluation rate of the system proposed in this article is higher than that of the Audry system.

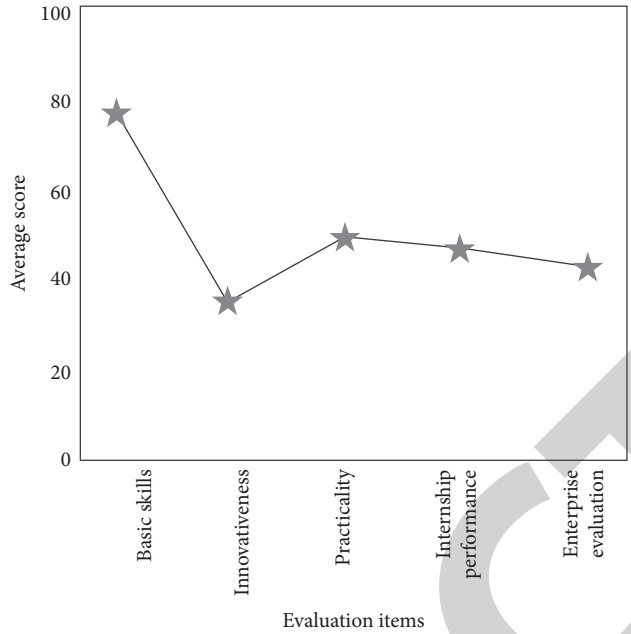

Figure 5: Results of optimizing the effectiveness of higher vocational business English teaching.

Table 1: Comparison results of evaluation systems.

Serial number of voice model	Endpoint monitoring system		Audry system		HMM system		The system proposed in this article	
	Evaluation rate (%)	Evaluation time (ms)	Evaluation rate (%)	Evaluation time (ms)	Evaluation rate (%)	Evaluation time (ms)	Evaluation rate (%)	Evaluation time (ms)
1	98.253	24.569	98.776	15.698	92.125	13.698	99.818	12.635
2	98.126	20.119	99.123	16.002	91.003	12.589	99.268	12.964
3	97.663	22.369	98.695	15.289	92.535	18.216	98.968	13.563
4	96.595	19.848	97.664	15.669	94.216	17.625	98.901	14.536
5	97.212	22.147	98.013	16.987	89.215	12.336	99.053	13.684
6	93.214	28.693	98.096	17.002	89.336	13.528	99.525	16.279
7	95.113	27.629	96.215	16.592	91.025	14.256	98.773	17.061
8	94.126	28.139	95.125	15.365	92.216	12.693	98.693	12.113
9	98.001	22.169	97.662	15.841	93.114	13.547	98.525	11.986
10	97.629	25.551	98.218	16.035	95.216	14.006	99.147	13.516
11	95.365	24.336	99.003	15.256	90.963	13.694	99.981	12.589
12	96.333	27.219	98.675	14.969	90.003	13.546	98.927	14.369
13	97.125	29.329	98.762	16.259	91.326	12.589	98.796	12.654
14	96.123	28.647	96.251	16.576	88.779	17.216	99.669	12.156
15	93.655	27.664	95.796	15.295	94.252	12.697	99.785	12.954
16	94.558	25.125	98.256	16.286	93.251	12.254	99.367	13.816
17	95.216	23.958	98.698	15.321	94.105	13.664	98.864	16.021
18	97.001	24.569	99.126	17.069	91.189	14.654	99.125	13.624
19	97.921	20.325	99.331	16.696	92.336	15.329	98.138	14.941
20	96.129	23.693	98.276	15.643	90.017	14.369	98.714	12.694

In brief, the online English speech teaching evaluation system 7 designed in this article has some advantages over mainstream business English teaching evaluation systems in the aspect of 5 "recognition rate" and "evaluation time." Hence, the proposed system is highly effective.

5. Discussion

5.1. Adjusting the Teaching Objectives. The evaluation work of business English teaching competency is influenced by multiple factors, and the experiments and research on business English teaching level are conducted first, and the data system and resource analysis system of business English teaching level are established. Through the application of the combination of information as well as clustering solution to assess business English teaching ability and establishing the objectives and statistical system of English teaching ability evaluation, the quantitative budgeting ability of business English teaching capacity evaluation can be significantly improved. This can be seen from the effect of the sequencing of courses on the

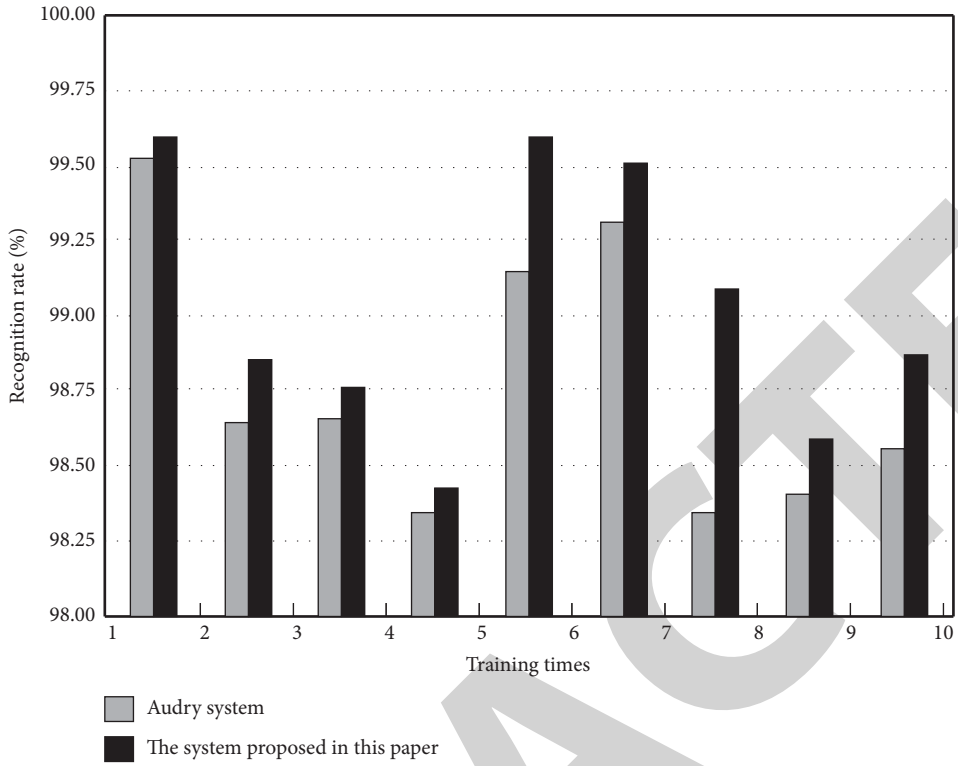

Figure 6: Comparison of the evaluation rates between the Audry system and the system proposed in this article.

rationality of the arrangement of business English classrooms in an institution, and the sequencing of business English classrooms in an institution stands for the feasibility of the whole class schedule in that institution.

5.2. Enhancing the Design of Optimized Courses for Business English Teaching. In view of the situation of imprecise classification of traditional international education model and evaluation indicator system competency evaluation calculation, the research scholars proposed the method of indicator system competency evaluation calculation by combining fuzzy greedy calculation method with information. Firstly, the research system of constrained parametric indicators is formed. Subsequently, the capacity of the data and information system is assessed by using the quantitative recursive method to achieve the access to the resources of capacity control features [14, 15]. The evaluation of the evaluation indicator system is completed by classifying and summarizing the indicator parameters, editing the corresponding teaching resource plan, and completing the evaluation of the evaluation indicator system. Using this calculation method to evaluate the international education model and evaluation index system, and to carry out a high degree of integration and analysis of information, can improve the accuracy of resource teaching ability evaluation.

5.3. Establishing a Sound Teaching Test and Evaluation System. The optimal evaluation of business English teaching in China has been carried out based on final evaluation for a long time, with final exams and level 4 and 6 exams as the main means of examination, but the evaluation of students' English learning process is relatively neglected. In college English level 4 and 6 exams and English level 4 and 8 exams, emphasis is given to the grades and pass rates. The question type of university English level exams has a great flaw in design. Not only the basic direction of internationalization of university English education is greatly deviated, but also many contents. In particular, business English skills, translation skills, and other aspects of the review of the weakness of our higher vocational education, and the phenomenon of inability to use English for oral communication properly is still relatively serious. Therefore, the current business English teaching requires innovative changes and optimization of the testing and evaluation system.

6. Conclusions

In accordance with the above analysis, it can be observed that there are many problems in the optimization process of business English teaching based on the interactive virtual reality genetic algorithm. English teachers in higher vocational education institutions need to carry out reforms in accordance with their teaching level, so as to implement the adjustment and innovation of the previous national teaching programs for business English, effectively enrich the role and function of the optimization of business English teaching, effectively improve the level of international English teaching, and adapt to the internationalization of higher vocational education and the development trend in economic globalization more effectively. In this article, an

Hindawi
Journal of Electrical and Computer Engineering
Volume 2024, Article ID 9840526, 1 page
https://doi.org/10.1155/2024/9840526

Retraction

Retracted: Analysis of Comprehensive Artificial Neural Network Computer Media Aided Construction of Economic Forecasting Model

Journal of Electrical and Computer Engineering

Received 23 January 2024; Accepted 23 January 2024; Published 24 January 2024

This article has been retracted by Hindawi following an investigation undertaken by the publisher [1]. This investigation has uncovered evidence of one or more of the following indicators of systematic manipulation of the publication process:

(1) Discrepancies in scope

(2) Discrepancies in the description of the research reported

(3) Discrepancies between the availability of data and the research described

(4) Inappropriate citations

(5) Incoherent, meaningless and/or irrelevant content included in the article

(6) Manipulated or compromised peer review

The presence of these indicators undermines our confidence in the integrity of the article's content and we cannot, therefore, vouch for its reliability. Please note that this notice is intended solely to alert readers that the content of this article is unreliable. We have not investigated whether authors were aware of or involved in the systematic manipulation of the publication process.

Wiley and Hindawi regrets that the usual quality checks did not identify these issues before publication and have since put additional measures in place to safeguard research integrity.

We wish to credit our own Research Integrity and Research Publishing teams and anonymous and named external researchers and research integrity experts for contributing to this investigation.

The corresponding author, as the representative of all authors, has been given the opportunity to register their agreement or disagreement to this retraction. We have kept a record of any response received.

References

[1] T. Li, "Analysis of Comprehensive Artificial Neural Network Computer Media Aided Construction of Economic Forecasting Model," *Journal of Electrical and Computer Engineering*, vol. 2022, Article ID 7981393, 8 pages, 2022.

Hindawi
Journal of Electrical and Computer Engineering
Volume 2022, Article ID 7981393, 8 pages
https://doi.org/10.1155/2022/7981393

Research Article

Analysis of Comprehensive Artificial Neural Network Computer Media Aided Construction of Economic Forecasting Model

Tianfeng Li

Nanyang Institute of Technology, Nanyang, Henan 473004, China

Correspondence should be addressed to Tianfeng Li; 160706222@stu.cuz.edu.cn

Received 30 December 2021; Accepted 1 March 2022; Published 30 March 2022

Academic Editor: Muhammad Rashad

As a complex system engineering, economic forecasting involves many fields and disciplines, and its accuracy largely depends on the selected forecasting method and forecasting model. The construction of the traditional economic prediction model mainly depends on the theories of economic statistics and metrology, which cannot meet the prediction needs of the new era. ANN model has a more flexible nonlinear quality and learning mode so that it can effectively adapt to the prediction scenario of a nonlinear economic system. ANN is an abstract model of the human brain neuronal network based on the information-processing perspective and composed of different networks to achieve a specific representation of logical strategies. ANN's self-learning function, associative storage function, and the ability to find optimal solutions at high speed have led to its in-depth application and research in an increasing number of fields. In addition, ANN research work has continued to advance, has made great progress in many fields represented by economic forecasting, has successfully solved many practical problems, showing a more intelligent adaptation in the field of economics, and therefore has an important research value. Based on this, this paper first analyzes the economic system prediction, then studies the ANN medium model and learning algorithm, and finally verifies the effectiveness of the ANN economic prediction model integrating computer medium.

1. Introduction

After years of in-depth integration and development of the global economy, economic integration and trade diversification have made remarkable achievements in the past few decades. However, in recent years, the development of the global economy is very unstable [1]. On the other hand, in order to maintain the steady development of the social economy, it is inseparable from the prediction and planning of economic info, so as to provide scientific and objective decision-making basis and data support for economic development [2]. In this context, through the collection and analysis of various indicators of economic operation, the establishment of economic prediction model is of great value for reasonably predicting the trend of economic development in a certain period of time.

In order to ensure the healthy development of their macro-economy, governments will inevitably formulate some economic decisions and intervention measures. The formulation of these economic control policies and intervention measures depends on the prediction of the future economic situation, which requires relevant institutions and personnel to adopt scientific means and strategies to make an accurate prediction of the economic situation. The accuracy of economic forecasting largely depends on the selected forecasting method and forecasting model [3]. The construction of the traditional economic forecasting model mainly depends on the theories of economic statistics and metrology. With the iterative progress and utilization of modern info tech such as artificial intelligence, IoT, and cloud computing, the construction of economic forecasting model has been supported by new tech, which has laid a solid technical premise for the regulation of economic activities and the formulation of strategies [4].

As a complex system engineering, economic forecasting involves many fields and disciplines. On the one hand, it is determined by the complexity of macro- and microeconomic activities; on the other hand, it is also determined by

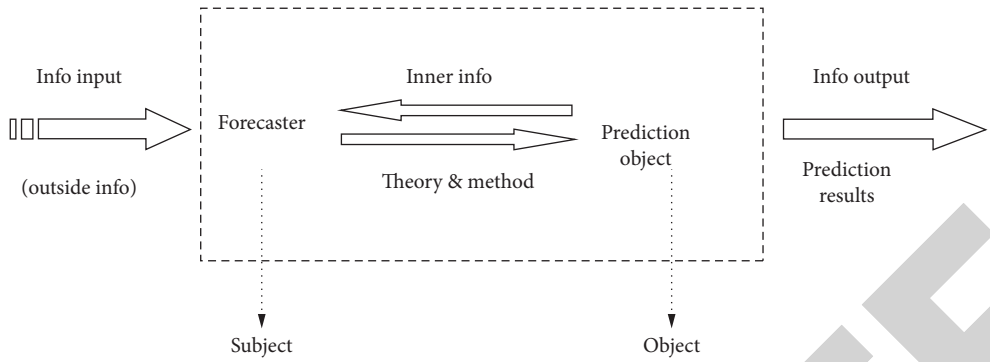

Figure 1: Elements of economic system prediction.

the nonlinearity and uncertainty of the economic system [5]. These inherent characteristics make economic prediction very difficult. Facing the serious challenge of economic prediction modeling, economic prediction research increasingly depends on quantitative data support. In this process, many kinds of prediction models and algorithms have emerged, such as time series analysis, econometrics, and VAR methods. Among them, as a mainstream prediction model method, VAR is a large-scale structure prediction model, which is composed of many variables [6]. However, whether econometric models, time series analysis, or VAR models belong to the category of linear models, which are difficult to predict nonlinear economic systems, resulting in a large optimization space for the prediction accuracy of these models, which is difficult to effectively meet the prediction needs of macroeconomy.

Traditional economic forecasting models either put forward many unrealistic presuppositions for the economic system or rely on the data generated by historical economic activities, so as to predict a very small number of economic quantities [7]. Due to the nonlinear and uncertain characteristics of the economic system, it is difficult to accurately realize the evolution prediction modeling of the economic system, resulting in great limitations of the traditional economic prediction model [8]. This requires breaking through the limitations of traditional prediction theory and practical models, finding new economic prediction methods to deal with the complex and diversified economic environment, reducing the risk of economic decision-making, and improving the prediction accuracy of economic system, so as to provide technical support for corresponding institutions to specify correct economic regulation policies and carry out corresponding response measures, so as to accelerate economic activities to better achieve the predetermined objectives.

In the info age, various computer media have made rapid progress. The computing medium represented by the ANN model has gained in-depth attention and research in the construction of economic prediction model because of its prediction accuracy advantage in the field of multivariable time series. The development of ANN theory provides a new opportunity for economic forecasting. ANN model has a more flexible nonlinear quality and learning mode. Thanks to its concise constituent units and flexible learning simulation mode and ability, it can be effectively applied to nonlinear economic system forecasting [9]. There is a certain inevitable trend behind a large number of disordered activities in the economic system. Through the analysis and calculation of economic data, it could study the law of economic development and predict economic activities. ANN model has the ability of self-study, association, and storage, so it can quickly guide the complex relationships and laws between nonlinear things. Therefore, it has good adaptability and matching in economic model prediction.

In short, under the background of the rapid development of computer medium, the economic system is more complex, diverse, and visual. As a continuous pursuit of human activities, economic growth is an important indicator to measure social development. Due to the complexity of the economic system, its healthy and orderly development is inseparable from the competent intervention and regulation of economic acquisition, and these adjustment and intervention measures are inseparable from the effective prediction of the economic system [10]. With the help of the ANN model, an advanced medium, it can effectively predict the impact of economic regulation measures on the whole economic system, so as to provide technical support for relevant institutions to make corresponding decisions and plans. Therefore, it is of great practical value to study the construction of ANN economic prediction model integrating computer medium.

2. Research on the Economic Forecasting System

The prediction of the economic system is the result of using known knowledge and means to deduce and judge the development trend and situation of the economic system in a certain period of time in the future. The constituent elements of economic system prediction are shown in Figure 1, mainly including input info, prediction object, prediction theory, and model adopted, as well as output prediction results and info. The prediction of economic system should follow the principles of continuity, correlation, similarity, variability, and randomness. At the continuity level, it is mainly because the past activities of the economic system will have an impact on the current and future behavior [11]. At the relevance level, it is mainly because the economic system, as an open system, is dependent on external factors. At the level of

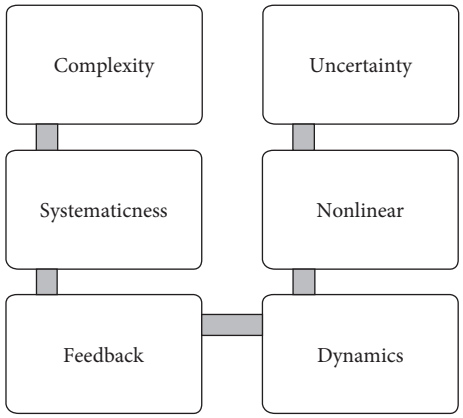

Figure 2: Typical characteristics of economic system.

similarity, variability, and randomness, it means that the relevant prediction activities should follow the change law of the economic system and find out the relevant influencing factors.

At the level of forecasting characteristics of economic system, because economic phenomena can be recognized and utilized, it has a certain regularity to carry out economic forecasting. The accuracy of economic forecast also has the typical characteristics of relativity and limitation, because the economic system will inevitably be affected by factors that cannot be mastered. When the results of economic prediction are inconsistent with the actual economic operation, it cannot explain that the prediction of the economic system is failed, because there are many human active interventions in economic activities, which affect the operation results of the economic system. The economic system has several typical characteristics as shown in Figure 2.

At the level of economic prediction test, common prediction test methods include relative error, average prediction error, average absolute error, mean square error, and average absolute percentage error. These different economic forecast test methods can effectively verify the consistency between the forecast results and the actual situation.

2.1. Classification Method. The methods of economic system prediction include qualitative prediction, quantitative prediction, and comprehensive prediction. Among them, the qualitative prediction of economic system is mainly based on subjective judgment, so it can only roughly estimate the development trend of things. Secondly, at the level of quantitative prediction, a targeted quantitative model is established through the collection of data and info of the economic system, so as to calculate the development trend of the economic system [12]. The comprehensive prediction organically integrates the advantages of the first two prediction methods to ensure that the prediction results are as accurate as possible. The forecast of typical fields can generally be divided into short-term forecast, medium-term forecast, and long-term forecast according to their duration, as shown in Table 1. In addition, according to the scope of prediction, it can be divided into macro- and microprediction, in which the prediction of economic system belongs to typical macroprediction.

Table 1: Classification of forecast periods in typical domains.

Forecast periods (years)	Tech	Industry	Economics
Short term	1–3	1–10	1–5
Medium term	3.5	10–20	5–10
Long term	5–10	>20	>15

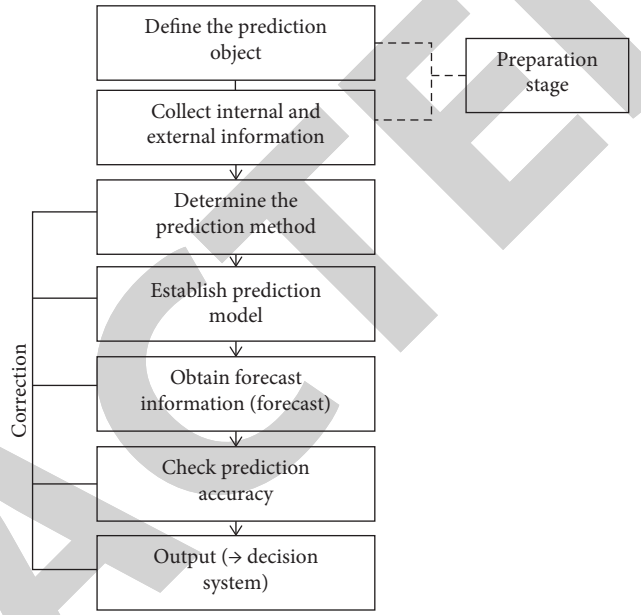

Figure 3: Typical process of marketing service in power supply enterprises.

In the process of economic system prediction, it should first clarify the prediction object and collect internal and external info of the economic system. After completing the preparation stage, it is necessary to further determine the prediction method and model, obtain the prediction info, check the prediction accuracy until the prediction info is output, and ensure the accuracy of the prediction results through continuous iterative optimization. The typical process of economic system prediction is shown in Figure 3.

In addition, in the process of economic system prediction, it is inevitable to receive the interference of many factors, which will adversely affect the accuracy of prediction. Generally speaking, the development of economic system prediction is mainly limited by objective factors, the role of randomness and mutation factors, and the accuracy of the selected prediction models and methods, social factors, and intelligent structure.

3. ANN Computer Medium

In recent years, the computer medium has made remarkable progress, and its in-depth utilization in many fields has significantly accelerated the development of all walks of life. However, with the in-depth utilization of computer medium, the disadvantages of traditional computer medium have gradually emerged [13]. Firstly, the info processing flow of a typical computer medium is shown in Figure 4.

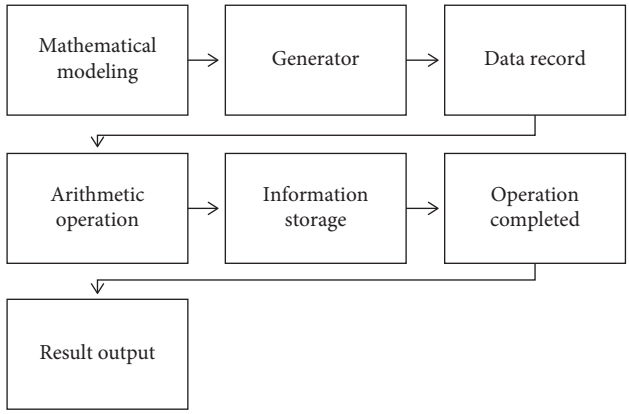

Figure 4: Typical info processing flow of computer medium.

It can be seen from Figure 4 that this flow depends on the set program steps, and the info processing mode is more centralized and serial, which has great limitations in the processing of intelligent info and other scenarios. Therefore, it is necessary to find a new medium, expand the mechanism of info processing and storage, and realize the efficient solution of related matters. As a top-down method, ANN medium is suitable for low-level mode processing. ANN medium simulates brain neural function by simulating human brain neural structure, so as to quickly process a large number of neuronal info and dynamic behavior. ANN medium can better solve and deal with the problems faced by traditional computer medium, especially its advantages in spatio-temporal info storage, parallel search, self-organizing association, spatio-temporal data statistics, and so on [14].

At present, ANN medium mainly aims to solve the problems of global, structural, and programmability and realize the overall stability. The artificial neural network medium uses the connection mechanism to model the cognitive information processing process and replaces the algorithm by establishing neural computing. Secondly, at the level of intelligent info processing, the utilization of ANN medium includes optimization control, signal processing, and sensor info processing. In addition, at the level of software simulation and hardware implementation, software simulation is carried out on the traditional computer medium to form an ANN simulator, so as to verify the new model and complex network characteristics [15]. At the realization level of neural network computer medium, biological simulation and digital-analog interconnection are realized.

In terms of storage capacity, the storage capacity of the ANN medium is greatly related to the network. The upper and lower limits of info expression capacity of ANN medium with n neurons are shown as follows:

$$C < \log_2\left(2^{(n-1)^{2^n}}\right)^n, \tag{1}$$

$$C \geq \log_2\left(2^{(0.33[n/2]^2)}\right)^{[n/2]}. \tag{2}$$

Secondly, at the level of computing power, ANN medium can mainly realize mathematical approximate mapping, estimation of probability density function, and formation of topological continuity and statistical isomorphic mapping and extract relevant knowledge from binary database. It can also realize nearest neighbor pattern classification and data clustering and solve optimization problems. ANN medium can better solve the problems of feature extraction, pattern classification, associative memory, low-level perception, and adaptive control. With the deepening of the utilization of ANN medium, its integration with traditional computer medium can effectively give full play to their advantages and accelerate the specified connection between target nodes.

The utilization of ANN prediction model media in economic system prediction further enriches the theory and practice of economic growth prediction and brings a new innovative perspective for the prediction of economic system operation. Secondly, the utilization of ANN prediction model can provide new decision-making tools and intellectual support for macroeconomic departments and can accurately predict the operation situation and trend of economic system in a certain period of time. In addition, by establishing the growth model based on ANN medium technology, the fitting ability of the economic prediction model is ameliorated.

3.1. ANN Medium Model. The basic composition of the ANN medium is shown in Figure 5. This medium is mainly used to strengthen the competition between neurons in the layer.

The relationship between each element node is shown in equations (3) and (4). Where w_{ji} is the connection weight between neuron i and neuron j; u_i is the neuron state of neuron i; v_j is the output of neuron j, that is, an input of neuron i; θ_i is the threshold of neuron i. Function f expresses the input-output characteristics of neurons.

$$u_i = \sum_{j=1}^{n} w_{ji} v_j - \theta_i, \tag{3}$$

$$v_i = f(u_i). \tag{4}$$

If the threshold θ_i as a special weight, the output of neuron i can be expressed as the state shown in (5), in which $w_{0i} = -\theta_i$, $v_0 = 1$.

$$v_i = f\left(\sum_{j=0}^{n} w_{ji} v_j\right). \tag{5}$$

In order to express the nonlinear transformation ability of neurons with continuous functions, S-type functions are often used.

$$f(u_i) = \frac{1}{1 + e^{-u_i}}. \tag{6}$$

At the level of connection mode, there are mainly intralayer connection, circular connection, and interlayer connection. Among them, intralayer connection is an intraregional connection, circular connection is used to continuously strengthen its own activation value, and

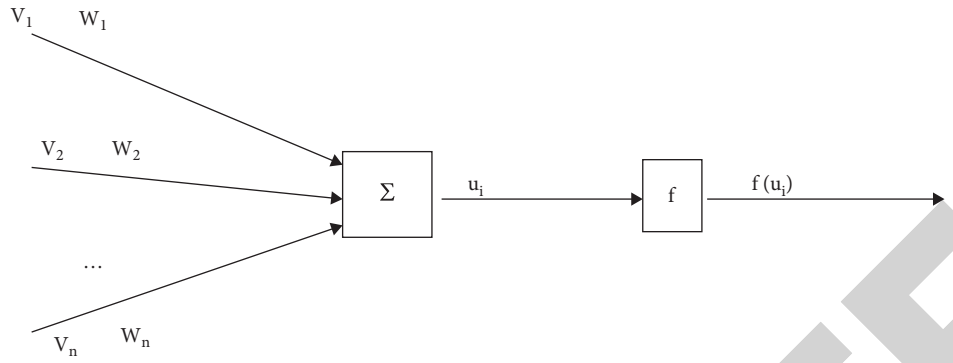

Figure 5: The basic composition of ANN medium.

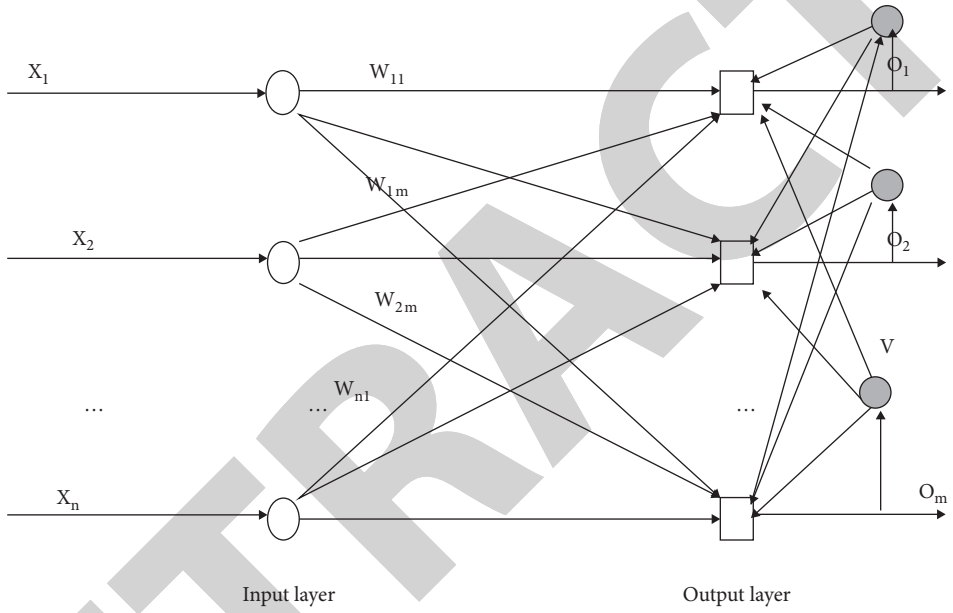

Figure 6: Simple single-stage horizontal feedback network architecture.

interlayer connection is the connections between neurons in different layers, so as to realize interlayer signal transmission. At the level of network info flow type, it mainly includes feedforward network and feedback network. Among them, the former is carried out layer by layer from the input layer to each hidden layer and then to the output layer; in the latter, each node can not only receive input from the outside but also output to the outside. In addition, the layered structure of ANN medium is divided into horizontal feedback, layer feedforward, and layer feedback. The simple single-stage horizontal feedback network is shown in Figure 6.

3.2. ANN Medium Model and Learning Algorithm. The processing of single output perceptron is applied to the neurons in the output layer of multioutput perceptron one by one. Firstly, the weight matrix is initialized, and then, the cycle number control method is used for cycle control to perform the specified number of iterations on the sample set. Or the precision control method or comprehensive control method shall be selected according to the actual problems. In the initial test stage, the accuracy requirements are low. After the test is completed, the actual accuracy requirements are given. The mathematical model of the perceptron is shown as follows:

$$\text{net}_j = \sum_{i=1}^{n} w_{ij} x_i, \tag{7}$$

$$\begin{aligned} o_j &= sgn\left(\text{net}_j - T_j\right) = sgn\left(\sum_{i=0}^{n} w_{ij} x_i\right) \\ &= sgn\left(\mathbf{W}_j^T \mathbf{X}\right), \end{aligned} \tag{8}$$

$$\mathbf{W}_j = \left(w_{1j}, w_{2j}, \ldots w_{ij}, \ldots, w_{nj}\right)^T, \tag{9}$$

where o_j is the output and $\mathbf{W}_j$ is the input.

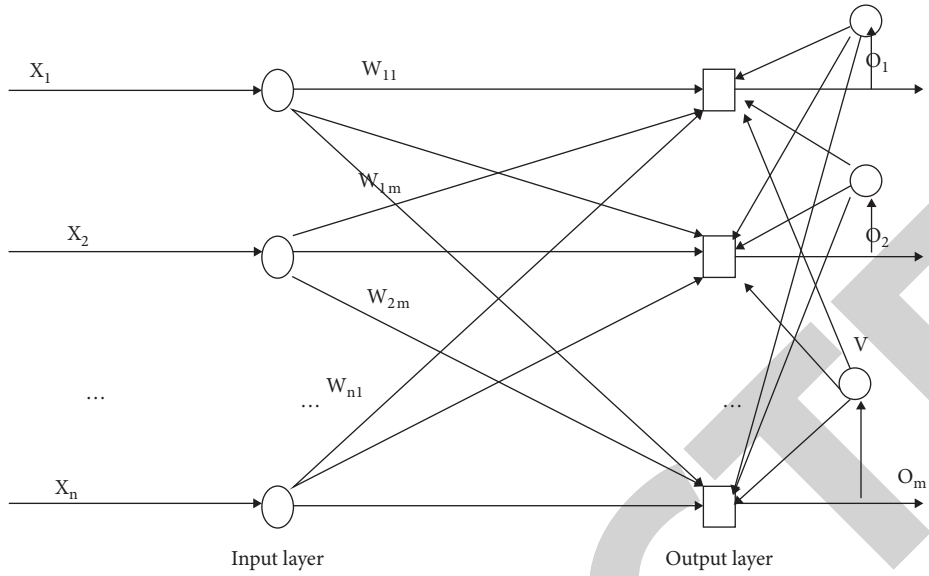

Figure 7: Topology of BP network medium.

For the problem of linear indivisibility, the closed or open convex domain is divided by a two-level network, and the nonconvex domain is identified by a multilevel network, and special attention should be paid to the adjustment of the connection weight of the hidden layer. By combining multiple single-level networks and fusing the network group with other single-level network groups, a two-level network can be formed. The network can be used to divide a closed or open convex domain on the plane, and a nonconvex domain can be divided into multiple convex domains. The three-level network can be used to identify nonconvex regions. The XOR problem is realized by constructing a two-level network with two neurons in the first layer and one neuron in the second layer.

Because the learning rules of perceptron neural network can only train single-layer neural network, while single-layer neural network can only solve linear separable classification problems, and multilayer neural network can be used for nonlinear classification problems, it is necessary to find a learning algorithm for training multilayer network. BP algorithm can be better applied to the learning of multilayer network and has wide applicability and effectiveness, which is also the main reason why most ANN medium adopts the form of BP network. The topology of the BP network medium is shown in Figure 7. In the BP network structure, the dimension of its input/output vector, the number of layers of the network hidden layer, and the number of neurons are directly related to the problem.

3.3. Training Process. The training samples of the BP network medium are input vector and ideal output vector. The weight is initialized, a sample (X_j, Yj) is taken from the sample set in the forward propagation stage, and X_j is inputted into the network and calculated the corresponding actual output O_j. In the error propagation stage, the difference between the actual output O_j and the corresponding ideal output Yj is calculated, and the weight matrix is adjusted in the way of minimizing the error. The error measure of the network with respect to the jth sample is shown as follows:

$$E_j = \frac{1}{2}\sum_{k=1}^{m}\left(y_{jk} - o_{jk}\right)^2. \tag{10}$$

The error of the output layer is used to adjust the weight matrix of the output layer, and the error of the direct leading layer of the output layer is estimated with this error, and then, the error of the leading layer of the output layer is used to estimate the error of the previous layer. In this way, the error estimates of all other layers are obtained, and these estimates are used to modify the weight matrix, so as to establish the process of transmitting the error shown by the output to the input step by step in the direction opposite to the input signal.

The order of receiving samples in the BP network medium has a great impact on the training results. It is easier to accept later samples. Generally speaking, it is difficult to arrange an appropriate order for the samples in the set, and the sample order will affect the results, so it is necessary to eliminate the influence of sample order. The input, output, precision control parameters, and learning rate are initialized with different small pseudo-random numbers. Secondly, the cycle control parameter is set as the precision control parameter plus one; the maximum number of cycles, cycle number control parameter equal to zero; for each sample, the weight modification amount and output error of output layer and hidden layer are calculated, and then, the weight matrix of output layer and hidden layer is modified. The ameliorated measure can effectively solve the accuracy problem caused by the sequence of samples and the jitter problem of training.

4. Model Construction Method and Results

At the microeconomic level, the cost prediction model constructed by ANN medium can predict the future

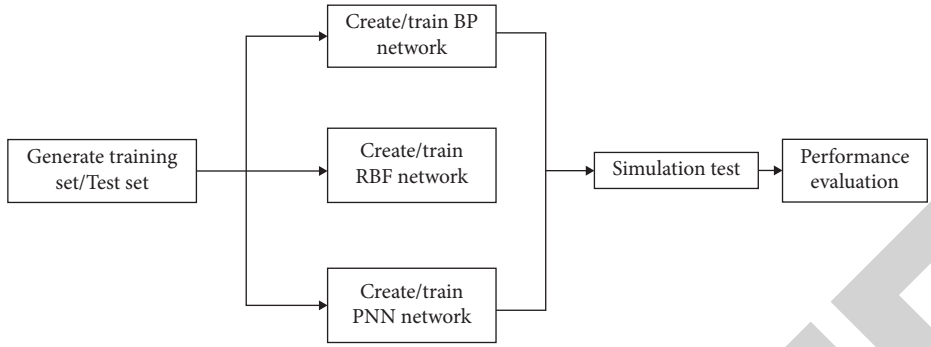

Figure 8: Simulation and prediction process based on BP network.

operating costs of enterprises in various industries and conduct simulation experiments on sales, so as to accurately predict future sales. In the field of macroeconomic system, ANN medium can be used to predict and warn the budget, inflation, and economic development cycle, and macro operation situation of the economic system. At the economic market level, the ANN model can accurately predict the profitability and future trend of the economic market. In addition, in the financial field, the use of the ANN model can establish a scientific and objective credit evaluation model, so as to evaluate the credit rating, financial status, risk rating, and expected benefits of relevant institutions and individuals. At the level of operation evaluation and decision-making assistance of the socio-economic system, the ANN model can objectively evaluate relevant industries, sustainable development, industrial planning, and economic strategy and truly reflect the actual situation of economic system.

4.1. Construction Method. The trained BP network is used for simulation prediction, and its process is shown in Figure 8. Firstly, the training and test sets are generated, and the samples are divided into training set and test set. The training samples are used for network training, and the test samples are used to test the generalization ability of the network. Secondly, the simulation is tested, and the final results are evaluated by creating training BP network, RBF network, and PNN network. After the network is created and trained, the input variables of the test set are sent to the network, and the output of the network is the prediction result. By calculating and comparing the error between the predicted value and the real value of the test set, the performance of the network can be evaluated according to the error results: the smaller the relative error is, the better the performance of the ANN prediction model is.

In addition, through sample collection, normalization, and random selection of training samples and test samples, the prediction error is calculated by test samples to evaluate the generalization ability of the network. If the generalization ability meets the requirements, the trained BP neural network can predict/classify. Otherwise, the network parameters need to be adjusted to continue learning until the generalization ability meets the requirements.

Table 2: The economic system parameters selected.

Parameters	Periods (values), unit: 100 million CNY				
Training samples	2005	2006	2007	2008	2009
	183085.8	219438.5	270092.3	319244.6	348517.7
Test samples	2010	2011	2012	2013	2014
	412119.3	487940.2	538580.0	592963.2	643563.1
Prediction samples	2015	2016	2017	2018	2019
	688858.2	746395.1	832035.9	919281.1	986515.2

Table 3: ANN model prediction output results.

Year	Comparison results, unit: 100 million CNY		
	PV	AV	Error (%)
2020	1014868.6	1015986.2	0.11

4.2. Results Analysis. At the level of economic system index selection and data processing, it is mainly based on macroeconomic theory. Therefore, the input variables of the ANN prediction model in this paper come from the production function. The economic system parameters selected in this paper are shown in Table 2. Secondly, the input indexes need to be preprocessed to speed up the learning and convergence efficiency of the ANN prediction model. In the process of forecasting the economic system, the actual time series observation data are input into the ANN economic forecasting model network, so as to obtain the prediction output at the next time, and carry out continuous iteration until the final result is obtained.

In order to verify the effectiveness of ANN economic prediction model integrated with computer medium, it is necessary to train, simulate, and verify the network model with the help of a computer software medium. This paper chooses MATLAB software medium to form the BP network model. After setting the training parameters, the train function is called in the software to train the BP model. The input variables of the economic system selected in Table 2 are predicted by the BP model, in which the data from 2005 to 2009 are used as training samples, the data from 2010 to 2014 are used as test samples, and the data from 2015 to 2019 are used as prediction samples. The forecast samples are inputted into the model to obtain the economic forecast value of 2020, and the results are shown in Table 3. It can be seen from the

Hindawi
Journal of Electrical and Computer Engineering
Volume 2023, Article ID 9843297, 1 page
https://doi.org/10.1155/2023/9843297

Retraction

Retracted: Filtering Algorithm for Positioning Accuracy of the Logistics Tracking System Based on the 3D Virtual Warehousing Logistics Demonstration System

Journal of Electrical and Computer Engineering

Received 15 August 2023; Accepted 15 August 2023; Published 16 August 2023

This article has been retracted by Hindawi following an investigation undertaken by the publisher [1]. This investigation has uncovered evidence of one or more of the following indicators of systematic manipulation of the publication process:

(1) Discrepancies in scope

(2) Discrepancies in the description of the research reported

(3) Discrepancies between the availability of data and the research described

(4) Inappropriate citations

(5) Incoherent, meaningless and/or irrelevant content included in the article

(6) Peer-review manipulation

The presence of these indicators undermines our confidence in the integrity of the article's content and we cannot, therefore, vouch for its reliability. Please note that this notice is intended solely to alert readers that the content of this article is unreliable. We have not investigated whether authors were aware of or involved in the systematic manipulation of the publication process.

Wiley and Hindawi regrets that the usual quality checks did not identify these issues before publication and have since put additional measures in place to safeguard research integrity.

We wish to credit our own Research Integrity and Research Publishing teams and anonymous and named external researchers and research integrity experts for contributing to this investigation.

The corresponding author, as the representative of all authors, has been given the opportunity to register their agreement or disagreement to this retraction. We have kept a record of any response received.

References

[1] G. Sun and F. Qiao, "Filtering Algorithm for Positioning Accuracy of the Logistics Tracking System Based on the 3D Virtual Warehousing Logistics Demonstration System," *Journal of Electrical and Computer Engineering*, vol. 2022, Article ID 5963140, 9 pages, 2022.

Hindawi
Journal of Electrical and Computer Engineering
Volume 2022, Article ID 5963140, 9 pages
https://doi.org/10.1155/2022/5963140

Research Article

Filtering Algorithm for Positioning Accuracy of the Logistics Tracking System Based on the 3D Virtual Warehousing Logistics Demonstration System

Guie Sun and Fengjuan Qiao

Chongqing Vocational College of Transportation, Chongqing 402247, Jiangjin, China

Correspondence should be addressed to Guie Sun; sunguie@cqjy.edu.cn

Received 22 October 2021; Accepted 4 January 2022; Published 31 January 2022

Academic Editor: Muhammad Rashad

Under the background of the global integrated supply chain, the work of logistics is more and more complicated. Warehouse management is now an important part of logistics. The optimization of the logistics tracking system in the building material market proves that the tracking result of the system is highly reliable. The system has the advantages of small size, low cost, accurate positioning, real-time convergence, and high performance.

1. Introduction

The continuous development of China's economy is inseparable from the development and support of logistics enterprises. At the same time, as a reasonable comprehensive service form in industrialization, it occupies an important position in the current economic development [1, 2]. The packaging, storage, transportation, inspection, processing, and even the packaging and distribution of goods before and after constitute the current logistics system [3, 4]. Now, the requirements of logistics informatization require logistics enterprises to solve the one-stop service system, provide strong support for the one-stop supply chain, and make the whole supply chain obtain the highest economic benefits, which is the overall goal of logistics enterprises [5, 6]. Warehousing management plays an important role in logistics management. A good warehousing system can speed up the flow of materials, reduce costs, ensure the normal operation of services, and realize the effective management and utilization of resources [7, 8].

This paper studies the way of the three-dimensional virtual warehouse logistics demonstration system and logistics tracking system. Using this demonstration system can timely and accurately find the location of goods, and then the GPS data, through the system positioning accuracy filtering strong tracking, can realize the real-time and effective monitoring and tracking of goods. It can get the positioning data and the data of the monitoring center in time.

2. Structure and Hardware Design of the Logistics Tracking System

2.1. Structure of the Logistics Tracking System. In the research process of the traditional logistics tracking system positioning accuracy filtering algorithm, usually, a two-dimensional map is mainly used to describe the movement environment of the logistics tracking system. However, because the two-dimensional map can only describe relatively high environmental plane information, it cannot provide relative information. Therefore, it has a great influence on the completion of the positioning accuracy filtering algorithm of the logistics tracking system. Mostly, the construction of a three-dimensional environment is very important for the positioning accuracy filtering algorithm of the logistics tracking system, and the signing and forwarding of business documents are carried out at the same time. The

main work of the logistics team and the control manager is to construct the information management system of the transportation fleet and the transportation vehicle and to set the deployment method of the specific cargo to the logistics transportation task [9]. This time, the train passes through the route and the central station and has formulated a systematic and target product element control plan, transportation application vehicle schedule, product element-product vehicle allocation combination, and logistics transportation invoice information collection and input management.

2.2. Hardware Design of the Logistics Tracking System. The hardware circuit diagram of the logistics tracking system is shown in Figure 1. The CPU used in this system is MSP430f147 macroprocessor developed by Texas Instruments (TI). The power supply voltage of this series of macroprocessors is low.

Users can use the function modules of the system to call the corresponding system functions for data operation [10, 11]. Therefore, from the perspective of application, it can be seen that controlling users' access to system functions can realize the access control of user information and can effectively improve the performance of the tracking system. The technical fault reporting measures of the logistics tracking and positioning information system at the use level can use software to complete the access control of the user side in the information system, and the corresponding theoretical essence is the authorization of the system function authority; that is, the completion of each function of the system can only be used after the authorized user [12, 13].

Following the existing relational database management system as an example, the authorization is configured. The permissions of the SQL server can be divided into four types of users: system administrator, database holder, acceptor of the database object, and other users of the database, as shown in Figure 2.

3. Filtering Algorithm for Positioning Accuracy of the Logistics Tracking System

3.1. Design of the Storage Environment Based on the 3D Virtual Logistics Demonstration System. Before planning the global path of the warehouse logistics tracking system, it is necessary to complete the modeling of the warehouse storage environment and improve the warehouse storage status of the warehouse storage logistics tracking system. The warehouse storage environment modeling in this section selects the 3D virtual warehouse logistics demonstration system. The 3D reconstruction technology of computer multimedia is also called cell decomposition method. It divides the environment of the warehouse logistics tracking system into area and volume [14], divides it into two-dimensional or three-dimensional grids with consistent shape, and describes other components in the warehouse environment in small lattice as units for abstract explanation. Build a warehouse environment that is easy to understand in the logistics tracking system.

The length of the warehouse system is described as M, and the width is described as N. Taking a corner of the warehouse as the origin, the grid coordinates of the upper left corner are set as (0, 0) to build a rectangular coordinate system. Assuming that the cargo boundary is a, when the size block of 3D reconstruction technology a is regarded as a cell grid and the grid of the warehouse environment is changed to several small grids, the number of each grid can be described as follows: the grid number of ceil (n/a) different columns is described by the cell (M/a), in which ceil represents upward arrangement [15].

Two-dimensional and one-dimensional space structures are used in the storage environment after gridding.

In the process of positioning accuracy filtering algorithm, it is transformed and used according to the requirements of planning algorithm. The detailed mapping relationship is as follows:

$$\text{bianhao} = (x-1) \times \text{ceil}\left(\frac{m}{a}\right) + y. \tag{1}$$

3.2. Construction of the Mathematical Model of Location Accuracy Filtering Algorithm in the Logistics Tracking System. Regardless of the point and the correct path of the point, the path planning problem is divided into two parts according to whether the initial point of the warehouse logistics tracking system has exports. One of them is that the initial point of the warehouse logistics tracking system is at the time of export. It can be considered as a typical TSP problem. Another is that if the initial point is not at the exit, then the end point of the initial point can be considered as a constant TSP problem, namely, ST-PSP problem. The mathematical model of the typical TSP problem can be expressed by formula (2), and the best path $P = \{u_1, u_2, \cdots, u_k\}$ can be calculated.

$$\min Z(P_\alpha) = \sum_{i=1}^{k=1} d\left(u_{\alpha_i}, u_{\alpha_{i+1}}\right) + d\left(u_{\alpha_i}, u_k\right). \tag{2}$$

In the formula, P_α is used to describe the reorganization set $d(u_{\alpha_i}, u_{\alpha_{i+1}})$ of the K path point sequence of the Manhattan distance α_i between two points.

If the potential field ant colony algorithm is used to solve the typical TSP problem, all the path points can be regarded as group individuals and can be adaptive function selection formula (2). For TSP and ST-PSP problems, potential field ant colony algorithm can only obtain the best access order of global path points, not the path, which cannot meet the requirements of the mobile wheeled logistics tracking system. It is necessary to obtain an accurate global planning path through 3D reconstruction technology.

3.3. Positioning Accuracy Filtering Algorithm Based on the Three-Dimensional Reconstruction Technology. In the grid environment, in the process of planning the global path of the logistics tracking system through 3D reconstruction technology, the OPEN table and CLOSE table are set, and the

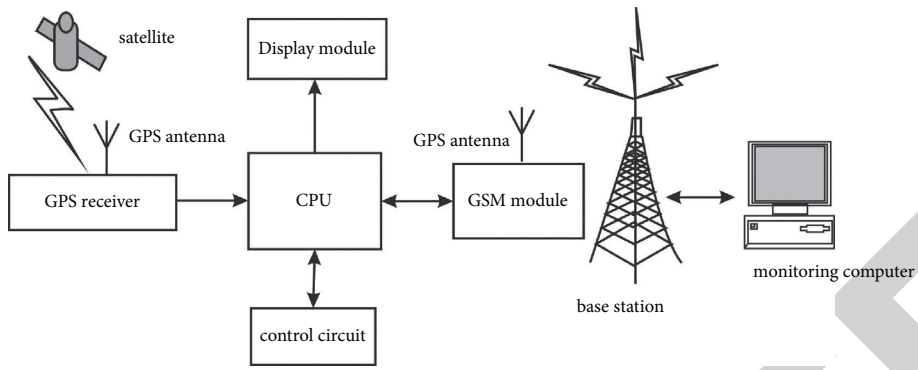

Figure 1: Structure of the logistics tracking system.

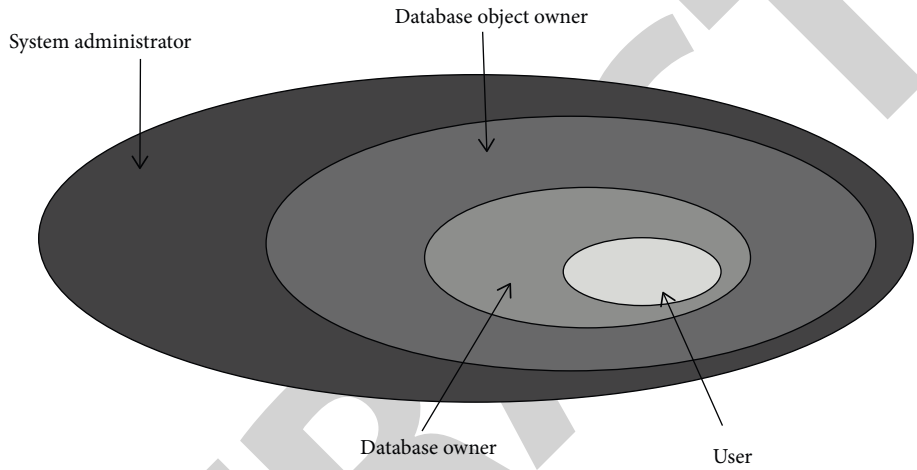

Figure 2: : Permission level of the SQL server.

initial point is added to the OPEN table during initialization. The current CLOSE table is empty. The initial point is

$$f(s) = h(s), \tag{3}$$

where $f(s)$ is the initial point evaluation function. $h(s)$ is used to describe the estimated interval between the initial node and the end point.

The OPEN table is empty. If there is no target location, the retrieval will be stopped, and there is no valid path. On the contrary, when the OPEN table is empty, repeat the following steps before obtaining the target node:

(1) Select a node with a small f value in the OPEN table, add it to the CLOSE table, and delete the corresponding value in the OPEN table. Assuming that the node with the smallest f value of the adjacent node of the initial point is q, the initial point is considered as the parent node.

(2) All the adjacent nodes of the current point P are calculated, assuming that the adjacent nodes are u_i. Then, $f(u_i)$, $h(u_i)$, and $g(u_i)$ are obtained. Here, $g(u_i)$ explains the interval between the selection point and the object node, the following determination is made:

① If the terminal is u_i, then jump out of the three-dimensional reconstruction technology algorithm, take the end point as the starting point, trace back from the parent node to the initial point, obtain the batch of the warehouse logistics tracking system, and select the shortest route.

② If u_i is an unreachable point, skip the point.

③ If u_i is in the CLOSE table, skip the point.

④ If u_i is not in either of the OPEN table or the CLOSE table, it is added to the OPEN table and is the parent node of u_i.

⑤ If u_i is in the OPEN table, find the g value of the new path and judge whether it is the smallest. If yes, p is the parent node of u_i, and update f, h, and g at the same time; on the contrary, no change is made.

(3) Save the search track and use the parent node to trace back to the initial point.

Positioning accuracy filtering model of the non-differential phase precision dynamic single-point positioning system:

$$\begin{cases} X_k = F_{k/k-1}X_{k-1} + T_{k-1}U_{k-1}, \\ Y_k = H_kX_k + N_k. \end{cases} \tag{4}$$

The statistical characteristics are $E(U_k) = 0$, $E(N_k) = 0$, dynamic noise vector U_k, and observation noise vector W_k; all of the dynamic noise vectors and the observation vectors are white noise vectors with an expected value of 0, $\operatorname{cov}(U_k, U_j) = Q_k\delta_{kj}$, $\cos(N_k, N_j) = R_k\delta_{kj}$, and $\cos(U_k, N_j) = 0$ where X_k and Y_k are the state vector and observation vector at k time, respectively; $F_{k/k-1}$ is the state transition matrix; U_k is the dynamic noise at k time; $T_{k/k-1}$ is the system control matrix; H_k is the k-time observation matrix; N_k is the observation noise at k time; Q_k and R_k are, respectively, the variance matrix of the system dynamic noise and observation noise. δ_{kj} is the Kronecker function:

$$\delta_{kj} = \begin{cases} 1\,(k = j), \\ 0\,(k \neq j). \end{cases} \tag{5}$$

For simplicity, firstly, the matrix vector with constant surrounding ambiguity is considered, and the constant speed model is adopted for the dynamic model.

Pre-estimated value:

$$X_{k/k-1} = F_{k/k-1}X_{k-1/k-1}. \tag{6}$$

Variance matrix:

$$P_{k/k-1} = F_{k/k-1}P_{k-1/k-1}F_{K/K-1}^T + T_{k-1}Q_{k-1}T_{k-1}^T. \tag{7}$$

Calculate the Kalman gain matrix:

$$K_k = P_{k/k-1}H_k^T\left(H_kP_{k/k-1}H_k^T + R_k\right)^{-1}. \tag{8}$$

Calculate the filtering value $X_{k/k}$ of the positioning accuracy of the system and its variance matrix $P_{k/k}$:

$$\begin{aligned} X_{k/k} &= X_{k/k-1} + K_k\left(Y_k - H_kX_{k/k-1}\right), \\ P_{k/k} &= \left(I - K_kH_k\right)P_{k/k-1}\left(I - K_kH_k\right)^T + K_kR_kK_k^T. \end{aligned} \tag{9}$$

The recursive initial value is $X_{0/0} = E(X_0)$ and $P_{0/0} = \operatorname{var}(X_0)$.

The filter maintains this capability when it reaches a stable state and has relatively low sensitivity to initial values and noise statistical properties [6].

$$\begin{aligned} P_{k+1/k} &= \lambda_{k+1}F_{k+1/k}P_{k/k}F_{k+1/k}^T + Q_{k+1}, \\ \lambda_{k+1} &= \operatorname{diag}\left(\lambda_{(k+1),}\lambda_{2(k+1)}, \lambda_{3(k+1)}, \ldots, \lambda_{n(k+1)}\right), \\ \lambda_{i(k+1)} &= \begin{cases} \alpha_iC_{k+1} & \left(\alpha_iC_{k+1} > 1\right), \\ 1 & \left(\alpha_iC_{k+1} \leq 1\right). \end{cases} \\ C_{k+1} &= \frac{\operatorname{Tr}\left[v_{0(k+1)} - R_{k+1} - H_{k+1}Q_kH_{k+1}^T\right]}{\sum_{i=1}^n \alpha_i\left(F_{k+1/k}P_{k/k}F_{k+1/k}^TH_{k+1}^TH_{k+1}\right)}, \\ v_{0(k+1)} &= \begin{cases} \widetilde{Y}\widetilde{Y}_1^T & (k = 0), \\ \dfrac{\rho v_{0(k)} + \widetilde{Y}_{(k+1)}\widetilde{Y}_{(k+1)}^T}{1+\rho} & (k \geq 1, 0 \leq \rho \leq 1). \end{cases} \end{aligned} \tag{10}$$

The value of a in equations (9) and (10) is determined by a priori knowledge. It can be seen that when the state changes suddenly, the increase of estimation error $\widetilde{Y}_{(k+1)}\widetilde{Y}_{(k+1)}^T$ will increase the error variance matrix $v_{0(k+1)}$; accordingly, the weighting coefficient $\lambda_{i(k+1)}$ increases, the tracking ability of the filter is enhanced, and the reliability is improved. During the simulation, the system and observation noise change suddenly. The adaptability of the two algorithms to noise change is compared.

Simulation initial value is $x_0 = \begin{bmatrix} 1000 & 50 \end{bmatrix}^T$, $P_0 = \begin{bmatrix} 100 & 0 \\ 0 & 10000 \end{bmatrix}$, $\alpha = 1.2$, and $\rho = 0.6$. The simulation results are shown in Figures 3 and 4.

Figures 3 and 4 show that the ability of the previous system positioning accuracy filtering algorithm to deal with noise mutation is relatively weak; especially, when the difference between the noise model and the fixed model in the simulation is large, the divergence phenomenon occurs in the filtering. The system positioning accuracy filtering algorithm can adapt to the noise change in the filtering process, but the filtering accuracy is reduced.

4. Design and Implementation of Positioning Accuracy Filtering Algorithm for the Logistics Tracking System

4.1. Getting Initialization Information.

(1) The management of basic information includes adding, modifying the use of identity, and does not delete the basic information.

(2) When the basic information with the master-slave relationship is recorded in the main table, the usage flag is set to 0 (no longer used) to judge whether the usage flag of all the subrecords in the table is 0. If not all 0, the usage ID of the main table cannot be changed. First, notice that the user sets the usage flag for all child records to 0.

(3) The record display area of the add basic information page displays all the records in the table and finally displays the record marked as 0.

(4) All codes of the basic information table are automatically generated by the system. The number increases from 1, and 0 is added before the length is 0.

(5) There is a master-slave relationship table. The first few digits of the table code are the main table code.

(6) For the basic information related to the correspondence of Co., Ltd., no separate menu item is set, and the corresponding link is added in the record display area of the addition page to pop up the correspondence correction screen of the corresponding Co., Ltd.

(7) For the basic information related to the corresponding relationship of a joint stock company, when the usage flag is changed to 0, the system will delete the corresponding relationship with all the joint stock companies. After the user agrees, all the

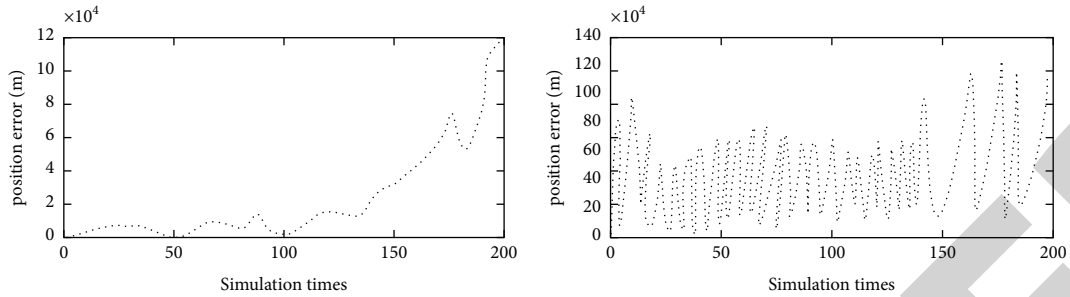

Figure 3: Position error simulation results of two algorithms. (a) Conventional Kalman filter. (b) Strong tracking Kalman filter.

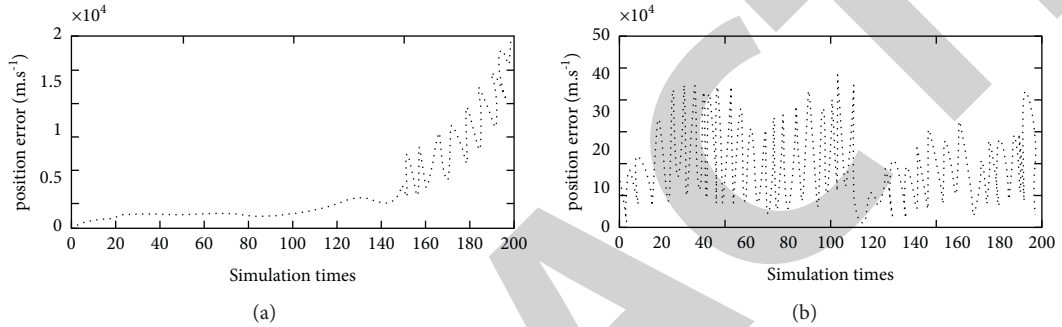

Figure 4: Speed error simulation results of two algorithms. (a) Conventional Kalman filter. (b) Strong tracking Kalman filter.

records corresponding to the joint stock company will be deleted automatically.

(8) There are many information records of factory cars and stock limited companies, which are inconvenient to retrieve and maintain. The sorting function is added to the record display area table of the factory cars and stock information addition page. Click the corresponding column name to sort the records (ASC or DESC) in the order of click.

(9) The primary key or code of the basic information cannot be modified.

4.2. Acquisition of Change Information and Exchange Information of Transportation Logistics. The change information of railway transportation logistics within the enterprise, the logistics change information of railway transportation within the enterprise, and the logistics exchange information inside and outside the enterprise have the characteristics of information change. The change of information can be represented by the change of specific data, and the change process of data can be represented by data flowchart in Figure 7. In order to facilitate the program, it can be transformed into a more direct program flowchart.

4.2.1. Internal Railway Transportation Logistics Change Information. Taking the loading process as an example, the flowchart is shown in Figure 5.

The loading of vehicles is divided into two parts: the loading of station vehicles and the loading of factory vehicles. The loading registration interface of station vehicles and the loading registration interface of factory vehicles are set. The loading investigation and maintenance interface of station vehicles is set. The loading time is registered as the sign of vehicle completion in the process of vehicle registration.

4.2.2. Internal and External Logistics Exchange Information. Take the train number delivery business process as an example; the process is shown in Figure 6.

During the delivery of goods, the train will be sent from the locomotive to the handover line at the time of delivery. This handover line is mainly a virtual tracking system, but the vehicle needs to be identified according to the vehicle number. The system will judge whether the number distinguishes the vehicle according to color. After confirming the delivery, if other data items need to be determined, the data will be extracted according to the relevant information form. After the completion of the operation, the train number can be removed from the existing table, and the corresponding train number table and train number detail table can be filled in at the same time. The logistics tracking information management system can display the tracking logistics information and carry out statistical management at the same time.

(1) Tracking operation processing subsystem: the tracking operation processing subsystem plays a core role in the overall positioning accuracy filtering algorithm of the railway transportation logistics

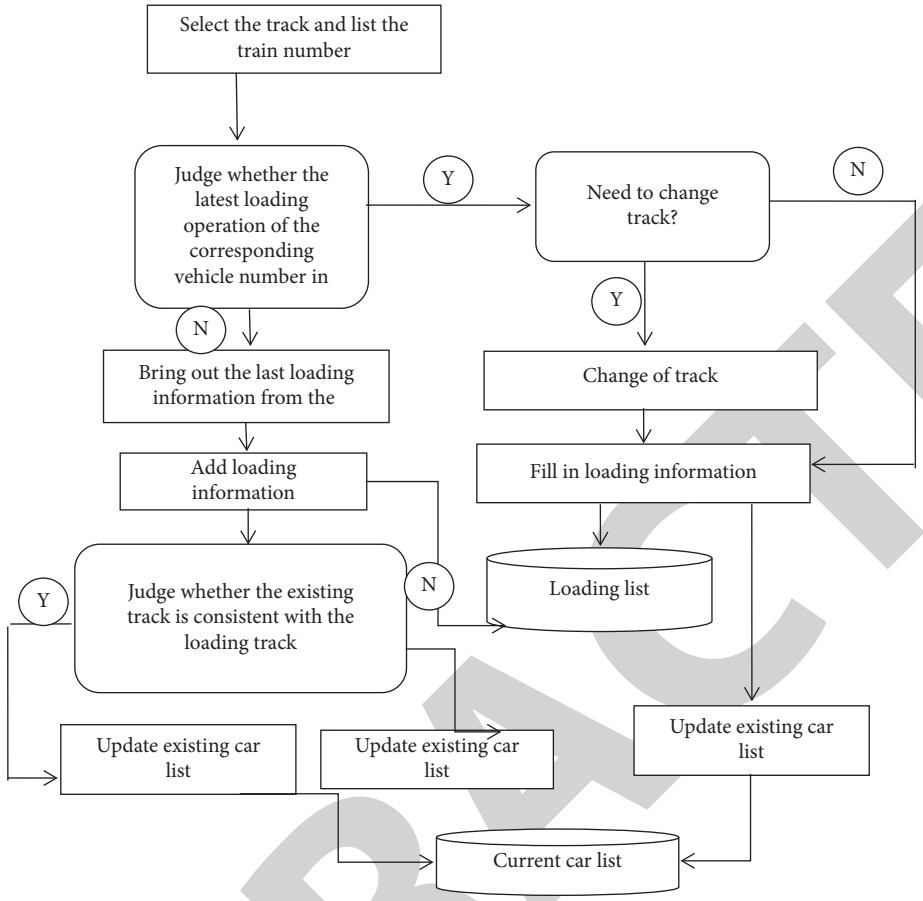

Figure 5: Loading process flowchart.

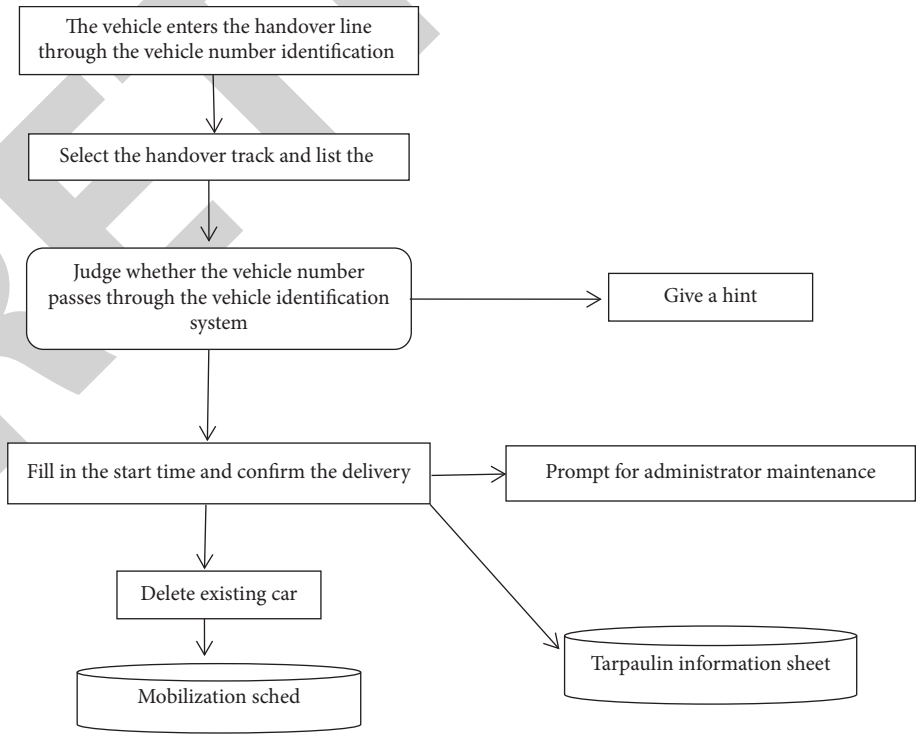

Figure 6: Flowchart of train number delivery business.

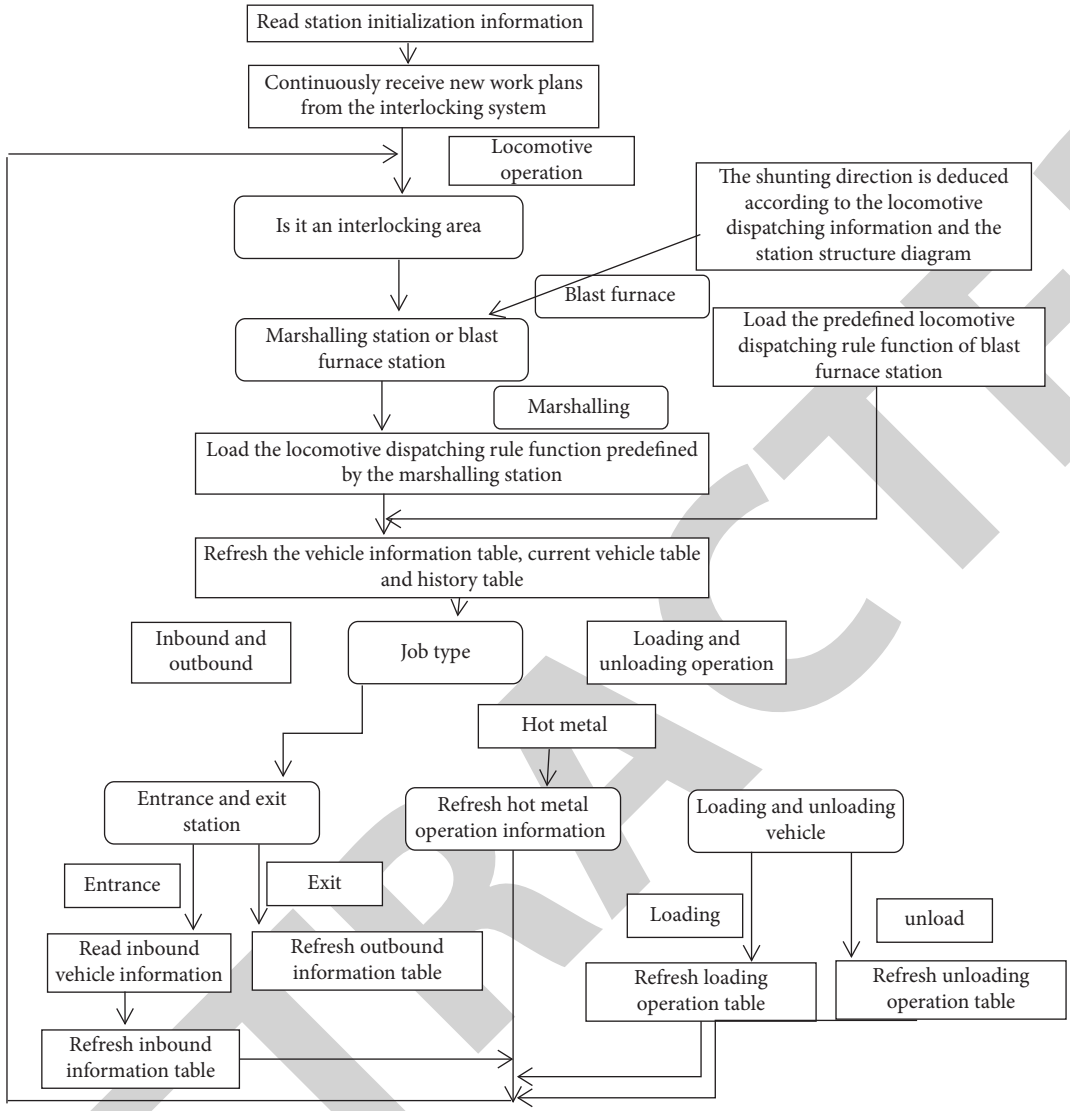

Figure 7: Schematic flowchart of the tracking calculation subsystem.

tracking system. The simple flow of the tracking operator system is shown in Figure 7.

(2) As shown in Figure 8, the logistics tracking information management subsystem structure is mainly composed of browser/web server + web application server and database server. In this type of architecture, the web application server can process the business logic function of the intermediate service, so as to ensure that the electronic client on the user side can send HTTP request to the web server and send the request to the web application server in time.

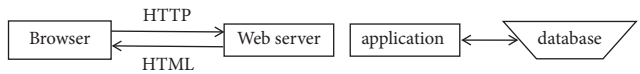

Figure 8: Four-tier architecture of B/S.

Finally, according to the obtained data request information, the web application server sends it to the system database server synchronously. The database server sends the obtained data to the web application server and uses the web server to send the data to the customer.

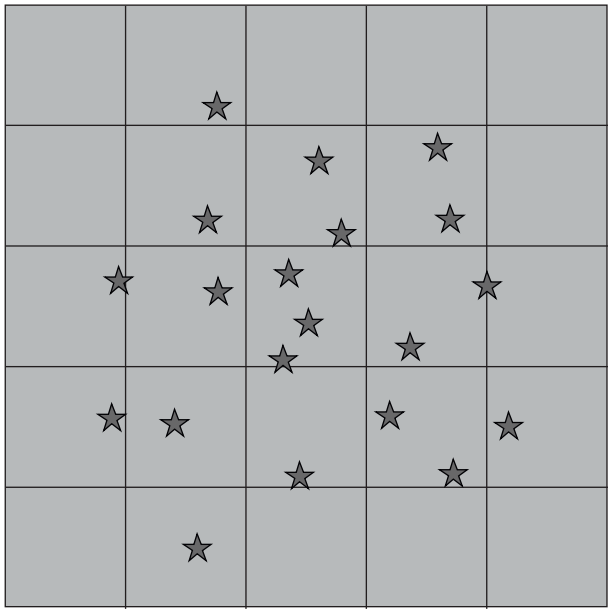

Figure 9: Test results of the unused filter.

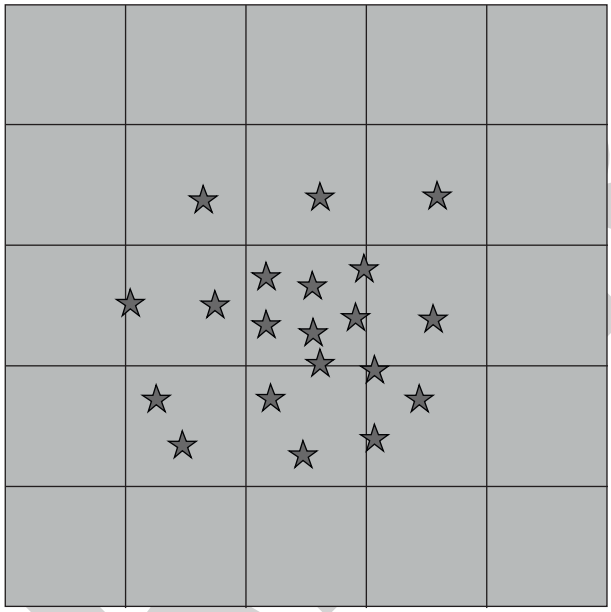

Figure 10: Test results of positioning accuracy filtering using the strong tracking system.

The implementation of the logistics tracking information management subsystem adopts Java Server Pages Technology (JSP) and realizes the connection of the database through JDBC.

5. Test Result

In order to verify the role of the powerful system positioning accuracy filtering algorithm in GPS positioning, the powerful tracking system positioning accuracy filtering and GPS positioning without using the filter algorithm are compared at fixed points. It is obvious from Figures 9 and 10 that using the strong tracking system positioning accuracy filtering algorithm can effectively suppress the satellite position drift and improve the satellite positioning accuracy.

6. Conclusions

The three-dimensional virtual warehouse logistics demonstration system has the advantages of small volume, low cost, good convergence, and high precision. The strong tracking method of system positioning accuracy filtering is used to locate and track the logistics system data, which can accurately and efficiently determine the detailed location of items according to the received data, effectively improve the accuracy and level of monitoring and management technology, and solve the problem of complex and changeable environment in the tracking process. After many experiments, GPS has high positioning accuracy and good performance in the background of obstacles and can receive and process information in real time and accurately. With the continuous updating of industry technology, improving the positioning accuracy in different environments is still an important research direction in the future.

Data Availability

The data used to support the findings of this study are available from the corresponding author upon request.

Conflicts of Interest

The authors declare no conflicts of interest.

Acknowledgments

The name of this research project is Research on the Application of "Internet Course Sizheng" in the Professional Courses of Logistics Management in Higher Vocational Colleges—taking "Procurement and Supply Practice" as an example. The project number is CJJY201901. The authors thank the project for supporting this article.

References

[1] M. El Midaoui, E. M. Ben Laoula, M. Qbadou, and K. Mansouri, "Logistics tracking system based on decentralized iot and blockchain platform," *Indonesian Journal of Electrical Engineering and Computer Science*, vol. 23, no. 1, pp. 421–430, 2021.

[2] Z. Chen, "A logistics status real-time tracking system based on wireless sensor network," *International Journal of Online Engineering*, vol. 14, no. 05, pp. 218–221, 2018.

[3] J. Xing, "An intelligent logistics tracking system based on wireless sensor network," *International Journal of Online Engineering*, vol. 14, no. 01, pp. 701–717, 2018.

[4] M. Schröder and P. Cabral, "Eco-friendly 3D-Routing: a GIS based 3D-Routing-Model to estimate and reduce CO2-emissions of distribution transports," *Computers, Environment and Urban Systems*, vol. 73, no. JAN, pp. 40–55, 2019.

[5] X. Li, W. Jianguo, and J. Yuan, "A new logistics distribution route optimization algorithm for fresh agricultural products based on the fusion of genetic algorithm and ant colony

Hindawi
Journal of Electrical and Computer Engineering
Volume 2023, Article ID 9838757, 1 page
https://doi.org/10.1155/2023/9838757

Retraction

Retracted: Based on Knowledge Recognition and Using Binomial Distribution Function to Establish a Mathematical Model of Random Selection of Test Questions in the Test Bank

Journal of Electrical and Computer Engineering

Received 15 August 2023; Accepted 15 August 2023; Published 16 August 2023

This article has been retracted by Hindawi following an investigation undertaken by the publisher [1]. This investigation has uncovered evidence of one or more of the following indicators of systematic manipulation of the publication process:

(1) Discrepancies in scope

(2) Discrepancies in the description of the research reported

(3) Discrepancies between the availability of data and the research described

(4) Inappropriate citations

(5) Incoherent, meaningless and/or irrelevant content included in the article

(6) Peer-review manipulation

The presence of these indicators undermines our confidence in the integrity of the article's content and we cannot, therefore, vouch for its reliability. Please note that this notice is intended solely to alert readers that the content of this article is unreliable. We have not investigated whether authors were aware of or involved in the systematic manipulation of the publication process.

Wiley and Hindawi regrets that the usual quality checks did not identify these issues before publication and have since put additional measures in place to safeguard research integrity.

We wish to credit our own Research Integrity and Research Publishing teams and anonymous and named external researchers and research integrity experts for contributing to this investigation.

The corresponding author, as the representative of all authors, has been given the opportunity to register their agreement or disagreement to this retraction. We have kept a record of any response received.

References

[1] Y. Chang, "Based on Knowledge Recognition and Using Binomial Distribution Function to Establish a Mathematical Model of Random Selection of Test Questions in the Test Bank," *Journal of Electrical and Computer Engineering*, vol. 2021, Article ID 2250300, 8 pages, 2021.

Hindawi
Journal of Electrical and Computer Engineering
Volume 2021, Article ID 2250300, 8 pages
https://doi.org/10.1155/2021/2250300

Research Article

Based on Knowledge Recognition and Using Binomial Distribution Function to Establish a Mathematical Model of Random Selection of Test Questions in the Test Bank

Yuan Chang

Shaanxi Institute of International Trade & Commerce, Xi'an 712046, Shaanxi, China

Correspondence should be addressed to Yuan Chang; 20061024@csiic.edu.cn

Received 5 November 2021; Accepted 23 November 2021; Published 23 December 2021

Academic Editor: Muhammad Rashad

With the in-depth development of social reforms, the scientificization of enterprise online examinations has become more and more urgent and important. The key to realizing scientific examinations is the automation and rationalization of propositions. Therefore, the construction and realization of the test question bank is also more important. In the realization of the entire test question database, how to select satisfactory test questions randomly from a large number of test questions through the selection of test questions so that the average difficulty, discriminability, and reliability of the test are satisfactory? These requirements are also more important. Among them, random selection of questions is an important difficulty in the realization of the test question bank. In order to solve the difficulties of random selection of these test questions, the author combines the experience of constructing the test question bank and uses the discrete binomial distribution to draw conclusions. Random variables established the first mathematical model for topic selection. By determining the form of the test questions and the distribution of the difficulty of the test questions and then making it use a random function to select questions, this will achieve better results.

1. Introduction

With the application and development of computers in the teaching field, the compilation and application of the test question bank have become more and more important. Random selection of questions is a difficult point in the construction of the test question bank. The test questions obtained from a large number of test questions are related to the average difficulty of the test, the question type, and the difficulty of each question, as well as the question type and difficulty distribution of each section [1]. There are generally three methods for selecting questions in the current test question bank. First, the user directly uses the random function to randomly select the test questions by inputting the required question types and sections, which is difficult to guarantee the difficulty of obtaining the test paper. Second, the user presents the question type, difficulty level, section distribution, and other requirements of each question in detail and then uses a random function to choose the question within the range suggested by the user. This can make the selected test questions really meet the user's requirements, but the workload is too much and too troublesome. Third, users are allowed to display or print all test questions in the test question bank and then manually (experts) select and write test questions [2]. This method of selecting questions can more accurately select the test papers that meet the requirements, but this method is also too cumbersome for users, and it is difficult to reflect the strength of the test question bank.

2. The Establishment of the Mathematical Model

In the test question composition process, the selection probability of each test question in the test question bank should be equal (the probability of each test question being selected is the same), and there are only two possibilities for each question, that is, to be selected or not to be selected; this

is random. Each test question drawn is discrete and independent, that is, the results of each drawing do not affect each other, that is to say, the probability of each drawn test question does not depend on the results of other drawn questions. In other words, these N extractions are independent [3]. Therefore, the event of randomly selected test questions conforms to the n-fold Bernoulli test; that is, the event of randomly selected test questions conforms to the binomial distribution of discrete random variables $B(n, p)$. As shown in formula (1), it can also be expressed as formula (2):

$$P_n(k) = \binom{n}{k} p^k q^{n-k}, \quad k = 0, 1, 2, \cdots, p < 0, q > 0, p + q = 1, \quad (1)$$

$$P_n(k) = \binom{n}{k} p^k (1-p)^{n-k}, \quad k = 0, 1, 2, \cdots, 1 > p > 0. \quad (2)$$

And the mathematical expectation (also known as the mean value) of the binomial distribution $B(n, p)$ can be expressed as

$$\begin{aligned} E(x) &= \sum_{k=0}^{n} k \binom{n}{k} p^k (1-p)^{n-k} \\ &= \sum_{k=0}^{n} k p_n(k) = np. \end{aligned} \quad (3)$$

For this reason, in the model, k can be used to represent the difficulty level, which is generally defined as $k = 0,1,2, \ldots$, pk represents the probability that the difficulty level is k, n is the total number of difficulty levels of the test question bank, and $E(r)$ represents the average difficulty level of the question bank.

It can be seen from Figure 1 that, for a binomial distribution $B(n, p)$ with a fixed n and P, when k increases, the probability $P\{x = k\}$ first monotonically increases to the maximum value and then monotonically decreases, so the probability $P\{X = k\}$ has a higher probability in the middle, but a lower probability at the two ends. Therefore, in actual operation, if the difficulty level is set to 9, then $n = 10$, a total of 11 difficulty levels. From equation (3), P can be obtained from the average difficulty level $E(z)$, and then, P, n, and k can be substituted into equation (2) to calculate the probability that the event occurs exactly k times (difficulty level) in the n-fold Bernoulli test, that is, the proportion $P_n(k)$ of the test questions of each difficulty in the total number of questions. If $P_n(k)$ is multiplied by the total number of questions, the number of questions that should be drawn for each difficulty level can be obtained [4].

In the actual system, the difficulty coefficient is used for general test questions to express the difficulty of the test paper such as the degree of difficulty of the ith question: $r_i = 1 - \overline{x}_i / a_i$, that is, the average loss rate of the ith question. Among them, a_i is the full score of the ith question and $\overline{x}_i$ is the average score of the ith question; the average difficulty coefficient of the test paper: $r = 1 - \overline{y}/a$, that is, the average loss rate of the test paper. Among them, α is the full score of the test paper (usually 100 points) and $\overline{y}$ is the average of the candidates' total scores. The expected value of a set of test papers determines its difficulty, and candidates' test scores should roughly match it. On the contrary, the number of questions of various difficulties in the test paper must be roughly consistent with it, so we can achieve the purpose of controlling the average score of the test by setting the difficulty level of the test paper.

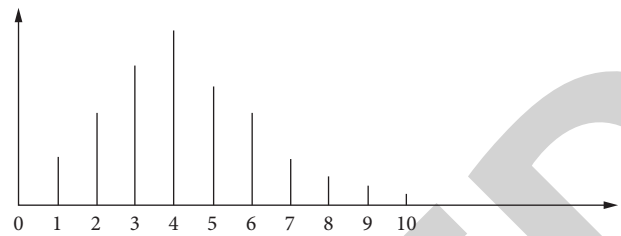

Figure 1: Binomial distribution $B(n, p)$ graph.

The relationship between the difficulty coefficient and the difficulty level is shown in Table 1:

3. Data Modeling of Test Question Bank Based on Knowledge Recognition

Teachers always divide test papers into several question types (such as fill-in-the-blank questions and multiple choice questions) when writing, and each question type is composed of several questions. When asking specific questions, teachers should consider the knowledge points of the problem and the difficulty of the problem. Therefore, when inputting questions, teachers are required to identify and input keywords, and the difficulty coefficient represents the knowledge score of the examination according to the subject knowledge score [5]. Figure 2 is a data modeling based on the knowledge tree structure of the test question bank.

Course examination is an important means to test the quality of teaching and the realization of teaching goals. In recent years, the separation of subject examinations has been continuously promoted. Many colleges and universities have carried out the construction of test question banks. The use of test question banks to compile test papers has the advantages of objectiveness and accuracy, standardized management, and strict confidentiality. This article discusses the methods, status quo, existing problems, and improvement strategies of college test question bank construction as follows:

(1) The number of courses constructed by the test question bank is relatively small, and additional construction is required. Due to the unreasonable structure of the existing test question bank itself, in order to improve the curriculum standards, the curriculum standards are revised in time according to the curriculum practice. A set of complete and feasible curriculum standards is the guideline for professors to implement, which is also an important basis for thesis proposal.

(2) The construction of the teacher integration question bank is a complex project, and the quality of the test questions is the main factor that determines the quality of the question bank. Therefore, in order to

Table 1: The relationship between the degree of difficulty and the level of difficulty.

Degree of difficulty	0	0.1	0.2	0.3	0.4	0.5	0.6	0.7	0.8	0.9	1
Average score	100	90	80	70	60	50	40	30	20	10	0
Difficulty level	0	1	2	3	4	5	6	7	8	9	10

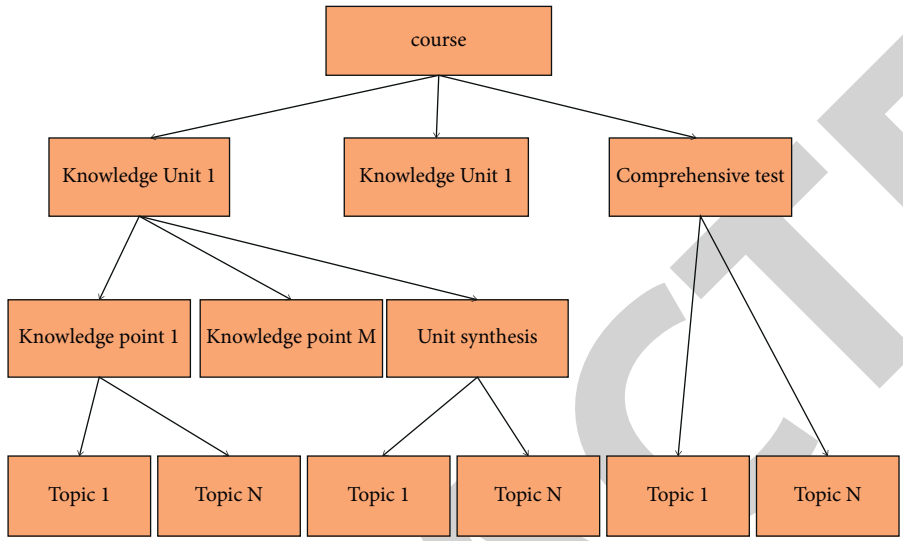

Figure 2: Data modeling of the question bank based on the knowledge tree structure.

build a high-quality question bank, there must be a well-trained professional technical team. It mainly includes two aspects. One is sufficient quantity. The project's restricted faculty cannot complete the construction and use of the question bank. The second is good quality. It is necessary to strengthen the training of teachers' modern theory and examination methods, which can promote the transformation of teachers' ideas, and they can further study examination theory and test question skills, so as to make the completed test question bank more scientific.

(3) At present, the use of random test question bank is prone to inconsistencies in teaching and examination. Therefore, teacher management, teacher action plan, group lesson preparation, teacher supervision, examination paper review, and other links need to strengthen supervision. The teacher implements the curriculum standard proposal group of the teaching method according to the curriculum standard, which effectively creates the conditions for the application of the test question bank classification and the separation of teaching and testing.

(4) The test question bank management software still has some functional defects, such as repeated use of random test questions and inability to search for keywords. Therefore, the smart lock function should be added after the single question is used, that is, each question cannot be reused within a certain period of time after it is used once, so as to ensure that the overlap of different test papers in the same class is less than the prescribed ratio. Secondly, increase the keyword index of test questions, that is, each test question is marked with a certain number of keywords. If selecting different test questions with the same keywords from the same test paper, the system will automatically ask to avoid repeated assessments of the same knowledge points or remind each other test questions.

4. Application of Binomial Distribution Function

4.1. Probability Inference Problem. When $n0$ (≥ 50) is large, from the central limit theorem theory, X–B (n, $P0$), the approximate probability mathematical model of the Y interfield in XXX is as [6]

$$P\{X \leq k\} = P\left\{X \leq \frac{k - n_0 p_0}{\sqrt{n_0 p_0 q_0}}\right\} = \Phi\left(\frac{k - n_0 p_0}{\sqrt{n_0 p_0 q_0}}\right) = p. \tag{4}$$

Among them, check the normal distribution probability value table to determine the value of $\Phi(x)$.

Inference: when $P < P0$, it can be considered that the actual scene event has not occurred, and when $P \geq P0$, it can be considered that the actual scene event has occurred.

4.2. The Problem of Estimating the Overall Probability and Inferring the Sampling Capacity. Suppose the sampling capacity is n, the sampling frequency of the problem is f_n/n, and the character frequency of the problem is $f_n \sim B(n, p)$,

so the probability mathematical model of the problem is as [7]

$$P\left\{\left|\frac{f_n}{n}-p\right|\le\delta\right\}\ge 1-\alpha. \tag{5}$$

When n is large, the central limit theorem is applied as

$$P\left\{\left|\frac{f_n}{n}-p\right|\le\delta\right\}\ge$$

$$P\left\{-\sqrt{\frac{n}{pq}}\delta\le\frac{f_n-np}{\sqrt{npq}}\le\sqrt{\frac{n}{pq}}\delta\right\} \tag{6}$$

$$\approx 2\Phi\left(\sqrt{\frac{n}{pq}}\delta\right)-1.$$

In formula (6), $q=1-P$, which is as

$$\Phi\left(\sqrt{\frac{n}{np}}\delta\right)\ge 1-\frac{\alpha}{2}. \tag{7}$$

Inversely check the normal distribution probability value table and get the probability critical value $u_{a/2}$ as

$$\Phi\left(u_{\alpha/2}\right)\ge 1-\frac{\alpha}{2}, \tag{8}$$

$$\sqrt{\frac{n}{np}}\delta\ge u_{\alpha/2}, \text{which is}: n\ge\frac{u_{\alpha/2}^2}{\delta^2}pq. \tag{9}$$

Estimate the unknown quantity P in (9) to obtain

$$n\ge\frac{u_{\alpha/2}^2}{4\delta^2}. \tag{10}$$

The inferred value of the sampling capacity that meets the accuracy and reliability requirements is as

$$n=\left[\frac{u_{\alpha/2}^2}{4\delta^2}\right]+1. \tag{11}$$

4.3. Inference Problem of Overall Capacity. Assuming that the number of individuals with probability P traits in the population is X, then $X\sim B\ (N,\ P)$; then, the probability mathematical model of the population capacity IV satisfying the problem is shown in

$$P\{X\ge M\}\ge 1-\alpha. \tag{12}$$

When N is large, the central limit theorem is applied as

$$P\{X\ge M\}=P\left\{\frac{X-pN}{\sqrt{Npq}}\ge\frac{M-pN}{\sqrt{Npq}}\right\}$$

$$=\Phi\left(\frac{pN-M}{\sqrt{Npq}}\right). \tag{13}$$

Thus, the overall capacity N satisfies

$$\frac{pN-M}{\sqrt{Npq}}\ge u_a. \tag{14}$$

4.4. Error Inference Problem Using Expected Value as the Estimator. Suppose the estimated reliability is $1-\alpha$ and the error is x; then, the probability mathematical model of the problem is as [8]

$$P\{|M-PN|\le x\}\ge 1-\alpha. \tag{15}$$

When N is large, the central limit theorem is applied as

$$P\{|M-PN|\le x\}$$

$$=P\left\{-\frac{x}{\sqrt{pqN}}\le\frac{M-pN}{\sqrt{pqN}}\le\frac{x}{\sqrt{pqN}}\right\} \tag{16}$$

$$\approx 2\Phi\left(\frac{x}{\sqrt{pqN}}\right)-1.$$

Formula (17) can be obtained by formulas (15) and (16):

$$\Phi\left(\frac{x}{\sqrt{pqN}}\right)\ge 1-\frac{\alpha}{2}. \tag{17}$$

Anyway, check the normal distribution table has $\Phi\left(x/\sqrt{pqN}\right)\ge 1-\alpha/2$, so take $x/\sqrt{pqN}\ge u_{\alpha/2}$; the estimated error number is shown as

$$x=\left[u_{\alpha/2}\cdot\sqrt{pqN}\right]+1. \tag{18}$$

Therefore, the $1-\alpha$ confidence interval of the number of individuals with probability P traits M is $[pN-x, PN+x]$.

4.5. Random Paper Grouping Algorithm. As shown in Figure 3, it is the process of random test paper generation algorithm based on binomial distribution [9].

There are five principles that need to be met during the development of test question composition technology, including the comprehensiveness, the cultivation of examinee's ability and intellectual development, the difficulty of test questions, and the importance of giving full play to the guiding role of test questions in the study methods of test takers. The proposition should be expressed as clearly as possible and describe the correct expression or instruction. In order to meet the above principles, the work of organizing papers is really complicated. There are still some shortcomings in using computers to solve the problem of volume formation. The following are the problems and corresponding solutions:

(1) The main purpose of the test paper formation system is to find some test papers that meet the user's requirements in the existing question bank. Therefore, the data in the question database must first match the text of the question and the corresponding answer. If the distribution of test questions is irregular, searching becomes very difficult. Therefore, the test paper system must use normalized index data to

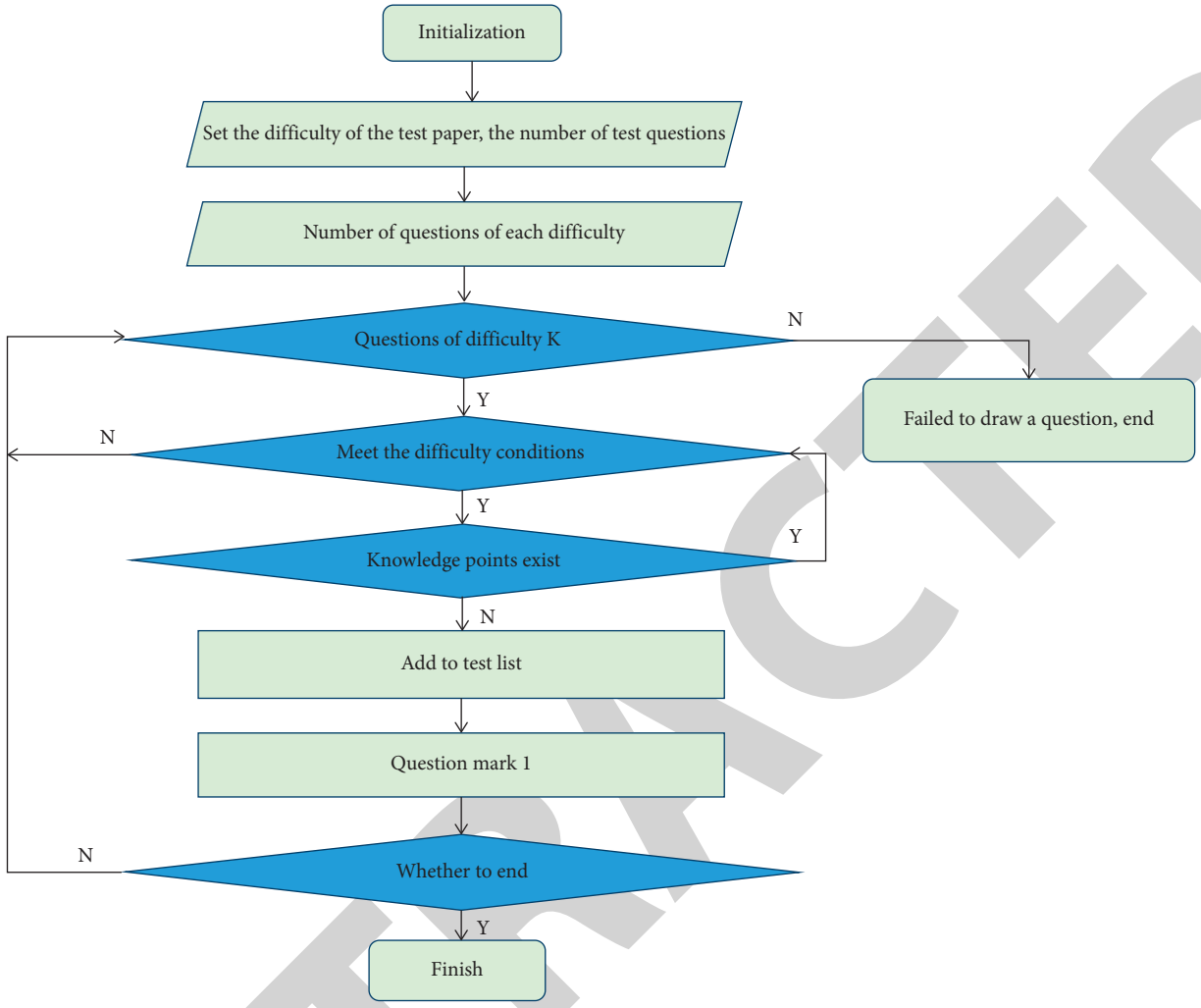

Figure 3: The flow of the random grouping algorithm.

describe the test questions. Relevant data in the test indicators, such as scores and answer time, can be clearly summarized. However, the data on difficulty and isolation in the abstract is rather vague. The indicators of these test questions are not static. According to the actual test results, it should be revised continuously.

(2) The design of the test paper structure and the indicators of some test questions come from the experience of the test paper maker, which has caused the influence of human factors. For example, the experience recognized by the test paper maker cannot be accepted and confirmed by the co-participants. Some content is effective, and some content is invalid due to changes in time and environmental conditions. In response to the above problems and in the software research process, experts discovered the defects in the process based on preliminary experience and then further improved the test paper system. In the service process, relevant personnel can further improve the test paper based on the continuous advancement of knowledge and technology.

5. Improvements to the Algorithm of Generating Papers

The method of randomly compiling papers is to randomly select test questions from a set of test questions according to the type of test questions, the complexity of the test questions, and the degree of differentiation of the test questions. Although the random combination method is a popular test question combination method, there are still many problems. The following are related problems and solutions:

(1) The traditional method of random grouping of papers is based on computers and programs to run and group papers. This paper composition method is too rigid and lacks human thinking mode, and the quality of its database is relatively poor, which will degrade the efficiency of paper composition. Therefore, relevant personnel have developed an

expert-based test paper algorithm, which utilizes an expert database and intelligent reasoning mechanism. This enables the computer to simulate the way of thinking of experts to solve problems in related fields. The expert library should contain a large amount of knowledge in a specific field, as well as attributes such as knowledge level and mastery, all of which help to improve the efficiency of grouping volumes.

(2) Experts in professional fields and education experts jointly complete traditional test papers. This kind of test paper largely reflects the subjective thoughts of the tester and ignores the actual situation of the testee. Therefore, the test questions in the test question bank may not be suitable for all testers. The test paper generation algorithm based on the article reaction theory estimates the actual ability value of the examiner through a nonlinear mathematical model, and it adjusts the test content of the examiner according to this value. The test paper grouping algorithm is based on the actual ability of the examiner, and this does not depend on the specific test question bank and test crowd.

(3) The traditional paper synthesis algorithm cannot realize parallel operation and cannot carry out large-scale paper synthesis. Therefore, related researchers have developed a genetic algorithm based on the traditional test paper synthesis algorithm. The algorithm is an optimization algorithm that simulates the survival of human beings in nature and the evolution of genetic genes. In the process of algorithm evolution, according to the material characteristics and evaluation function of the test questions, it is determined how the test questions in the chromosome will be inherited, mutated, and mutated, so as to realize the function of computer combination.

5.1. System Demand Analysis. At present, the society and education industries use traditional manual testing methods to complete the examination process. However, the types and requirements of exams are constantly changing and improving. For teachers, the workload will be greater, which will affect work efficiency and teaching quality. The examination questions themselves are a tedious process. There is great resistance to this proposition. Judging from the current educational environment, the traditional artificial model is no longer applicable [10].

The advancement of science and technology and the development of the network have brought tremendous impetus to the construction of informatization in colleges and universities. The traditional question bank can no longer meet the needs of current campus development. With the help of campus resources and network resources, it is necessary for school education to use network technology to develop a scientific and standardized test question bank. The systematic development of the network test question bank can greatly reduce the burden of test questions on teachers, and at the same time, this can improve the efficiency of the examination process and then provide objective, fair, reasonable, and high-quality test papers [11]. The principle of this system development is shown in Figure 4.

6. The Design of Random Selection System

6.1. System Architecture Design. The architecture adopted by this system is the BS model mentioned above. This article divides the structure of the system into three layers, namely, the user interface layer, the specific function layer, and the data layer [12], as shown in Figure 5.

6.1.1. User Interface Layer. The user interface layer runs on the user's computer, and the user can use it to access the system, through which human-computer interaction is realized. The user interface of the system can be composed of administrators and examinees. Other users log in to the system according to their roles to obtain its interface information.

6.1.2. Specific Functional Layer. The functional layer is the intermediate link between the user interface layer and the data layer. The functional layer mainly includes task management, user management, question bank management, monograph management, and other tasks. When the system is running, this layer provides its functional services to the user interface layer on the one hand and can access the database on the other hand. The specific function class has two main advantages; one is the program structure is simple and flexible, and the other is the realization of the main functions of the system. So, this layer is easy to change when needed, or reduce some functions; as long as the code is modified, the desired effect can be achieved, and this can greatly improve the overall efficiency of development [13].

6.1.3. Data Layer. The data layer is mainly to provide data support for the upper specific functional layer, and the data of these databases are completely independent of the specific functional model and it is the development basis of all systems. In the system implementation part of this article, the data layer is mainly composed of user table, question type dashboard, account table, test paper dashboard, and score table.

6.2. System Function Module. According to the specific analysis of the question bank system requirements and the overall operation requirements of the education industry on the question bank system, the question bank system designed in this article is mainly divided into six modules [14], as shown in Figure 6.

6.3. System Database Design. The question bank system designed in this paper uses Oracle database. Oracle is a relational database system developed by Microsoft. It has good scalability and high integration. Oracle database also

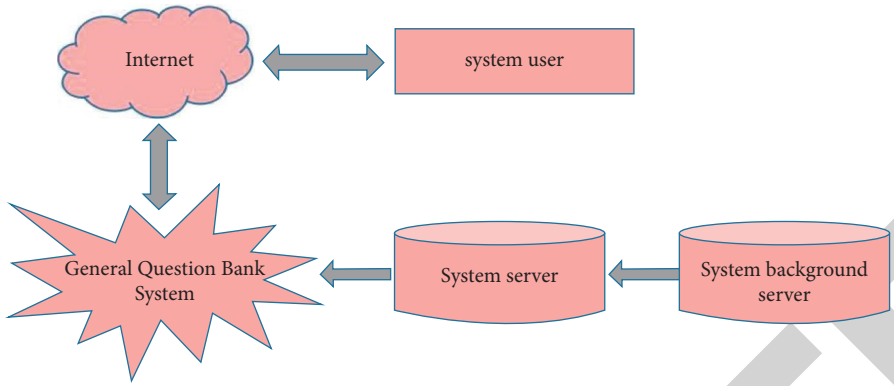

Figure 4: Principle of system development.

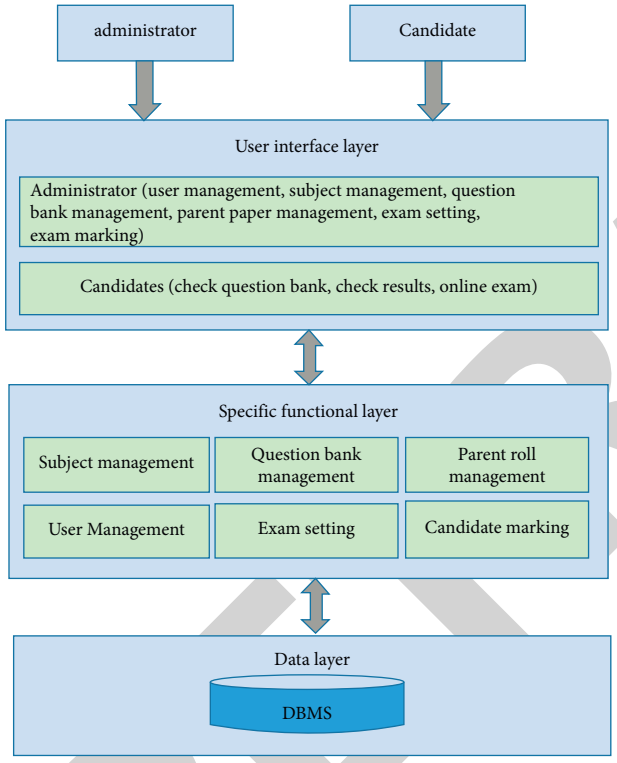

Figure 5: System structure division diagram.

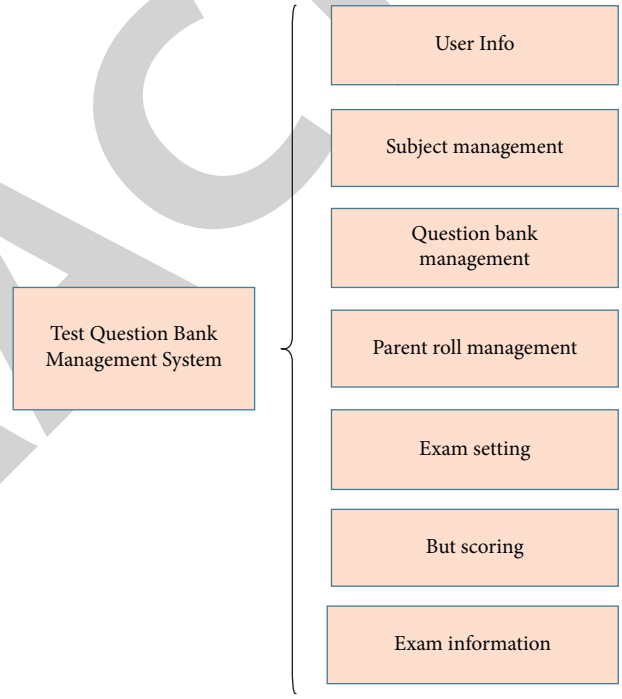

Figure 6: System function module diagram.

has cross-platform features, which can be well adapted to multiple different server platforms.

Oracle database is a comprehensive database platform, which can provide enterprises with complete data management. In the relational data and many structured data used in the system, the database engine can provide storage functions with high security and strong reliability [15].

7. Conclusions

This article uses the binomial distribution function $B(n, p)$ of discrete random variables to establish a mathematical model for random selection of questions. It can well solve the problem of difficulty distribution in the preparation of the test question bank. On this basis, the random function is used to randomly select questions within this difficulty distribution range. If the question type, section scope, and